August 2024

THE SUBCUTANEOUS LD_{50} OF IVALIN, EXTRACTED AND PURIFIED FROM *GEIGERIA ASPERA*, IN TWO MURINE MODELS

DR SARA LINDSEY LOCKE

UNIVERSITEIT VAN PRETORIA
UNIVERSITY OF PRETORIA
YUNIBESITHI YA PRETORIA
Denkleiers • Leading Minds • Dikgopolo tša Dihlalefi

THE SUBCUTANEOUS LD_{50} OF IVALIN, EXTRACTED AND PURIFIED FROM *GEIGERIA ASPERA*, IN TWO MURINE MODELS

BY

SARA LINDSEY LOCKE (20064226)

SUBMITTED IN PARTIAL FULFILMENT OF THE REQUIREMENTS FOR THE DEGREE

MMedVet (Toxicology) in the Faculty of Veterinary Science, Department of Paraclinical Studies, University of Pretoria

29 August 2024

SUPERVISOR: PROFESSOR CHRISTO BOTHA
CO-SUPERVISOR: PROFESSOR JAN MYBURGH

DECLARATION OF ORIGINALITY

I declare that this dissertation, which I hereby submit for the degree MMedVet (toxicology) at the University of Pretoria, is my own work and has not previously been submitted by me for a degree at this or any other tertiary institution.

The experimental work reported in this dissertation was carried out at the Onderstepoort Veterinary Animal Research Unit (OVARU), the sections of Pharmacology, Toxicology and Pathology of the Department of Paraclinical Sciences, and the Electron Microscopy Unit of the Department of Anatomy, at the Faculty of Veterinary Science, University of Pretoria, under the expert supervision of Professor Christo Botha and Professor Jan Myburgh.

Sara Locke

_____

DR. SARA LINDSEY LOCKE

_____

PROF. CHRISTO BOTHA (SUPERVISOR)

_____

PROF. JAN MYBURGH (CO-SUPERVISOR)

August 2024

ETHICS STATEMENT

The author, whose name appears on the title page of this dissertation, has obtained the required research ethics approval for the research described in this work. The author declares that they have observed the ethical standards required in terms of the University of Pretoria's Code of ethics for scholarly activities.

ACKNOWLEDGEMENTS

Firstly, I would like to thank the University of Pretoria for affording me the opportunity and privilege to study further in my chosen field. Additionally, I am extremely grateful to have received a staff rebate for the tuition fees involved in the degree, which has greatly assisted me in partly funding my studies.

I would like to thank my supervisor, Prof. Christo Botha, for his patience, guidance, and involvement in my work. Thank you for your challenging questions, your timely and constructive feedback and your insights and professionalism.

I would also like to thank other members of the University staff:

Prof. Jan Myburgh for agreeing to co-supervise this project.

Prof Vinny Naidoo for assistance with statistical analysis and the study model design.

Mrs. Ilse Janse van Rensberg, Dr. Richard Mavuganidze and all other staff members from the OVARU for their involvement with caring for and collecting samples from the animals during the data collection phases of the study.

Dr. Sarah Clift from the section of Pathology (Department of Paraclinical Studies) and Prof. Martina Crole from the Department of Anatomy and Physiology for assisting with necropsy and tissue sampling for histopathology.

Dr. Sarah Clift and Dr. Lida Avenant from the section of Pathology (Department of Paraclinical Studies) for histopathology interpretation.

Ms. Rephima Phaswane, Dr. Sarah Clift and Dr Lida Avenant from the section of Pathology (Department of Paraclinical Studies) for desmin immunohistochemistry analysis and interpretation.

Mrs. Antoinette Lensink from the Department of anatomy and physiology for assisting with transmission electron microscopy (TEM) analysis and interpretation.

Dr. Yolandi Rautenbach and Ms. Carien Muller from the section clinical pathology, Department of Companion Animal Clinical Studies for assistance with biochemistry and haematology analysis and last, but definitely not least,

Mr. Frank Smith for assistance with EPA AOT 425 statistical package software installation.

A special note of thanks is further made of Dr. Sarah Clift's involvement in this project. Dr Clift was instrumental in interpretation of muscle pathology in this study. Her time, effort, enthusiasm and dedication are greatly appreciated!

ABSTRACT

"Vermeersiekte" or vomiting disease in ruminants is one of the most economically significant toxicities in South Africa and is caused by chronic ingestion of sesquiterpene lactone compounds present in plants of the *Geigeria* genus. Affected livestock demonstrate stiffness and paralysis, mega-oesophagus with regurgitation of ingesta, production losses and mortality due to actin and myosin damage in the striated muscle of the heart, diaphragm, skeletal muscle and oesophagus. *In vitro* studies in murine myoblastic cell lines suggest that disruption of desmin intermediate cytoskeletal filaments could be the cause of the muscle lesions. The aim of this study was to determine whether a rodent model is appropriate for *in vivo* study of ivalin's toxicodynamics in ruminants and to determine median lethality in rats exposed to the same compound.

We exposed 3 groups of CD-1 mice (6 mice per group) to subcutaneous ivalin, extracted from *G. aspera,* at doses of 175, 250 and 325 mg/kg BW. The control group (n = 6) received only the PEG 400 vehicle. Subsequently, we exposed Sprague-Dawley rats to ivalin in a sequential dosing procedure, according to the OCED Test Guideline (TG) 425 for Acute Oral Toxicity in rodents. Mortality, clinical signs, histopathology, muscle ultrastructure and desmin immunohistochemistry were evaluated. All mice, except one in the lowest dosing group, died within 24 hours of dosing and the LD_{50} was estimated at 164 mg/kg BW. Three of the 5 rats exposed to ivalin also died acutely and a maximum likelihood estimate method was used to calculate an LD_{50} of 135.4 mg/kg BW. There were no significant striated muscle histopathological or ultrastructural changes in exposed animals compared to the controls, and desmin immunoreactivity was highly variable in both exposed and control mice and rats.

Acute single-dose parenteral exposure of rodents to purified sesquiterpene lactones does not provide a viable laboratory animal model for further study of *Geigeria* spp. ingestion in ruminants. Acute ivalin toxicity in laboratory rodents following parenteral subcutaneous exposure induces sudden mortality with minimal muscle pathology and is in contrast to the more protracted muscular disease which occurs following chronic ingestion of sesquiterpene lactones from *Geigeria* plants in domestic ruminants. Median lethality is similar across the two rodent species and the lack of significant muscle lesions suggests toxicity at these doses is due to another mechanism, most likely mitochondrial energy pathway disturbances. This pilot study provides a starting dose for further investigation of sesquiterpene lactone plant extracts and chronic lower-dose exposure studies comparing oral and intravenous administration in both ruminants and rodents could potentially drive understanding of toxicokinetic and -dynamic differences between exposure routes and species. Additionally, the differences in clinical and pathological findings observed between acute and chronic toxicity could be elucidated.

TABLE OF CONTENTS

LIST OF TABLES

LIST OF FIGURES

LIST OF ABBREVIATIONS

ALT	Alanine transaminase
AST	Aspartate transferase
BW	Body weight
CK	Creatinine kinase
CNS	Central nervous system
EMH	Extramedullary haematopoiesis
GGT	Gamma-glutamyltransferase
GLDH	Glutamate dehydrogenase
OECD	Organisation for Economic Co-operation and Development
PO	Per os
SC	Subcutaneously
TEM	Transmission electron microscopy

`

1 SYNOPSIS

1.1 Introduction

Plant toxicoses in livestock contribute significantly to agricultural economic losses in South Africa. Vermeersiekte in sheep and cattle, caused mainly by ingestion of *Geigeria* species, is one of the most important of these and causes striated muscle pathology with resultant oesophageal dilatation, regurgitation of ruminal content, as well as stiffness and paralysis (Grosskopf, 1964; Kellerman *et al*., 2005).

Whilst the histopathological and ultrastructural changes are well described (Pienaar *et al*., 1973; van der Lugt and van Heerden, 1993), the exact mechanism of action of the toxic principles contained in *Geigeria* plants, the sesquiterpene lactones, is not. Efforts to elucidate this are hampered by several factors, including large variability in toxicity in plant material and the need for large volumes of plant extract required to dose sheep. Median lethal doses for sesquiterpene lactones extracts have not been determined in sheep or cattle.

Recent studies in murine myoblastic cell lines suggest that disruption to desmin intermediate cytoskeletal elements may underlie muscle pathology (Botha *et al*., 2019; Botha *et al*., 2020), but this has not been replicated in animal models. Validation of a small animal laboratory model and determination of median lethality for at least one sesquiterpene lactone from a species of *Geigeria* would therefore be practically and economically useful to further study sesquiterpene lactone toxicodynamics in ruminants and to confirm *in vitro* findings seen in muscle cell lines.

1.2 Aim

To evaluate murine laboratory animal models for further study of sesquiterpene lactone-induced toxicity, using ivalin extracted and purified from *Geigeria aspera*.

1.3 Objectives

- To determine the subcutaneous LD_{50} of ivalin in Sprague-Dawley rats.
- To evaluate relevant biochemistry and haematology parameters in CD-1 mice and Sprague-Dawley rats following subcutaneous administration of ivalin.
- To evaluate pathological findings in CD-1 mice and Sprague-Dawley rats following subcutaneous administration of ivalin, and to compare findings with those previously demonstrated in ruminants.

- To evaluate desmin immunohistochemistry findings in CD-1 mice and Sprague-Dawley rats following subcutaneous administration of ivalin and to compare findings with those previously demonstrated in murine C2C12 myoblast cell lines.

2 LITERATURE REVIEW

2.1 "Vermeersiekte" in livestock

Vermeersiekte, or "vomiting disease" as it is colloquially known to farmers, is a plant poisoning of significant economic importance in sheep in South Africa. Vermeersiekte also affects cattle and has been estimated to account for 13% of all phyto- and mycotoxin-related livestock mortalities in the country (Kellerman *et al.*, 1996). The most significant historical outbreaks have occurred in the drier Northern Cape and North West provinces, and to a lesser degree on the highveld in Free State and Mpumalanga provinces (figure 1) (Kellerman *et al.*, 1996; Kellerman *et al.*, 2005).

Figure 1: Historical distribution of vermeersiekte in South Africa. Reproduced from Kellerman et al.*, 1996.*

Vermeersiekte can cause significant animal losses. In one outbreak in 1929 and 1930, over 1 million animals died in a single season in the Griqualand West region of the Northern Cape province (Vahrmeijer, 1981). In 1954, a further outbreak in the same area saw a loss of *c.* 55 000 animals (Grosskopf, 1964). Kellerman *et al*. (1996) estimated that at the time of publication, annual losses due to mortalities amounted to around R6 million. Losses attributed to reduced production and reproduction (decreased milk and wool production, ill-thrift, poor lambing rate) were not included in this figure but could be expected to be significant (Grosskopf, 1964; Kellerman *et al.*, 1996). More recent annual losses have not been published.

2.2 The genus *Geigeria*

Vermeersiekte is caused by plants belonging to the genus *Geigeria*, a member of the Asteraceae family, and commonly known in South Africa as the vermeerbossies or "vomiting bushes". There are various *Geigeria* species which cause vermeersiekte in ruminants including:

- *G. ornativa* O. Hoffm. (= *G. passerinoides* Harv. = *G. africana* Griess. subsp. *ornativa* [O. Hoffm.] Merxm.).
- *G. aspera* Harv. var. *aspera*.
- *G. burkei* subsp. *burkei* var. *zeyheri* (= *G. zeyheri*).
- *G. burkei* Harv. subsp. *burkei* var. *hirtella* Merxm.
- *G. pectidea*.

Other species such as *G. filifolia, G. acaulis* and *G. obtusifolia*, though not historically associated with the disease, are also considered able to induce vermeersiekte (Botha *et al.*, 1997; Kellerman *et al.*, 2005).

Geigeria ornativa is regarded as the most important species associated with vermeersiekte. It occurs mostly in the drier northern and north-western parts of South Africa, as well as in the neighbouring countries, Namibia and Botswana. Its distribution roughly overlaps outbreaks of the disease (figure 2) and *G. ornativa* therefore causes periodic vermeersiekte in the Northern Cape province (Kellerman *et al.*, 2005). It is an annual or weakly perennial species of on average 100 mm in height, with rough ribbon-like leaves and a typical daisy-like flowerhead (figure 3). The numerous seeds, which can be widely distributed by wind, rain and animals, may lie dormant and viable for up to 13 years. *Geigeria filifolia* is very closely related to *G. ornativa*, such that the two plants can be regarded as the same species (Vahrmeijer, 1981).

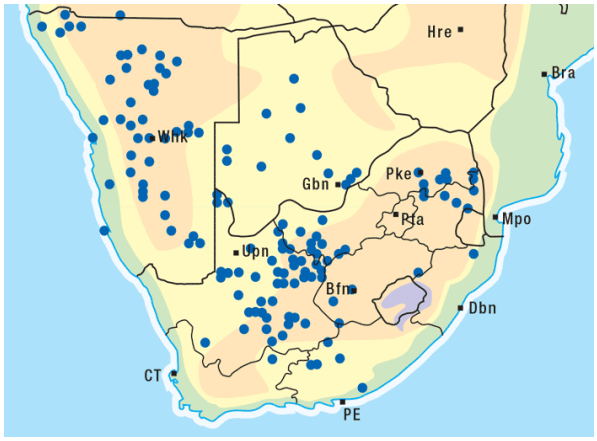

Figure 2: Distribution of Geigeria ornativa *in South Africa. Reproduced from Kellerman* et al.*, 2005.*

Figure 3: Geigeria ornativa.

Geigeria aspera, by contrast, prefers the open savannah and higher rainfall of the highveld (figure 4), causing sporadic problems in parts of Free State and Mpumalanga province (du Toit, 1928; Kellerman et al., 2005). It is described as a slightly woody shrublet of around 200 mm in height, with a perennial root system and weakly perennial aerial parts. The leaves are shorter than *G. ornativa,* but the flower heads are similar (figure 5) (Vahrmeijer, 1981). Whilst *G. aspera* is not as widely distributed as *G. ornativa*, it is estimated to be 10 times more toxic (Kellerman *et al*., 2005).

Several other *Geigeria* species have been associated with vermeersiekte. *Geigeria pectidea* has been incriminated historically in the field and caused minor outbreaks in the Northern Cape (Griqualand West region) (Steyn, 1935; Kellerman *et al.*, 2005). *G. burkei* subsp. *burkei* var. *zeyheri* induced the disease experimentally (Kellerman *et al.*, 2005) and a variety of this plant, *G. burkei* Harv. subsp. *burkei* var. *hirtella* Merxm caused an outbreak in Limpopo province (Botha *et al.*, 1997).

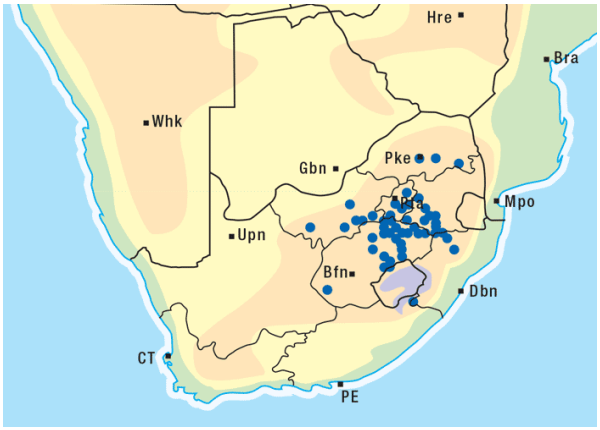

Figure 4: Distribution of Geigeria aspera *in South Africa. Reproduced from Kellerman* et al.*, 2005.*

Figure 5: Geigeria aspera.

Other members of the Asteraceae family have also been implicated in disease outbreaks in small stock that resemble vermeersiekte. In the USA, plants belonging to the genera *Hymenoxys* (bitterweeds) and *Helenium* (sneezeweeds) elicit a similar illness in sheep called "spewing disease" (Hardy, 1931; Schmutz *et al.*, 1974). More recently in South Africa, *Ursinia nana*, a plant known to contain sesquiterpene lactones (Bohlmann and Gupta, 1982), was suspected to have caused vermeersiekte in sheep in the Eastern Cape in camps where *Geigeria* species were found not to grow (Myburgh, 2020).

2.3 Toxicity of *Geigeria* species

The *Geigeria* species have been investigated for their comparative toxicity; *Geigeria aspera* is considered most toxic, 10 times more so than *G. ornativa*. *G. pectida* and *G. burkei* var. *burkei* subsp. *zeyheri* are 3 times more toxic than *G. ornativa* (Rimington, 1936a; Kellerman *et al.*, 2005). Therefore, although most frequently incriminated in disease outbreaks, *G. ornativa* is the least toxic species. Within a species, toxicity can also vary and is purported to depend on season, rainfall, geography, soil

type, stage of growth and whether the plant has been dried or not (du Toit, 1928; Rimington, 1936a; Grosskopf, 1964; Kellerman *et al.*, 2005).

This variation in toxicity is somewhat evident in the literature. In a study by du Toit (1928), as little as 2.3 kg of *G. ornativa* given over 3 days induced toxicity in a sheep, however, in another trial by the same author it took 36.2 kg of the same plant ingested over 42 days to induce disease. Steyn (1935) gave 1.2 kg fresh *G*. *aspera* var. *aspera* to a sheep and induced mortality, but 2.6 kg of dried plant material produced only mild disease in another sheep. Van Heerden *et al*. (1993) reported a variation in latent period of between *c.* 19 – 33 days when sheep ingested 5 g/kg/day of dried, milled flowering *G. ornativa* together with lucerne and dairy meal.

These studies indicate that providing a definitive toxic dose and latent period may be difficult, however, it is generally accepted that animals need to graze on *G. ornativa* for 3 weeks to show toxic effects (Kellerman *et al.*, 2005).

2.4 Clinical picture in ruminants

Vermeersiekte mainly affects sheep, of all breeds, age and sex. Merino and Karakul are most frequently affected, followed by Dorpers, Persians and mixed breeds (du Toit, 1928; Grosskopf, 1964). This variability may relate to differences in grazing habits, nutritional requirements or perhaps farming preference of certain breeds in regions where *Geigeria* plants grow. Sheep with high nutritional requirements such as growing animals, lactating ewes or wool-producers are most at risk (Kellerman *et al.*, 2005).

Vermeersiekte is recognised as occurring in four different clinical forms; (1) regurgitation or 'vomiting', (2) ruminal bloat, (3) stiffness and (4) paralysis. In sheep, which are most susceptible, these forms may manifest in isolation or in combination with each other (du Toit, 1928; Steyn, 1943; Kellerman *et al.*, 2005). The disease has also been recorded in goats, which are more susceptible to the paralytic form, and cattle, where there is a predilection for development of both the stiff and paralytic forms (du Toit, 1928; Steyn, 1943; Grosskopf, 1964). Despite anecdotal claims by farmers, vermeersiekte has not been experimentally demonstrated in horses and donkeys, and has only been infrequently reported in some wildlife species (du Toit, 1928; Grosskopf, 1964).

Clinical disease in sheep is usually noticed days to several weeks after grazing on *Geigeria* spp. Afflicted animals in a flock usually tire easily, lag behind or frequently lie down and develop stiffness in gait. This progresses to weakness and paresis and animals will eventually remain recumbent. If lifted, they

typically tremble and arch their backs before lying down again. Complete paralysis may ensue (Hutcheon, 1893; du Toit, 1928).

Regurgitation of ingesta is often preceded by salivation and may be accompanied by diarrhoea and a cough (Hutcheon, 1893; du Toit, 1928; Steyn, 1943). A greenish staining or ruminal content is often noticed around the mouth and nose and in the upper respiratory tract (figure 6). Affected animals, which may appear otherwise healthy, may demonstrate an episode of regurgitation followed by a return to grazing, though ultimately, they lose body condition (Steyn, 1943). Regurgitation may also be stimulated by drinking or exertion (Hutcheon, 1893; du Toit, 1928). Spasmodic contractions of the oesophagus can also sometimes be observed either immediately after regurgitation or independently of it (Kellerman *et al.*, 2005). A fairly consistent lesion of oesophageal dilatation, diagnosed by neck ballottement or contrast radiography (figure 7), has been described in living animals, even when they do not regurgitate (Pienaar *et al.*, 1973; van Heerden *et al.*, 1993). The cough present is usually due to aspiration of ruminal content and this may progress to pneumonia and mortality (van Heerden *et al.*, 1993).

Figure 6: Sheep afflicted with vermeersiekte showing ruminal regurgitation from the mouth and nose. Photo on the top left courtesy reproduced from Kellerman et al.*, 2005.*

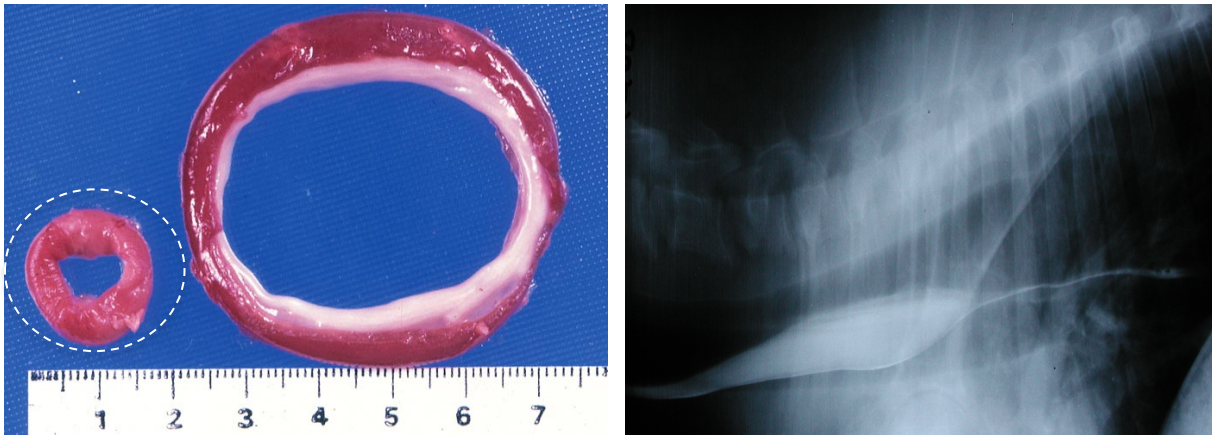

Figure 7: Oesophageal dilatation in a sheep with vermeersiekte.
Left: The oesophagus on the left of this image is normal (white circle, reproduced from J.J. van der Lugt et al, *1993) whilst the oesophagus on the right shows severe mega-oesophagus. Right: Mega-oesophagus demonstrated by radiography, following dosing of barium fluid (reproduced from Snyman* et al., *2008).*

The tympanic form of the disease is rare (du Toit, 1928), however sudden death from bloat, without other usual clinical signs, may result from large intake of plant material (Steyn, 1935).

The aspiration of ruminal content and subsequent foreign body pneumonia is probably the leading cause of death in affected animals and the mortality rate can be as high as 80%. Other causes of death listed in the literature include asphyxiation secondary to choking on ruminal content, and exhaustion/progressive deterioration from chronic regurgitation and diarrhoea (Rimington, 1936a; Steyn, 1943; Grosskopf, 1964). Losses due to direct mortality appear to depend on the length of time grazing on *Geigeria*-infested veld (and therefore perhaps the amount of plant material ingested chronically), nutritional status of the animals, presence of stressors and whether pneumonia develops. Death may occur in only a few days, but pneumonia-affected sheep may take weeks to succumb. Mortality can however be prevented, and the prognosis improves considerably if animals are removed from affected camps (Grosskopf, 1964).

2.5 Pathology and clinical pathology

Pathological changes have been well described in sheep affected by vermeersiekte. The regurgitation form of the disease was previously described as vomiting and was thought to be due to stimulation of chemoreceptors in the central nervous system (CNS), gastrointestinal (GIT) irritation or excessive rumination reflexes (Grosskopf, 1964). It has now been confirmed through radiography, necropsy visualisation of oesophageal dilatation (figure 7) and comprehensive histopathological evaluation, that the condition is due to muscle, rather than CNS pathology (van der Lugt and van Heerden, 1993).

Histopathological changes have been described in both skeletal and cardiac muscle in sheep, as well as in the oesophagus. Light microscopy in one study of muscle and oesophageal tissue, following both

natural and experimental exposure of sheep to *Geigeria ornativa,* demonstrated vacuolisation of randomly affected myocytes/myofibres or groups of muscle fibres. In some of the affected myocytes, the nuclei intruded into the vacuoles and the sarcoplasm was hyalinised (figure 8). In more chronically affected sheep, the muscle fibre size itself varied, with some of the hyalinised fibres being smaller and demonstrating proliferating nuclei (Pienaar *et al.*, 1973). In a later study, oesophageal, skeletal muscle, diaphragm and cardiac tissue from sheep experimentally dosed with *G. ornativa* revealed similar changes; hypertrophy, vacuolisation and necrosis of myofibres (figure 9) (van der Lugt and van Heerden, 1993).

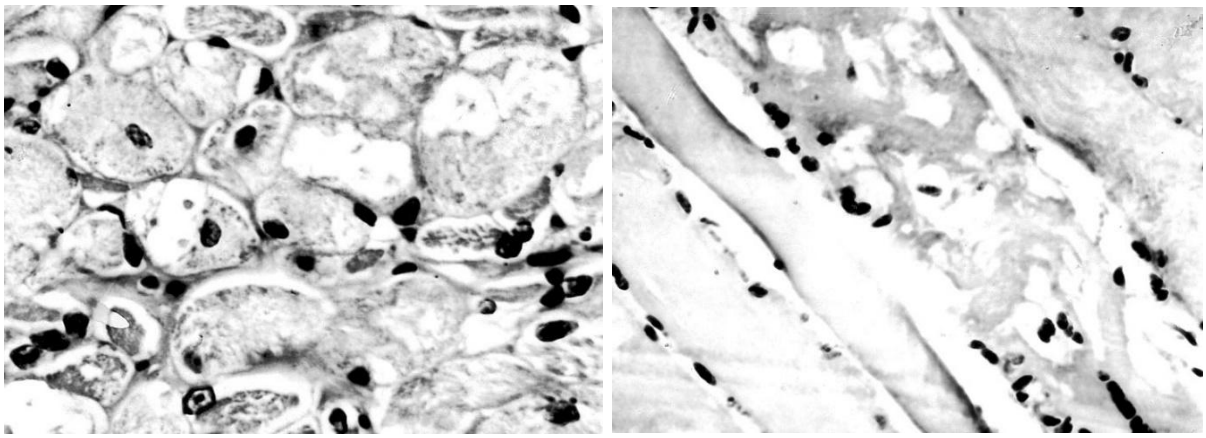

Figure 8: Histopathology of oesophageal and skeletal muscle following Geigeria ornativa *ingestion in a sheep. Muscle fibre vacuolisation and myonuclei centralisation in a transverse section of the oesophagus (left; H&E stain, x 500) and longitudinal section of skeletal muscle (right; H&E, x 200). Reproduced from Pienaar et al., 1973.*

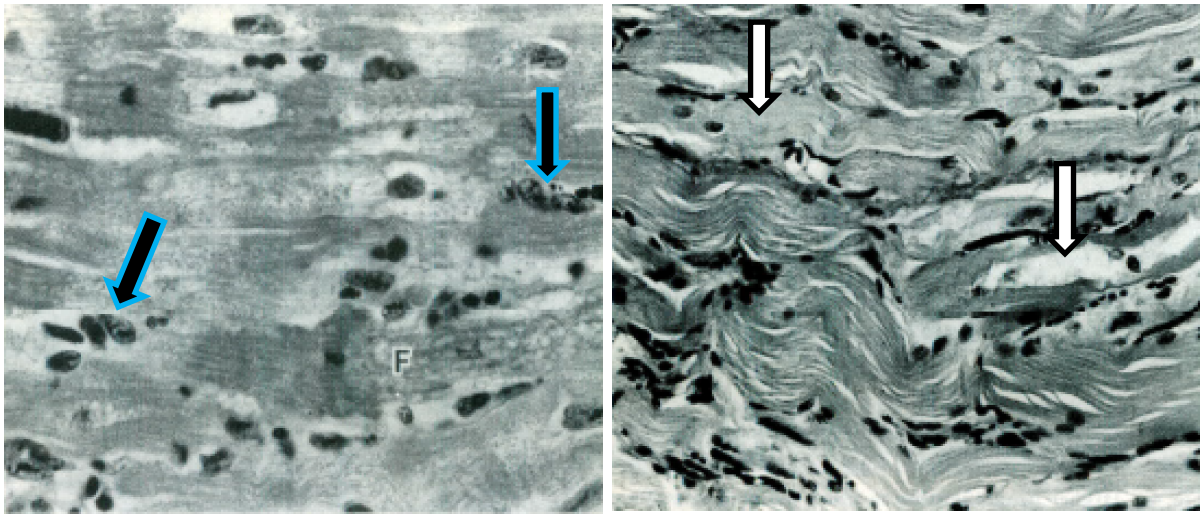

Figure 9: Histopathology of oesophageal and cardiac muscle tissue following Geigeria ornativa *ingestion in a sheep. Left: Vacuolar and myofibrillar disorganisation and sarcolemma nuclear proliferation (black arrows) in oesophageal muscle (H&E, x 200). Right: Left ventricular myocardial necrosis; presence of inflammatory mononuclear cells, vacuolar and granular appearance to myofibers (white arrows), pyknotic nuclei (H&E, x 200). Reproduced from van der Lugt and van Heerden, 1993.*

In both of the above-mentioned studies, ultramicroscopy revealed that the vacuoles observed in histology contained segments of myofibril degeneration within otherwise normal myofibres. In

addition, initial disappearance of the thick myosin myofilaments (with loss of the A-band) was followed by degeneration of the remaining thin actin filaments. In completely degenerate fibres, fine granular material, myofibril remnants and dark Z-line fragments were evident. Swollen and fragmented mitochondria with lysed cristae were also observed (figure 10 and 11) (Pienaar *et al.*, 1973; van der Lugt and van Heerden, 1993).

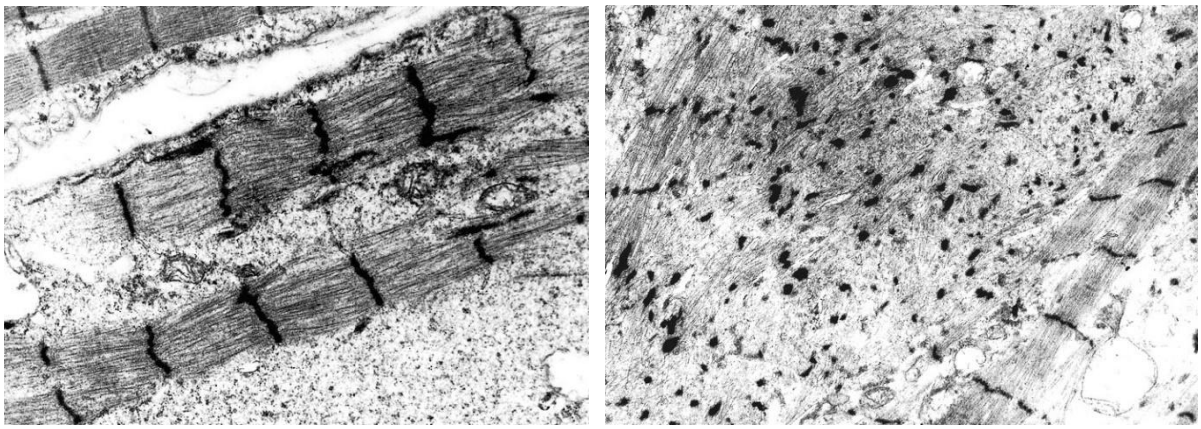

Figure 10: Ultrastructure of skeletal muscle following Geigeria ornativa *ingestion in a sheep.*
Left: Loss of A-band integrity; there is thickening and a tortuous appearance of the Z-line in the lower two myofibrils, compared to the top myofibril (TEM, x 12000). Right: A more severely affected myofibril with complete deterioration of myofibril structure and only clumped, fragmented Z-line components remaining (TEM, x 8000). Reproduced from Pienaar et al, *1973.*

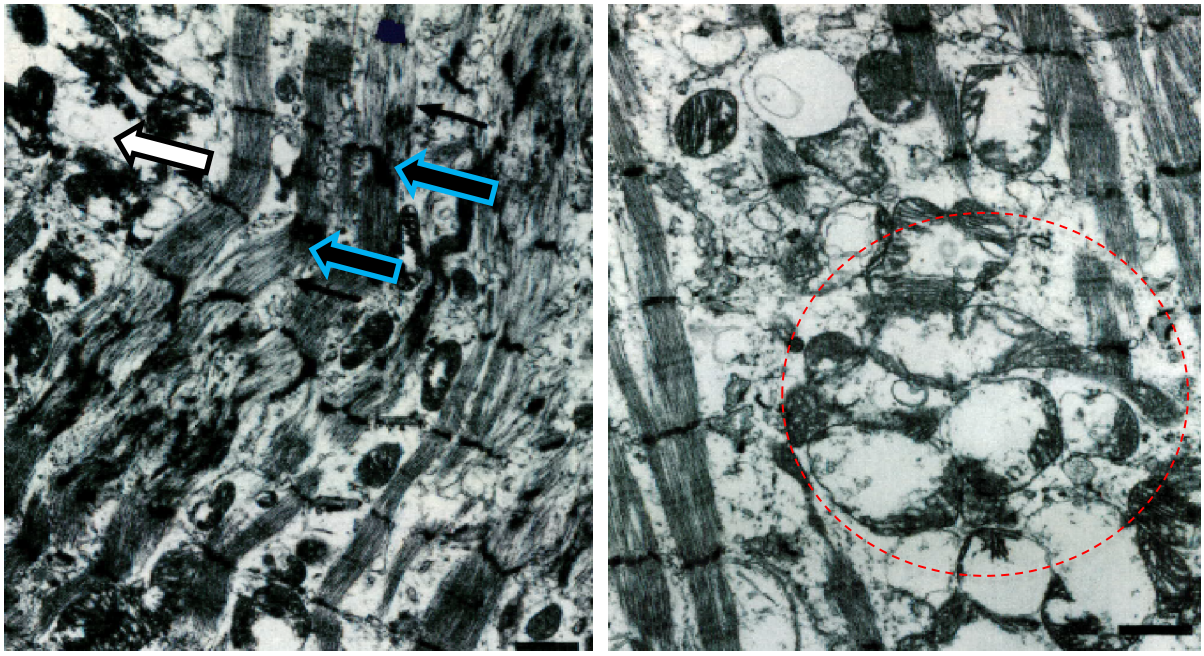

Figure 11: Ultrastructure of cardiac muscle following Geigeria ornativa *ingestion in a sheep.*
Left: Cardiac muscle with early myofibre degeneration; the myofibrils show separation and disruption, loss of thick filaments and focal areas of Z-line thickening and distortion (black arrows). There is some early mitochondrial swelling (white arrow) (TEM, Bar = 1 µm). Right: Mitochondrial swelling, fragmentation, vesiculation and cristae lysis (exhibited by mitochondria in circled area) (TEM, Bar = 1 µm). Reproduced from van der Lugt and van Heerden, 1993.

Hepatic changes have also been reported in sheep with vermeersiekte; hepatocyte degeneration, mild bile duct proliferation and portal triad fibrosis (van der Lugt and van Heerden, 1993). The latter finding may explain the biochemical changes noted by Fourie (unpublished work, 1992, cited by [Kellerman, *et al*., 2005]) of elevated levels of aspartate transaminase (AST) and γ-glutamyl transferase (GGT) in affected sheep. Botha *et al*. (1997) also reported elevated AST, glutamate dehydrogenase (GLDH), GGT, lactate dehydrogenase (LDH) and creatinine kinase (CK) in sheep dosed experimentally with *Geigeria burkei* Harv. subsp. *burkei* var. *hirtella* Merxm (Botha et al., 1997). Though raised AST levels are not specific to liver injury and may reflect concurrent muscle pathology in sheep, raised GGT and GLDH support the pathology findings from the above studies and indicate that the liver is probably also mildly affected by sesquiterpene lactones (Ford, 1974).

2.6 Treating and preventing vermeersiekte in the field

Several therapeutic interventions, including intravenous administration of cysteine and oral supplementation with ethoxyquin, both of which showed potential in treating animals affected by bitterweed ingestion in the USA (Rowe *et al.*, 1980; Kolm, 1984), have unfortunately not been effective in sheep affected by vermeersiekte (Joubert, 1983; Fourie, 1991). Another intervention which has been trialled without success in sheep experimentally dosed with *Geigeria filifolia* is piracetam (*Nootropil®*, UCB Pharmaceutical) (Joubert, 1983). Cognitive aversion to *G. ornativa* has shown promise, though is perhaps less practical to implement in the field, given that continuous exposure to the aversive mixture is required for aversion maintenance (Snyman *et al.*, 2002).

Disease prevention may be of greater benefit, although removal of plants by human intervention is problematic; manual removal is costly and of temporary benefit because of the length of seed survival, hormonal weed killers do not appear to be effective against plants or seeds sheltered by other bushes and parasitic insect biocontrol is unlikely to be of significance (Grosskopf, 1964; Vahrmeijer, 1981; Kellerman *et al.*, 2005).

Currently, the most practical and efficient manner of prevention lies in appropriate grazing management. Since disease outbreaks have been noted to occur where veld vegetation is very poor (Morris, 1945), and as *Geigeria ornativa* cannot maintain itself where vegetation cover is dense [(Schijff, cited by (Grosskopf, 1964)], good agricultural practices (where geographically possible) such as optimal stocking density, correctly placed watering points, rotational grazing and prevention of veld denudement can help prevent outbreaks (Morris, 1945). *G. aspera* is particularly responsive to good veld management as a means of control, as higher rainfall on the South African highveld allows quicker recovery of grass species (Grosskopf, 1964).

It should be noted that *Geigeria ornativa*, when ingested in small amounts, is high in protein and can be nutritious (Grosskopf, 1964). Given that it takes 3 weeks for poisoning to occur (Fourie, 1991; Kellerman *et al.*, 2005), high stocking densities to avoid ingestion of toxic doses in affected camps or rotational tactical grazing of pastures infested with the plants for less than 3 weeks can be applied (Kellerman *et al.*, 2005).

This said, limited understanding of the exact mechanism of toxicity has hampered research into novel preventative and treatment methods. There is furthermore no validated laboratory animal model available and the differences in toxicity between individual sesquiterpene lactones is unknown.

2.7 Current knowledge of vermeersiekte pathophysiology

2.7.1 The sesquiterpene lactones from the *Geigeria* and *Hymenoxys* genus

The active compounds in *Geigeria* spp. are now known to be α, ß-unsaturated-γ-sesquiterpene lactones (Kellerman *et al.*, 2005). Structurally they are mostly C15 compounds (figure 12 and 13). Rimington and Roets first isolated geigerin (figure 12) and its corresponding acid, geigeric acid, from *G. aspera* var *aspera* in 1936 and later that year, what they considered to be the true active principles from the same plant, vermeeric acid and the dilactone vermeerin (Rimington, 1936a; Rimington, 1936b). The structure of geigerin was confirmed in 1958 (Barton and Levisalles, 1958) and its stereochemistry evaluated in 1962 by X-ray analysis (Hamilton *et al.*, 1962). Vermeerin, (but despite several attempts, not vermeeric acid) was re-isolated in 1967 in South Africa from *G. ornativa* (Anderson *et al.*, 1967) and in the US from *Hymenoxys richardsonii* and *H. anthemoides*. The latter two plants cause a similar syndrome to veremeersiekte, 'spewing disease', in sheep in the US (Herz *et al.*, 1970).

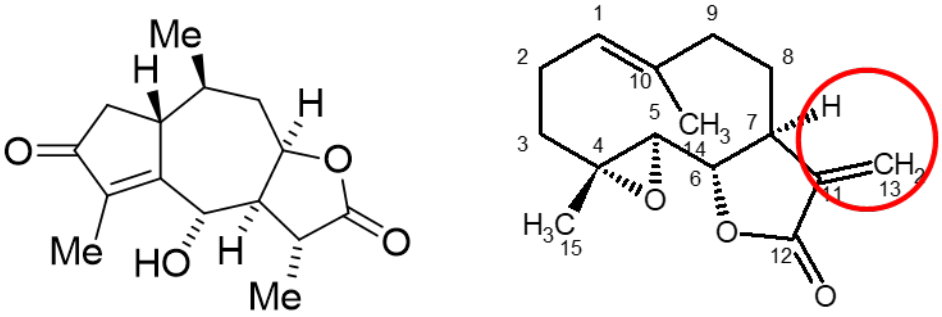

Figure 12: Chemical structure of the sesquiterpene lactones geigerin and parthenolide.
Geigerin (left) and parthenolide (right) (Botha et al., 2017; Botha et al., 2020). Note the absence of the exocyclic α-methylene-γ-lactone double bond at C-11 in geigerin compared to parthenolide (circled).

Other sesquiterpene lactones isolated from *Geigeria* spp include; geigerinin (De Villiers, 1959), gafrinin (de Villiers, 1961; Anderson *et al.*, 1968), griesenin (de Kock *et al.*, 1968), dihydrogriesenin (de Kock *et al.*, 1968; Vermeulen, 1978) and ivalin (figure 13) (Vogelzang *et al.*, 1978; Fouche *et al.*, 2021).

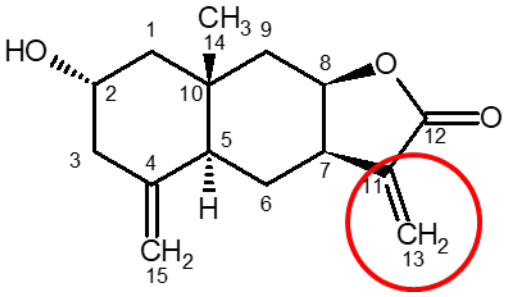

Figure 13: The structure of the sesquiterpene lactone ivalin.
Ivalin also contains an α-methylene-γ-lactone double bond at C-11 (circled) (Fouche et al., 2021).

Sesquiterpene lactones isolated from *Hymenoxys* spp include; floribundin (isolated from *H. richardsonii* and *H. greenei*, native to North America and *H. anthemoides*, native to South America), anthemoidin and themoidin (isolated from *H. anthemoides*), greenein (isolated from *H. greenei*) and hymenoxynin, paucin and hymenolide from *H. odorata*, also native to North America (Herz *et al.*, 1970).

2.7.2 Cytotoxicity of the sesquiterpene lactones

Sesquiterpene lactones form one of the largest groups of cytotoxic compounds of plant origin, appearing in at least 13 genera within the Asteraceae family (Rodriguez *et al.*, 1976), and are described as being cytotoxic to bacteria, fungi, some mammalian parasites, animals and humans (Picman, 1986). In human medicine, they have demonstrated potent anti-tumour properties in human neoplastic cell lines and both the correlation between molecule structure and cytotoxicity, and the mechanisms of toxicity have been investigated (Picman, 1986). Sesquiterpene lactones appear to inhibit tumour growth through a combination of mechanisms including; selective alkylation of key thiol-containing enzymes involved with cell division (Kupchan, 1974), interference with mitotic spindle formation [Bialecki et al (1974) as cited by (Picman, 1986)], inhibition of RNA synthesis (Klimek et al., 1981), inhibition of DNA synthesis and interference with glycolytic and mitochondrial energy processes (Hanson *et al.*, 1970; Hall *et al.*, 1980; Klimek *et al.*, 1981; Woynarowski *et al.*, 1981; Coleman *et al.*, 1984; Caspar *et al.*, 1986; Narasimhan *et al.*, 1989). Parthenolide (figure 12), a commercially available sesquiterpene lactone isolated from the feverfew plant (*Tanacetum parthenium*), has received recent attention as a potential anticancer agent (Gach *et al*., 2015; Chen *et al*., 2016) and studies on this compound suggest additional mechanisms of cytotoxicity such as perturbation of redox balance and protein folding homeostasis (Sun, 2010; Pei and Jordan, 2014).

In respect of vermeersiekte research in veterinary medicine, the cytotoxic effect of various sesquiterpene lactones in animal cell lines has also been evaluated. Murine skeletal myoblast (C2C12) cell lines exposed to varying concentrations of sesquiterpene lactones from *Geigeria aspera* demonstrate EC_{50} values of 3.75 mM, 0.003 mM and 3.8 mM for isogeigerin acetate, ivalin and geigerin, respectively. Thus, ivalin is much more toxic *in vitro* compared to isogeigerin acetate and geigerin (Fouche *et al.*, 2021). Botha *et al*. (2020) reported similar EC_{50} values for ivalin, following exposure of C2C12 cells for 24 – 72 h, of between 2.7 and 3.3 µM (Botha *et al.*, 2020). The EC_{50} values for parthenolide in this study ranged from 4.7 – 5.6 µM (Botha *et al.*, 2020).

Sesquiterpene lactone biological activity and hence toxicity has been ascribed to the double bond exocyclic-methylene group conjugated to the γ-lactone of the carbocyclic skeleton (figure 14). Furthermore, the presence of a functional group such as an epoxide or hydroxyl group, enhances the conjugated lactone reactivity (Rodriguez *et al.*, 1976). This may account for the difference in *in vitro* toxicity of ivalin and parthenolide, both of which contain an exocyclic-methylene group (figure 12 and 13), compared to isogeigerin and geigerin, which do not. Thus ivalin is approximately 1000 times more toxic than isogeigerin and geigerin but only twice as toxic as parthenolide (Botha *et al.*, 2020).

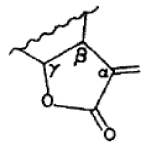

Figure 14: The α-methylene-γ-lactone group, thought to be responsible for biological activity in sesquiterpene lactones. This group is a major functional group for biological activity and hence toxicity.

2.7.3 Sesquiterpene lactone effect on cytoskeletal components

The exact cellular mechanism of sesquiterpene lactone muscle toxicity in vermeersiekte has not been fully elucidated, though recent *in vitro* studies have indicated that damage to the cell cytoskeleton could be involved (Botha *et al.*, 2019; Botha *et al.*, 2020). The cytoskeleton is comprised of 3 major polymers: actin microfilaments, microtubules, and intermediate filaments. In brief, their major functions include spatial organisation of intracellular content, transmission of mechanical and biochemical information from the microenvironment to the cell and coordinating cell movement and shape change (Fletcher and Mullins, 2010).

To evaluate the effect on cytoskeletal proteins and filaments, Botha *et al.* (2019) exposed desmin-expressing murine myoblasts (C2C12) to different concentrations of geigerin for 24, 48 and 72 h and evaluated cellular response using desmin immunocytochemistry staining. Other cytoskeletal proteins which were evaluated using this technique included synemin (previously called desmuslin) and alpha-

β-crystallin. Desmin is the major muscle-specific intermediate cytoskeletal filament. It is mainly expressed in striated (including cardiac) muscle, but is also present in smooth muscle, and plays an important role in maintaining the cytoskeletal architecture (Paulin and Li, 2004; Mermelstein *et al.*, 2005; Costa, 2014). Synemin is an intermediate filament which co-polymerizes with desmin at the Z-line in striated muscle and therefore also provides structural support (Mizuno *et al.*, 2001). Alpha-β-crystallin is a small chaperone heat shock protein which has cellular house-keeping roles such as preventing desmin aggregation during stress-induced muscle damage (Dubińska-Magiera *et al.*, 2014). Two other cytoskeletal elements, β-tubulin and F-actin were also evaluated in this study using fluorescence staining.

Botha *et al.* (2019) observed a concentration-dependent cytotoxic response under light microscopy, evidenced by disorganisation and dot-like perinuclear aggregation of desmin filaments in the cells. β-tubulin, F-actin and the other desmin-associated proteins (α-β -crystallin and synemin) were unaffected (figure 15) (Botha *et al.*, 2019).

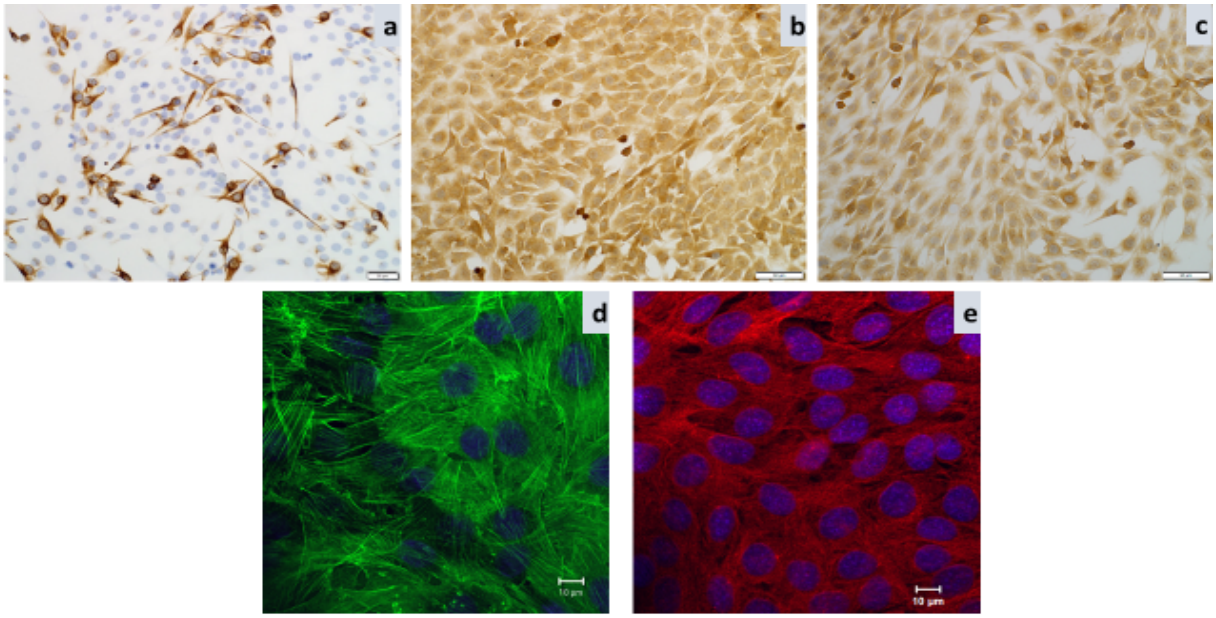

Figure 15: Effect of exposure of C2C12 myoblasts to 2.5 mM geigerin for 48 h.
Comparison of immunocytochemical staining for desmin (a), synemin (b) and αB-crystallin (c) x 20 (bar = 50 µm) and immunofluorescence staining for F-actin (d) and β-tubulin (e) x 63 (bar 10 µm) (Botha et al., 2019).

In a second study, Botha *et al*. (2020) confirmed that ivalin and parthenolide also induced disorganisation, aggregation and a decrease of desmin intermediate filaments following exposure of C2C12 myoblasts (figure 16).

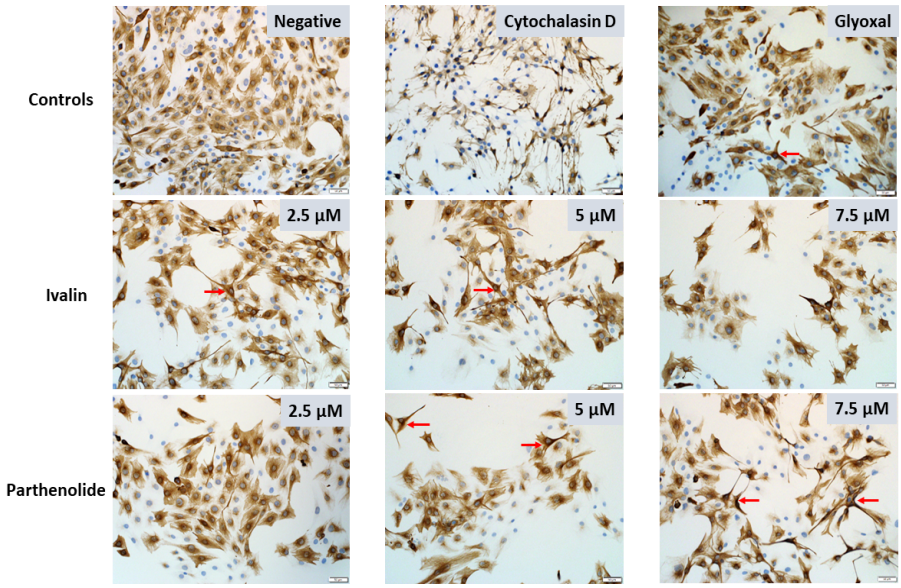

Figure 16: Desmin immunocytochemistry following exposure of C2C12 myoblasts to 2.5, 5 and 7.5 µM ivalin and parthenolide for 24 h.
Condensed, contracted desmin forming stellate-like cells (red arrows). Cytochalasin D (20 µM) and glyoxal (10 mM) were used as positive controls x 20 (bar = 50 µm) (Botha et al., 2020).

In myocytes, desmin forms a three-dimensional 'net-like' extra-sarcomeric scaffold that connects the contractile apparatus with the subsarcolemmal cytoskeleton as well as the nuclei and other cytoplasmic organelles, including the mitochondria (Paulin and Li, 2004; Mermelstein *et al.*, 2005; Costa, 2014) (figure 17). Desmin is anchored to costameres (connections linking the sarcomere and sarcolemma) present on the sarcolemma, by synemin and another protein, syncoilin (Capetanaki, 2002; Paulin and Li, 2004; Costa, 2014; Paul and Skalli, 2016).

Desmin is most abundant in cardiac myocytes, particularly at the intercalated disks, where it may play a role in force generation (Paulin and Li, 2004). It is also abundant at the myotendinous and neuromuscular junctions of skeletal muscles and in the smooth muscle of the elastic aorta, where it is required to maintain vascular tone and ensure blood supply (Paulin and Li, 2004). More recently, it was concluded that desmin plays a role in the regulation of proteostasis and muscle size, as well as during muscle atrophy (Agnetti *et al.*, 2022).

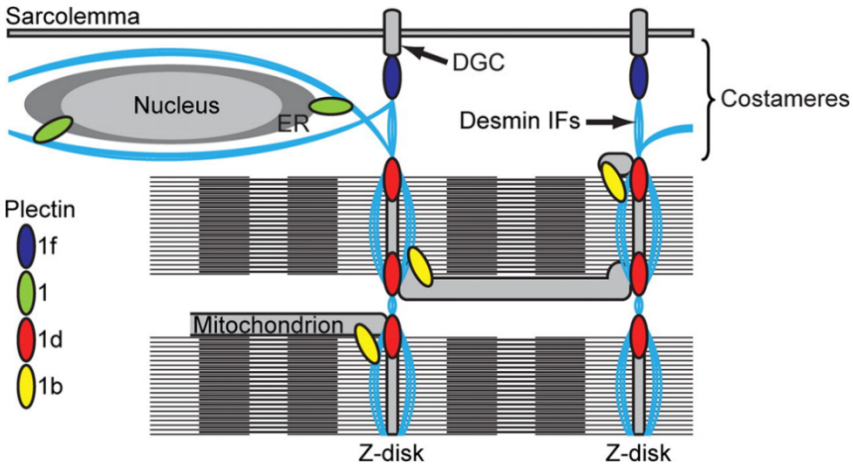

Figure 17: Schematic presentation of skeletal muscle desmin intermediate filaments and associated proteins. Desmin, shown in pale blue, connects the contractile apparatus to the dystrophin-glycoprotein complex (DGC) component of the costameres at the sarcolemma, via the Z-disks (Z-lines). Desmin strands can be crosslinked to each other, as well as to other cytoskeletal elements by proteins called plectins. In this schematic, 4 major plectins, 1d, 1f, 1b and 1 link desmin with the Z-disks (Z-lines), costameres, mitochondria and outer nuclear/endoplasmic reticulum (ER) membranes, respectively. (Konieczny, 2008; Fletcher and Mullins, 2010; Agnetti et al*., 2022). Image reproduced from Konieczny* et al*, 2008.*

Desmin is also known to interact with cellular organelles; it connects the extracellular matrix with the nuclear matrix and may be involved with mechanochemical signalling between the two compartments, as well as in gene expression activity (Capetanaki, 2002). Mitochondria are particularly linked structurally to desmin, and this appears to be crucial in optimising energy production; disruption of this spatial arrangement is a feature of muscle dysfunction secondary to desmin mutations, misfoldings or losses (Agnetti *et al.*, 2022). The exact mechanism of desmin-mitochondria interaction remains elusive but may involve; stabilisation of mitochondrial position, influence over mitochondrial membrane function, involvement with mitochondrial-endoplasmic/sarcoplasmic reticulum communication, control of mitochondrial fusion-fission or stabilisation of specific functional complexes within the mitochondria (Capetanaki, 2002).

Botha *et al.* (2019 and 2020) therefore proposed that the disorganisation and aggregation of desmin following exposure to increasing geigerin, ivalin and parthenolide concentrations was significant and could explain some of the striated muscle lesions observed in vermeersiekte (Botha *et al.*, 2019; Botha *et al.*, 2020). As desmin is concentrated mainly at the Z-lines of striated myofibres (Paulin and Li, 2004; Costa, 2014), the disorganisation and destruction of desmin could explain some of the Z-line abnormalities (thickening, zigzagging, fragmentation and clumping) that have been reported at the electron microscopic level in *Geigeria*-poisoned sheep (Pienaar *et al.*, 1973; van der Lugt and van Heerden, 1993). Furthermore, they postulated that given the role desmin plays in mitochondrial location and functioning, sesquiterpene lactone-induced desmin loss and disorganisation could contribute to energy deficiency within the cell.

2.7.4 Clinical effects of desmin abnormalities in mice

Studies on desmin-null mice support the hypothesis that muscle lesions observed following exposure to sesquiterpene lactones are due to desmin disruption and mitochondrial dysfunction. Though these animals appeared to develop normally *in utero*, the effects become noticeable after birth and are most pronounced in the heart. In brief, these animals develop dilated cardiomyopathy and heart failure with extensive cardiac calcification and fibrosis. Ultrastructurally, there is Z-line streaming, hypercontraction, and myofibril disorganisation. The intercalated disks appear abnormal, with slender elongated points of contact. There are also altered sarcolemmal elements, including fewer desmosomes, the point of intermediate filament attachment (Milner *et al.*, 1996; Thornell *et al.*, 1997; Milner *et al.*, 2000; Paulin and Li, 2004).

Regarding mitochondria, the microtubule-dependent molecular motor, kinesin, appears to lose its anatomical association with mitochondria and there is depletion of mitochondrial enzyme cytochrome c levels, but increased creatinine kinase activity. Mitochondria appear swollen, vacuolated, have reduced cristae density and tend to proliferate after work overload (Milner *et al.*, 2000). Paulin *et al.* (2004) evaluated these studies and proposed that desmin disorganisation disrupts kinesis and other microtubular elements associated with mitochondria, affecting their positioning in specific subcellular domains in the heart and leading to insufficient ATP for contraction. This results in increased creatinine kinase activity and mitochondrial proliferation and might account for cardiomyocyte degeneration and calcification through apoptotic signalling (Paulin and Li, 2004).

Pertaining to skeletal muscle, desmin-deficient mice demonstrate muscle weakness and quick fatigue. On ultramicroscopic evaluation, there is abnormal clumping and degeneration of subsarcolemmal mitochondria, irregular myofibril organisation, and Z-line streaming (Thornell *et al.*, 1997; Milner *et al.*, 2000; Paulin and Li, 2004). Other studies have demonstrated a loss of myofibrillar attachment to the sarcolemma at the costamere (O'Neill *et al.*, 2002), adipocyte accumulation and neuromuscular junction disorganisation with postjunctional folded forms (Agbulut *et al.*, 2001).

2.7.5 Sesquiterpene lactone interference with mitochondrial biochemistry

Aside from their effects on desmin, and which may indirectly affect mitochondrial functioning, the sesquiterpene lactones are also known from antineoplastic research to interfere directly with glycolytic and mitochondrial energy processes (Hanson *et al.*, 1970; Hall *et al.*, 1980; Klimek *et al.*, 1981; Woynarowski *et al.*, 1981; Coleman *et al.*, 1984; Caspar *et al.*, 1986; Narasimhan *et al.*, 1989). Furthermore, van Aswegen (1979) conducted *in vitro* studies using extracts from *Geigeria* spp and guinea pig liver mitochondria incubated in hexokinase. Oxygen consumption and inorganic

phosphorus (Pi), trapped as glucose-6-phosphate, were measured following sesquiterpene lactone exposure. Compared to the control, mitochondria incubated with 1 mM of a sesquiterpene lactone containing an α-methylene-γ-lactone, i.e., ivalin and dihydrogriesenin, demonstrated inhibition of oxygen and Pi consumption by up to 40%. In contrast, compounds where this bond was either not present (geigerin) or reduced (dihydroivalin and tetrahydrogriesenin), inhibited oxygen and Pi consumption by only 10% (van Aswegen., 1979). This is consistent with the *in vitro* findings of Rodriguez *et al.* (1976) and Botha *et al.* (2020) that biological activity of these compounds is driven by the presence of the α-methylene-γ-lactone functional group.

In a second study, van Aswegen *et al*. (1982) were able to demonstrate that the site of mitochondrial disruption by sesquiterpene lactones from *Geigeria* spp were complexes I and II, as well as the choline dehydrogenase complex of the respiratory chain. These compounds may also be weak uncouplers of oxidative phosphorylation (van Aswegen *et al*., 1982). These two studies, in conjunction with the proposed effects from desmin disruption, therefore intimate that the overall effects of sesquiterpene lactones on energy production within the cell could be significant.

2.8 Sesquiterpene lactone *in vivo* domestic animal toxicity studies

Individually extracted sesquiterpene lactones have previously demonstrated *in vivo* toxicity in both domestic and laboratory mammals, though the results have been equivocal (table 1). Though neither vermeeric acid nor geigerin appear to affect rabbits, vermeeric acid was acutely lethal to frogs. The doses used in these studies is unknown (Rimington, 1936a; Rimington, 1936b). Carnivores appear to develop gastrointestinal sensitivity, nausea and vomiting following oral exposure to vermeeric acid and geigerin. This is supported by necropsy findings of mild gastritis in these animals (Rimington, 1936a; Grosskopf, 1964). Geigerin, given at 1 g subcutaneously in a cat has also reportedly produced mild systemic toxicity (anorexia and listlessness) (Rimington, 1936a).

In sheep, the results of oral exposure to sesquiterpene lactones or *Geigeria* extracts has also been equivocal. Ten to 15 g of vermeeric acid given orally in sheep caused acute death in 5 to 24 hours (Rimington, 1936b) but in another study by the same authors, the same dose of geigerin produced no effect (Rimington, 1936a). In a personal communication, Adelaar (1956) reported to Grosskopf (1964) that when sheep were dosed with a *G. aspera* extract in 16% alcohol, some animals showed no effects, others mild ruminal dysfunction, whilst in a few animals, clinical signs consistent with vermeersiekte developed. Some animals also succumbed (table 1) (Grosskopf, 1964). What is apparent is the variation in response among animals and lack of correlation to dose. Interestingly, acute death without classical signs of vermeersiekte has also been recorded in sheep fed plant material; in an older

study, when fed exclusively on *Geigeria* plants, toxicity was induced in sheep in as little as 4 days. In some of these experiments, sheep died acutely without developing regurgitation or stiffness (du Toit, 1928).

It is also appreciable from these early studies that considerable amounts of plant extract are required to conduct toxicity studies in the species of interest. Grosskopf (1964) noted that 200 g of plant extract was needed to produce 1 g of extract, before isolation of individual compounds. The need for laboratory rodent models is therefore evident, in order to test isolated fractions of plant extract for toxicity and to explore toxic mechanism of action.

2.9 Sesquiterpene lactone *in vivo* laboratory animal toxicity studies

Early *in vivo* work has been reported in rodents (table 1). Ivalin was reported as toxic to guinea pigs at a dose of 0.25 g/kg when given subcutaneously (Coleman *et al.*, 1984). Similarly, dihydrogriesenin and geigerinin were found to be toxic to guinea pigs and mice at 0.25 g/kg, also when given subcutaneously. Neurological strychnine-like effects were noted (Vermeulen, 1978). In rats, variable responses to *Geigeria* extract have been noted (table 1) (Grosskopf, 1964). Median lethality of sesquiterpene lactones from *Geigeria* spp has however not been determined in rodents, nor has the mechanism of toxicity and its correlation with vermeersiekte in ruminants been explored.

Table 1: In vivo *studies evaluating clinical effects of sesquiterpene lactone extracts in domestic and laboratory animals.*

Sesquiterpene lactone	Animal	Dose (g) or dosage (g/kg BW)	Effect	Reference
Vermeeric acid	Rabbits	0.08 g	None	(Rimington, 1936b)
	Frogs	0.05 g, dorsal lymph sac	Paralysis, respiratory distress, mortality in 1 h	(Rimington, 1936b)
	Sheep (n = 1)	10 to 15 g PO	Stiffness, vomiting within 8 h Mortality in 40 h	(Rimington, 1936b)
Geigerin	Cat (n = 1)	0.1 g SC	Partial anorexia for 24 h, then recovery	(Rimington, 1936a)
	Cat (n = 1)	1 g PO	Vomiting, depression and anorexia prior to sacrifice at 24 h for necropsy	(Rimington, 1936a)
	Rabbits (n = 1)	0.13 g/kg PO	None	(Rimington, 1936a)
	Sheep (n = 1)	15 g over 2 days PO	None	(Rimington, 1936a)
***Geigeria aspera* extract in 16% alcohol**	Sheep (n = 1)	64 g over 16 days PO	Weakness, anorexia, regurgitation on day 29	Adelaar (1956) as cited by (Grosskopf, 1964)
	Sheep (n = 1)	48 g over 3 days PO	Died 2 h after last dosing	Adelaar (1956) as cited by (Grosskopf, 1964)
	Sheep (n = 1)	160 g over 10 days PO	Paresis, weakness, died on day 10	Adelaar (1956) as cited by (Grosskopf, 1964)
	Sheep (n = 1)	224 g over 14 days PO	None	Adelaar (1956) as cited by (Grosskopf, 1964)
	Sheep (n = 1)	80 g over 5 days PO	None	Adelaar (1956) as cited by (Grosskopf, 1964)
	Sheep (n = 1)	528 g over 24 days PO	Decrease in ruminal movements only	Adelaar (1956) as cited by (Grosskopf, 1964)
	Rat	6 g PO (daily, but duration of exposure not disclosed)	None	Myburgh (1956) as cited by (Grosskopf, 1964)
	Rats (n = 3)	0.2 g, 0.4 g, 0.6 g to one rat each	None	Minne (1956) as cited by (Grosskopf, 1964)
	Rats (n = 2)	4 g/kg	Died	Minne (1956) as cited by (Grosskopf, 1964)

***Geigeria aspera* fractions, including geigerin**	Cat	Not disclosed	Nausea and vomition, some deaths (not specific)	Adelaar (1956) as cited by (Grosskopf, 1964)
	Dogs (n = 2)	Not disclosed	Vomition	Adelaar (1956) as cited by (Grosskopf, 1964)
Ivalin	Guinea pigs	0.25 g/kg SC	Reported as toxic, but not lethal	(Coleman *et al.*, 1984)
Dihydrogriesenin and geigerinin	Guinea pigs and mice	0.25 g/kg SC	Reported as toxic, but not lethal	(Vermeulen, 1978)

Sample size, dose/dosage and route of exposure is included, where known. PO = per os, SC =subcutaneously.

2.10 Laboratory animal models in toxicology

In vivo laboratory animal models are regarded as key in biomedical research, including in veterinary toxicology. They contribute significantly to understanding of toxicity, toxicokinetics, mechanisms of disease, as well as in investigating prophylactic and therapeutic interventions. Laboratory animal models are often more cost effective than using the naturally affected veterinary species and the amount of toxic compound required to induce a toxicosis is significantly reduced (Domínguez-Oliva *et al.*, 2023).

To ensure that results obtained are extrapolatable to affected domestic animal species, a laboratory animal model needs to be chosen with consideration of anatomical and physiological features. This can make selecting a target species for ruminants difficult. However, despite being monogastrics, rodents remain the most accessible and affordable laboratory animal species employed in toxicity research (Makowska and Weary, 2021). Furthermore, the entire oesophagus in both mice and rats is striated, as in ruminants (McInnes *et al.,* 2017).

The Organisation for Economic Co-operation and Development (OECD) serves to provide a knowledge hub for internationally recognised and best-practice guidelines and policies. These include for toxicity testing in rodent models. Traditional acute toxicity testing guidelines, such as that described in the now deleted Test Guideline (TG) 401 in rodents, made use of lethality as the endpoint. Typically, 4 to 5 dosages were used, with 5 male and 5 female animals per group, thus a total of 40 to 50 animals (OECD, 1987). For animal welfare reasons, this has now fallen out of favour in the scientific community and the OECD provides 3 alternative designs for assessing toxicity of compounds in rodents. The most animal-friendly of these and which allows for estimation of lethality, sometimes with confidence intervals, is Test Guideline 425 (OECD, 2022).

2.11 The acute oral up-and-down toxicity procedure in rodents

TG 425 is based on the procedure from Bruce (1985), as adopted by the American Standard for Testing and Materials in 1990 (Bruce, 1985; ASTM, 1987). The value of this guideline is the small number of animals involved, estimation of median lethal dose (LD_{50}) with confidence intervals, provisions for observation of toxicity and collection of samples.

As the name suggests, the main test in TG 425 consists of single animal dosing in ordered progression, with a minimum time interval between dosing of 48 h. The first animal is dosed

based on the best available estimation of the LD_{50}. If it survives, the next animal is dosed lower by a specific numerical factor. If the animal dies, the next animal is dosed higher by the same numerical factor. This factor is calculated from the slope of a previous dose-response curve, if available. If either the LD_{50} or dose response curve is unknown, a default value of 175 mg/kg and 3.2 respectively, can be used. A combination of stopping criteria is used to halt testing immediately when an LD_{50} can be calculated and therefore to minimise animal wastage and suffering. The LD_{50} value is calculated using the maximum likelihood estimation method (OECD, 2022).

2.12 Purpose and benefits of the research

For this project, an initial pilot study in CD-1 mice was conducted, using doses described in the literature as being toxic, but not lethal, to mice and guinea pigs (Vermeulen, 1978; Coleman *et al.*, 1984). The mice study was designed to evaluate the effect of ivalin, extracted from *Geigeria aspera*, on murine skeletal muscle desmin. A follow-up study using Sprague-Dawley rats, conducted according to OECD TG 425 guidelines, was designed to assess desmin pathology in a second species and to validate an LD_{50} for future research in rodents and sheep.

3 MATERIALS AND METHOD

3.1 Study Design

Two separate studies were conducted in 2 species of rodents: CD-1 mice (*Mus musculus*) and Sprague-Dawley rats (*Rattus norwegicus*).

3.1.1 CD-1 mice

An *in vivo* randomised and controlled study using 24 mice, randomly allocated to 4 groups.

- Group 1: Ivalin (175 mg/kg BW) in vehicle
- Group 2: Ivalin (250 mg/kg BW) in vehicle
- Group 3: Ivalin (325 mg/kg BW) in vehicle
- Control group: Vehicle only

The vehicle used was polyethylene glycol 400 (PEG 400).

3.1.2 Sprague-Dawley rats

An *in vivo* study model, according to the global gold-standard OECD guidelines for toxicity testing in animals.

The study design used is detailed in OECD Test Guideline (TG) 425 for Acute Oral Toxicity in rodents, otherwise known as the "Up-and-Down Procedure" or UDP (OECD, 2022). The Main Test from OECD TG 425 was used.

Animals were dosed with ivalin one at a time, in a stepwise fashion, at a minimum of 48 hourly intervals. The first animal received a dose 1 dose-step below the best estimate of the LD_{50}. In this instance, the LD_{50} was estimated using Hill's modelling from the study described in 6.1.1 above in CD-1 mice at 164 mg/kg BW (see 7.2.1 below). If the animal survived, the dose for the next animal was increased by a dose-step and conversely if the animal died, the dose for the next animal was decreased by a dose-step.

The dose-step for this study was chosen, according to TG 425, as the antilog of (1/slope), where the slope was set at a fairly steep factor of 8, because of acute toxicity of the ivalin molecule in CD-1 mice in the study described in 6.1.1 above. TG 425 makes provision to extend the inter-dosing interval beyond 48 h if there is concern that the toxin will cause death in more than 48 h and this provision was utilised (see 6.3.2.2 below).

In the OECD TG 425, a combination of stopping criteria is used to keep the number of animals low. The study stops when the first of the following 3 stopping criteria is met:

1. 3 consecutive animals survive the upper bound dose*.
2. 4 reversals occur in any of 6 consecutive animals tested*.
3. At least 4 animals have followed the first reversal, and the specific likelihood-ratios exceed the critical value*

***Upper bound dose:** The upper bound dose is either 2000 or 5000 mg/kg BW and is only applicable for low toxicity molecules. This was not expected to be the case with ivalin.

Reversal: A situation where a non-response (survival) is observed at a dose, followed by a response (mortality) at the next dose tested, or *vice versa*. A reversal is therefore created by an opposite pair of responses.

Specific likelihood-ratio: A likelihood is a statistical measure of how strongly the data support an estimate of the LD_{50}. Ratios of likelihood values are determined and checked against a critical value. If the likelihood values exceed the critical value, dosing stops and the LD_{50} can be estimated.

The stopping criteria also reduce the effect of an inaccurate starting value, which in this case was an estimate. When the first stopping point is reached, the LD_{50} and if possible, a confidence interval is calculated (OECD, 2022).

A control group (n = 5) was used to monitor the health and husbandry of test rats to ensure that the ability of the study to provide reliable results was not compromised and to provide control samples for analysis. TG 425 stipulates that more than 10% mortality in the control group invalidates the study. No additional control rats were added during the study.

3.2 Animals

3.2.1 Animal Ethics Approval

The study protocols were both approved by the University of Pretoria Animal Ethics Committee and the Faculty of Veterinary Science Research Ethics Committee under the following project numbers:

CD-1 mice: REC 068-21

Sprague-Dawley rats: REC 038-23

3.2.2 Animal procurement, acclimatisation and preparation

3.2.2.1 CD-1 Mice

Twenty-four outbred mice (female, 10 weeks, weighing approximately 30 – 35 g) were purchased from Onderstepoort Biological Products (OBP, Onderstepoort, Pretoria) and transported to the Onderstepoort Veterinary Animal Research Unit (OVARU). Mice were clinically examined for abnormalities or disease, randomly assigned to a study group (see 6.3.2.1 below) and then ear-notched for identification. One animal, mouse 5, had a healed tail injury, but was otherwise healthy. Mice were treated topically with ivermectin for parasite control. Following this, a 14-day observation and acclimatisation period was allowed. Mice were weighed again on day 10 and treated with ivermectin again on day 12 of the acclimatisation period, respectively.

3.2.2.2 Sprague-Dawley Rats

Fifteen outbred Sprague-Dawley rats (female, 6 weeks, weighing approximately 200 g) were purchased from South African Vaccine Producers (SAVP, Sandringham, Johannesburg) and transported to the Onderstepoort Veterinary Animal Research Unit (OVARU). Rats were clinically examined for abnormalities or disease, randomly assigned to a study group (see

6.3.2.2 below) and ear-notched for identification. They were also treated topically with ivermectin for parasite control. Following this, a 14-day observation and acclimatisation period was allowed. Rats were weighed again on day 10 and treated with ivermectin again on day 12 of the acclimatisation period, respectively.

3.2.3 Housing and care

CD-1 mice and rats were housed in the rodent unit at the OVARU for the full duration of the study, according to document SOP 0193. The rodent housing uses Type II Tecniplast and Type II 1284L Tecniplast rodent cages, housing a maximum of 3 mice and 3 rats per cage, respectively. Rodent cages are transparent, and animals were kept together for visual social interaction between cages (figure 18). Room temperature was maintained at 22 – 24 °C. Relative humidity was maintained between 40 and 60%. Lighting was artificial with the photoperiod set at 12 h light/ 12 h dark.

The mice and rats were weighed individually on the second day of arrival and then weekly until the start of the study. After administration of the compounds, they were weighed every second day, or as needed.

A commercial brand of food, irradiated EPOL rodent pellet, was fed *ad libitum*. Mice and rats had access to unlimited supply of reverse osmosis purified water. Autoclaved rodent houses, sawdust bedding (mice), sawdust shavings (rats), paper tissues, toilet roll inners, fresh hay, wooden sticks and egg containers were used as environmental enrichment.

The animals were attended to twice daily by OVARU staff members and at least daily by a laboratory animal veterinarian. The facility makes use of a simple biosecurity protocol, whereby persons entering change into surgical scrubs (provided and laundered on site) or make use of clean laboratory coats and wear impermeable boots or shoe covers. Footbaths with F10 disinfectant are provided on entry and latex gloves are worn at all times.

Figure 18: Rodent Tecniplast housing in the OVARU.
Left: Sprague-Dawley rats. Right: CD-1 mice.

3.3 Dosing

3.3.1 Ivalin preparation

Ivalin, extracted from *Geigeria aspera*, was already available in the Natural Toxin Collection of the Section of Pharmacology and Toxicology, Department of Paraclinical Sciences. Polyethylene glycol (PEG 400) was purchased from the Onderstepoort Veterinary Academic Hospital (OVAH) pharmacy and sterile-filtered.

Ivalin was weighed, according to the individual animal weight prior to dosing, using a Mettler AT250 (Mettler Toledo, Ohio, USA) scale and dissolved into 0.2 ml PEG 400 vehicle for the mice and 0.5 ml PEG 400 vehicle for the rats, in a sterile 2 ml Eppendorf tube. Complete dissolution was facilitated by Vortex agitation (Heathrow Scientific, Illinois, USA) and a heated water bath (37° C). An additional 0.1 ml of sterile water was added to the prepared ivalin solutions to reduce viscosity for ease of parental administration. The solutions were drawn-up into 1 ml syringes for dosing.

3.3.2 Dose groups and administration of ivalin

3.3.2.1 CD-1 Mice

Mice were randomly assigned by a manual random lottery method to a study group and cage upon arrival so that the acclimatisation period also allowed for social development. Mice were then ear-notched according to their dosing group placement and cage (see table 2).

Table 2: Mouse ID numbers per study group and group ivalin dose.

Study group	Mice numbers and cage allocation	Ivalin dose per mouse
1 (exposed)	1 – 3 (cage 1) 4 – 6 (cage 2)	175 mg/kg in PEG 400
2 (exposed)	8 – 9 (cage 3) 10 – 12 (cage 4)	250 mg/kg in PEG 400
3 (exposed)	13 – 15 (cage 5) 16 – 18 (cage 6)	325 mg/kg in PEG 400
4 (control)	19 – 21 (cage 7) 22 – 24 (Cage 8)	PEG 400 only

Following the acclimatisation period of 14 days, on Day 1 of the study, mice were weighed first thing in the morning and the dose of ivalin per individual animal calculated. The individually labelled ivalin solutions were then prepared as described above in 6.3.1 and injected in the relevant animal, subcutaneously between the scapulae, using a 25-gauge needle and 1 ml syringe.

3.3.2.2 Sprague-Dawley Rats

Rats were randomly assigned to a study group upon arrival so that the acclimatisation period also allowed for social development. Rats were then ear-notched according to their dosing group placement (see table 3).

Table 3: Rat ID numbers per study group.

Study group	Rat numbers	Treatment
Exposed animals	1 – 2 (cage 1) 3 – 4 (cage 2) 5 – 6 (cage 3) 7 – 8 (cage 4) 9 – 10 (cage 5)	Ivalin in PEG 400, according to OECD TG 425
Control animals	11 – 12 (cage 6) 13 – 15 (cage 7)	PEG 400

As discussed in 6.1.2, animals were dosed with ivalin one at a time, in a step-wise fashion, according to table 4. Rats were injected subcutaneously between the scapulae using a 23-gauge needle and 1 ml syringe. Initially the time between dosing was set at 48 h, as prescribed

by the OECD guidelines (OECD, 2022). However, rat 1 did not die acutely, rather deteriorated chronically over 4 days before being euthanased, therefore the inter-dosing interval was extended to 4 days. Rats were furthermore observed for 14 days following dosing, as prescribed by the OECD guidelines.

Table 4: Step-wise ivalin dosing in rats.

Dose step number from starting dose										
-5	-4	-3	-2	-1	**Starting dose**	+1	+2	+3	+4	+5
Dose in mg/kg BW										
29	39	52	69	92	123	164	219	290	390	520

3.3.3 Animal fate and study end-point

The endpoint of the CD-1 mouse study was originally designed to be blood and muscle sampling, which would have been completed at necropsy, conducted 4 days after ivalin administration. Animals were scheduled to be sacrificed by overdose of isoflurane. Any animal showing undue suffering prior to this was also scheduled to be euthanased. Unfortunately, all animals in the exposed groups, except 1 (mouse 3), died acutely within 24 h of ivalin exposure. These animals were submitted for necropsy and muscle sampling, however it was not possible to collect blood samples as animals were either moribund at euthanasia or had died overnight. Control animals and the single surviving test group animal (mouse 3, test group 1) were euthanased as described above on day 5 following dosing and post mortem examinations and clinical pathology analyses completed.

In view of the high acute mortality shown in the mice, the second study was completed in rats, with a view to determine the median lethal dose in a species for which a validated model already existed (OECD, 2022), and to assess interspecies variation between murine laboratory animal models. As such, mortality was the primary endpoint in the Sprague-Dawley rat study, with subsequent blood and muscle sampling, where possible. In view of this being a lethality study, animals obviously in pain or showing signs of distress, or showing more than a 10% weight loss were euthanased. Rats which were euthanased for this reason were interpreted in the same way as rats which died naturally after toxin exposure, as outlined in the OECD TG 425 (OECD, 2022). All rats were euthanased by overdose of isoflurane, where natural death did not occur as a consequence of toxin exposure, and post mortem examinations and clinical pathology analyses completed.

3.4 Observations and sampling

3.4.1 Clinical and general observations

3.4.1.1 CD-1 Mice

Mice were observed daily and weighed weekly for the 2-week adaptation period. Weight was also recorded on the day of exposure, to determine ivalin dose. Animals were observed continuously for the first 30 minutes following dosing and once hourly during the first 4 hours thereafter. All mice in the exposed groups, except one, died acutely (see 7.1.1). Following this, the surviving animal (mouse 3 from exposed group 1) and the control animals were observed twice daily for 4 days after dosing. Signs of pain, stress and/or toxicity were assessed using the Mouse Grimace Scale (Langford *et al.*, 2010), Appendix 1, as well as facility recognised parameters including; staring coat, staining of medial canthus of eye, muscle tremors, stiffness, lethargy, weakness, appetite and weight loss, respiratory distress and recumbency. Toxicity was recorded descriptively. Mortality and time of death after exposure were recorded, and animals which were euthanased were included as deaths occurring due to ivalin exposure.

3.4.1.2 Sprague-Dawley Rats

Rats were observed daily and weighed weekly for the 2-week adaptation period. Weight was also recorded on the day of exposure for each individual animal, to determine ivalin dose. Following dosing, animals were weighed twice weekly, or more frequently if necessary. Animals were observed continuously for the first 30 minutes following dosing and once hourly during the first 4 hours thereafter. Following this, animals were observed twice daily for up to 14 days post dosing. Signs of pain, stress and/or toxicity were assessed using the Rat Grimace Scale (Sotocinal *et al.*, 2011), Appendix 2, as well as facility recognised parameters including; staring coat, staining of medial canthus of eye, muscle tremors, stiffness, lethargy, weakness, appetite and weight loss, respiratory distress and recumbency. Toxicity was recorded descriptively. Mortality and time of death after exposure were recorded, and animals which were euthanased were included as deaths occurring due to ivalin exposure.

3.4.2 Clinical pathology

3.4.2.1 CD-1 Mice

Blood samples were collected from the heart at euthanasia at the OVARU. A 23-gauge needle and 1 ml syringes were used for cardiopuncture and only clotting activator serum vacutubes

were used for collection due to the small volume of blood available (often less than 0.2 ml). Samples were sent directly to the Section of Clinical Pathology, Department of Companion Animal Clinical Studies, for analysis of ALT, GLDH, GGT, AST and CK. Animals euthanased for humane reasons were bled at euthanasia, the remaining animals were bled at study termination.

3.4.2.2 Sprague-Dawley Rats

Blood samples were collected from the heart at euthanasia at the OVARU. A 23-gauge needle and 5 ml syringe was used for cardiopuncture and blood was collected into EDTA, lithium heparin and clotting activator vacutubes. Samples were sent directly to the Section of Clinical Pathology, Department of Companion Animal Clinical Studies, for haematology, ALT, GLDH, AST, CK, venous blood gases, electrolytes and iCa analysis. Animals euthanased for humane reasons were bled at euthanasia, the remaining animals were bled at study termination.

3.4.3 Necropsy and tissue sampling

All animals were subjected to a full necropsy. This included a detailed examination of the gross appearance of the external surface of the body, orifices, and the thoracic and abdominal cavities and their contents. The liver, oesophagus, diaphragm, cardiac and skeletal muscles (*M. triceps brachii* and *M. gluteus maximus*) were collected and divided for histopathology, immunohistochemistry and transmission electron microscopy (TEM; rats only). Muscles were pinned onto cardboard to prevent contraction.

3.5 Sample preparation and analysis

3.5.1 Clinical pathology

Blood samples were collected directly into 2 ml microtubes (mice) or 5 ml vacutainer tubes (rats) and gently inverted for 30 seconds. Samples were taken directly to the Clinical Pathology laboratory, Department of Companion Animal Clinical Studies, and processed according to the sample type.

Blood biochemistry was conducted by a Roche Cobas Integra®-400 plus analyser (Roche diagnostics GmbH, Randburg, South Africa).

Blood gas analysis was conducted by a Siemens Rapidpoint 500® analyser (Siemens, Isando, South Africa) for pCO2, pO2, blood pH, Na^+, K^+, ionised Ca^{2+}, Cl^-, glucose, lactate and oxygenation capability (haematocrit).

Haematology was conducted using a multiparameter, automated Siemens ADVIA 2120i® analyser (Siemens, Isando, South Africa). A blood smear was also evaluated.

3.5.2 Histopathology and desmin immunohistochemistry

Samples for histopathology and immunohistochemistry, each no thicker than 0.5 cm, were collected in individually labelled containers containing 10% neutral buffered formalin.

Samples were allowed 24 h for fixation and then routinely processed, sectioned and stained with haematoxylin and eosin (H&E) for light microscopy. Immunohistochemistry was performed using a manual chromogen-based indirect immunoperoxidase technique. After hydration, samples were incubated with 3% hydrogen peroxide in methanol for 15 min, and then heat-induced epitope retrieval (HIER) was performed by microwave heating (96 °C) of the slides in EDTA buffer (pH = 9) for 21 min. A mouse monoclonal anti-human desmin M0760 antibody (DakoCytomation®, Glostrup, Denmark) was applied to the sections (1:200 dilution for 30 min), followed by application of Leica Novolink Polymer detection system (Leica Biosystems®, Newcastle Ltd, United Kingdom) according to the manufacturer's instructions. The 3,30-diaminobenzidine (DAB) chromogen, supplied with the Novolink system, was then applied to the sections for 1 – 2 min, followed by counterstaining with Mayer's haematoxylin for 20 s. Slides were rinsed in tap water for 10 min, routinely dehydrated, mounted with Entellan, and secured with a coverslip prior to examination under the light microscope.

3.5.3 Transmission Electron Microscopy

Only rat tissue was subject to ultrastructural analysis. TEM samples were collected into 2.5% glutaraldehyde/formaldehyde (0.075 M phosphate buffer, pH 7.4, room temperature) in individually labelled containers. Samples were allowed 24 h for fixation, washed 3 times in a 0.075 M phosphate buffer and then fixed in 1% osmium tetroxide for 1 – 2 h. Afterwards, samples were washed 3 times in distilled water in a fume cabinet and then dehydrated sequentially using 50%, 70%, 90% and 96% ethanol, followed by twice dehydration in 100% ethanol, for 10 minutes each. To further dehydrate the samples and to start the embedding process, the samples were successively placed in 100% propylene oxide (20 – 30 minutes), 2:1 propylene oxide to epoxy resin (1 h), 1:2 propylene oxide to epoxy resin (2 h) and finally in 100% epoxy resin for 3 h. Finally, the samples were placed in a mould with 10% epoxy and left in an oven at 65°C for 36 h. Polymerised blocks were sectioned using an ultra-microtome and the 80 – 90 nm sections were stained using 4% uranyl acetate (10 min) and Reynold's lead citrate (7 min) for viewing under the electron microscope.

3.6 Data analysis

3.6.1 Clinical signs and mortality

Clinical signs were recorded descriptively and time to mortality (or euthanasia) was recorded in hours post dosing. In CD-1 mice the percentage mortalities were calculated per study group. Weight changes were tabulated, and percentage weight losses calculated, where weight loss occurred, and compared with the normal losses between readings at the facility.

3.6.2 Median Lethal Dose (LD_{50}) calculations

3.6.2.1 CD-1 Mice

Though the study in mice was not designed to calculate a median lethal dose and there was a paucity of data points below a dosage of 175 mg/kg BW, a series of 3 scenarios were run using a Monte Carlo simulation, according to the Hill's Equation for pharmacodynamic modelling in Kinetica PK/PD modelling software (Thermo Fisher Scientific®, Philadelphia, USA), in order to determine an estimated LD_{50}.

3.6.2.2 Sprague-Dawley Rats

The LD_{50} was calculated using the maximum likelihood method. According to Dixon *et al*. (1991) the likelihood function is written as:

$L = L_1L_2...L_n$, where

L is the likelihood of the experimental outcome, given μ (the mean), σ (the standard deviation) and n (the total number of animals tested) (Dixon, 1991).

$L_i = 1 - F(Z_i)$ if the i^{th} animal survived, or, $L_i = F(Z_i)$ if the i^{th} animal died, where

F = cumulative standard normal distribution, $Z_i = [\log(d_i) - \mu]/ \sigma$; d_i = dose given to the i^{th} animal and σ = the standard deviation in log units of dose.

An estimate of the LD_{50} is given by the value of μ that maximises the likelihood L. An estimate of 0.125 was used for σ, corresponding to a slope of 8.

In exceptional circumstances, the LD_{50} is determined as follows:

1. Where stopping criteria 1 stops testing; in this case the boundary test dose is tested repeatedly or the testing stops at the upper bound test (see 6.1.2 above). The LD_{50} is then reported to be above the upper bound dose.

2. If all the dead animals have higher doses than all the alive animals then the LD_{50} lies between the doses for the live and dead animals. No exact value can be determined but an estimate of the LD_{50} can be provided using the maximum likelihood method if there is a value for σ. This may occur in stopping criteria 2 (see 6.1.2 above).
3. If the live and dead animals have only 1 dose in common and the dead animals have higher doses and all the living animals have lower doses, or *vice versa*, then the LD_{50} is equal to the common dose.

The likelihood-ratio stopping criteria 3 (see 6.1.2 above) is based on 3 measures of test progress that are in the form of the likelihood mentioned above. These measures are made after each animal tested after the 5th that does not satisfy criteria 1 or 2. If the criterion is met, testing stops, and the maximum likelihood method described above is used to calculate the LD_{50}. Confidence interval calculation provides information on the reliability of the test; a narrow confidence interval indicates that there is less uncertainty associated with the LD_{50} estimate. Following the LD_{50} calculation it was possible to calculate or estimate a confidence interval, through the methods described in the OECD guidelines (OECD, 2022).

Maximum likelihood calculations and confidence interval calculations were performed using the Acute Oral Toxicity (OECD TG 425) Statistical Programme (AOT 425 StatPgm) Version: 1.0, 2001 https://www.oecd.org/env/ehs/testing/section4software.htm, downloaded from the U.S. Environmental Protection Agency website (EPA, 2023).

3.6.3 Clinical pathology

Clinical pathology parameters obtained were tabulated, analysed for descriptive statistics (where possible) and compared to control animal values.

3.6.4 Pathology, desmin immunohistochemistry and TEM

Histopathology, ultrastructural findings and desmin reactivity were qualitatively evaluated and described.

4 RESULTS

4.1 Clinical signs and weight trends

4.1.1 CD-1 Mice

Table 5 shows the weight changes for each animal in the acclimatisation period and during the study. Mice were weighed according to the study protocol and OVARU facility study master schedule. All mice were clinically healthy prior to dosing. In some animals, minor fluctuations in weight occurred in the early acclimatisation period, however as there were no changes above 5%, these were considered normal by the facility veterinarian and most likely due to social interaction and food access stressors.

The dose, toxicity findings and mortality outcomes for each mouse are recorded in table 6. The mortality percentages per exposure group are recorded in table 7. Figure 20 depicts the corresponding dose-response curve for subcutaneous ivalin exposure in mice in this study.

All exposed group mice were quiet and subdued from several minutes after dosing. They began to show significant subcutaneous swelling at the injection site from 30 min after exposure, which in some cases extended all the way down the forelimbs (mice 1 and 15) (figure 19). One animal (mouse 7, group 2) died acutely within 3 h of dosing and a further 4 mice (mouse 6 from group 1 and mice 13, 14 and 16 from group 3) were euthanased for humane reasons at this time. All animals in the exposed groups (groups 1, 2 and 3) exhibited similar signs of toxicity according to veterinary clinical observations and assessment by the Mouse Grimace Scale (Langford *et al.*, 2010); orbital tightening, nose bulge, outward and backward rotation of the ear, and pulling back/clumping of the whiskers. Other clinical indicators of toxicity included staring coat, lethargy, weakness, appetite loss and recumbency. In mouse 7, prior to death, neurological signs (twitching and tremors) were noted. These signs were also exhibited in mice 13, 14 and 16, which prompted their immediate euthanasia. All remaining exposed group animals remained stable until late evening, but the majority were found dead the following morning. The single surviving animal from group 1 (mouse 3),

recovered completely, gained weight, and did not show any clinical abnormalities prior to euthanasia, as scheduled, 4 days after dosing.

Figure 19: Severe subcutaneous oedema in the forelimb of a CD-1 mouse.
Swelling, indicated by the black arrow, is observed in rat 15 during necropsy.

In control animals, there was mild swelling at the injection site only that diminished over the following days. None of these animals exhibited other signs of toxicity, showed stable weight trends (tables 5 and 6), and were euthanased, as scheduled, 4 days after vehicle dosing.

Table 5: *Weight trends in CD-1 mice exposed subcutaneously to ivalin during the acclimatisation and study periods.*

Mouse ID	26 July 2022 Day 2 of acclimatisation	3 August 2022 Day 10 of acclimatisation	8 August 2022 Day 1 of study (all dosed)	10 August 2022 Day 3 of study	12 August 2022 Day 5 of study
1	31.5	29.5	29.6	X	X
2	24.6	28.7	30.1	X	X
3	36.3	37.8	37.6	42.7	40.4
4	29.1	28.4	30.8	X	X
5	31.7	30.6	33.3	X	X
6	32.5	34.0	32.6	X	X
7	30.2	30.4	30.4	X	X
8	32.6	33.0	33.2	X	X
9	32.0	31.2	32.4	X	X
10	30.3	31.3	32.3	X	X
11	34.7	36.2	36.2	X	X
12	31.0	33.1	32.9	X	X

13	34.4	34.0	34.7	X	X
14	31.4	29.9	30.9	X	X
15	31.8	32.0	32.2	X	X
16	34.8	35.1	35.7	X	X
17	31.1	31.6	30.3	X	X
18	34.5	33.4	34.0	X	X
19	29.6	30.2	31.0	30.8	30.9
20	30.6	31.0	31.7	31.1	30.1
21	28.5	30.5	28.9	28.0	29.0
22	32.9	30.4	31.7	32.3	32.1
23	30.0	30.6	29.4	31.0	29.7
24	31.6	29.8	30.6	31.5	30.3

Exposed animals are highlighted in red. Control group animals are highlighted in green. X denotes mortality.

Table 6: Dosing information and clinical outcomes in CD-1 mice exposed subcutaneously to ivalin.

Mouse ID	Treatment Group	Exposed /Control	Pre-dosing weight (g)	Ivalin dose (mg/kg BW)	Ivalin dose (mg per animal)	Outcome (X/O*)	Comments
1	1	Exposed	29.6	175	5.18	X	Found dead 20 h post doing
2	1	Exposed	30.1	175	5.27	X	Found dead 20 h post doing
3	1	Exposed	37.6	175	6.58	O	Survived
4	1	Exposed	30.8	175	5.39	X	Found dead 20 h post doing
5	1	Exposed	33.0	175	5.78	X	Euthanased 19 h 50 min post dosing
6	1	Exposed	32.6	175	5.71	X	Euthanased 2 h 15 min post dosing
7	2	Exposed	30.4	250	7.60	X	Died acutely within 2 h of dosing
8	2	Exposed	33.2	250	8.30	X	Found dead 20 h post doing
9	2	Exposed	32.4	250	8.10	X	Found dead 20 h post doing
10	2	Exposed	32.3	250	8.08	X	Found dead 20 h post doing
11	2	Exposed	36.2	250	9.05	X	Found dead 20 h post doing
12	2	Exposed	32.9	250	8.23	X	Found dead 20 h post doing

13	3	Exposed	34.7	325	11.28	X	Euthanased 2 h 15 min post dosing
14	3	Exposed	30.9	325	10.04	X	Euthanased 2 h 15 min post dosing
15	3	Exposed	32.2	325	10.47	X	Found dead 20 h post doing
16	3	Exposed	35.7	325	11,60	X	Euthanased 2 h 15 min post dosing
17	3	Exposed	30.3	325	9.85	X	Found dead 20 h post doing
18	3	Exposed	34.0	325	11.05	X	Found dead 20 h post doing
19	4	Control	31.0	-	0.00	O	Survived
20	4	Control	31.7	-	0.00	O	Survived
21	4	Control	28.9	-	0.00	O	Survived
22	4	Control	31.7	-	0.00	O	Survived
23	4	Control	29.4	-	0.00	O	Survived
24	4	Control	30.6	-	0.00	O	Survived

Exposed animals are highlighted in red. Control group animals are highlighted in green. X = died, O = survived.

Table 7: Percentage mortality in CD-1 mice exposed groups in response to subcutaneous ivalin administration.

Group Dose	Number of animals	Number of mortalities	Percentage mortality
0 (Control)	6	0	0
1 (175 mg/kg BW)	6	5	83.33
2 (250 mg/kg BW)	6	6	100
3 (325 mg/kg BW)	6	6	100

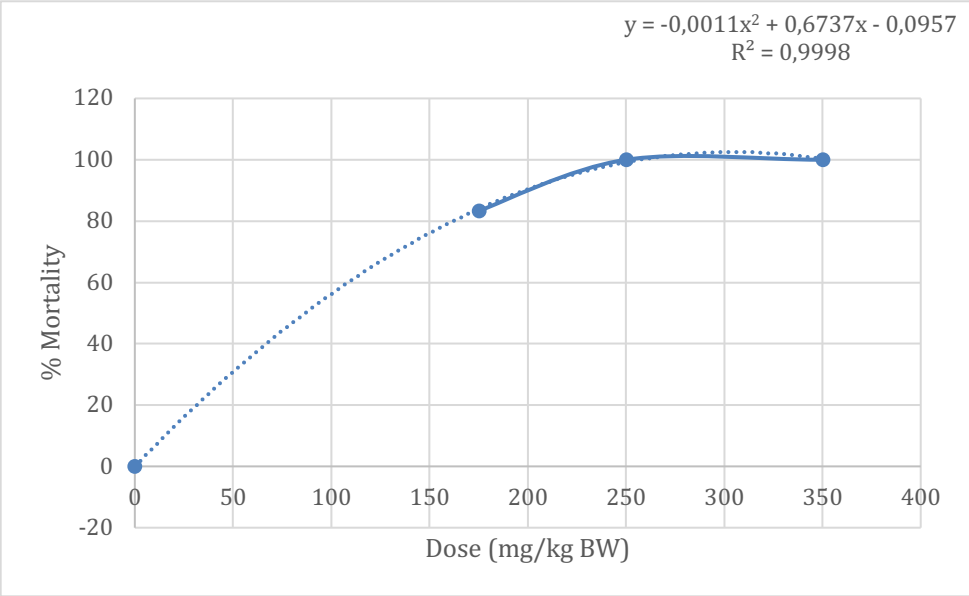

Figure 20: Dose-response curve for subcutaneous ivalin exposure in CD-1 mice.

4.1.2 Sprague-Dawley Rats

Table 8 shows the dose timing and weight changes for each animal during the acclimatisation and study periods. Rats were weighed according to the study protocol and facility master schedule, except where a pre-dosing weight was required or where there was concern over animal health post-dosing. These additional weighing points, recorded in table 8, are only applicable to certain animals. No animals experienced weight loss during the acclimatisation period; however, minor weight fluctuations of less than 10% were noted in unexposed animals after the study commenced. This was considered to be insignificant by the facility veterinarian, given the normal clinical status and behaviour of these animals.

Table 9 shows individual doses for each rat and overall clinical outcomes. Table 10 details the clinical toxicity noted over time for each exposed animal. All exposed rats showed significant

subcutaneous swelling and depression from around 30 minutes after exposure (figure 21). There was a degree of self-traumatisation that occurred in all rats, either at the site of administration (between the scapulae) or on the lateral limbs or cranioventral abdomen (over the sternum). This was particularly severe in rat 1 (figure 22). The lesions were alopecic, erythematous and showed crusting and thickening. Blue seal Vaseline® was applied to these lesions and all except those in rat 1 healed within 7 days. All rats exposed to ivalin that did not die or were not euthanased due to toxicity, were observed for 14 days post exposure.

Figure 21: Severe subcutaneous oedema in rat 2, extending down forelimbs and ventral thorax.

Rat 1 received the starting dose of 123 mg/kg BW, a single dose-step below the estimated LD_{50}. In this animal, the swelling regressed over the proceeding 48 h. Though it appeared to recover, remaining appetent and active, there followed a gradual clinical deterioration. This included significant self-traumatisation over the abdomen (figure 22) and a weight loss of greater than 10%. The animal was therefore euthanased on humane grounds 4 days after exposure.

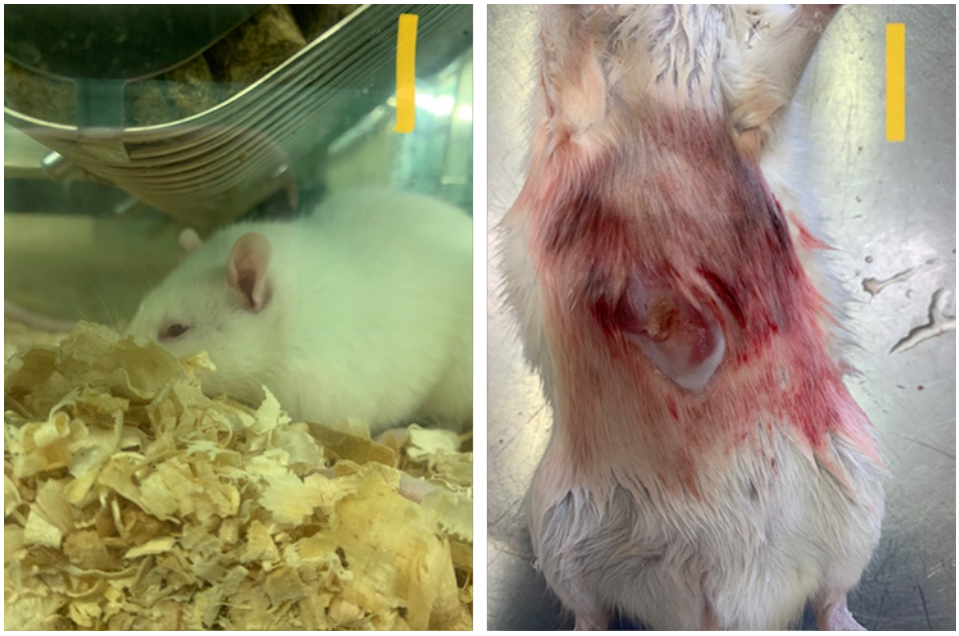

Figure 22: Post dosing depression and severe self-trauma over ventral abdominal area in rat 1. Note that the haemorrhage was due to post mortem exsanguination at the site of cardiopuncture.

Rat 2 received a higher dose than rat 1 of 164 mg/kg BW. The animal was dosed 48 h after rat 1, in accordance with study protocol. Based on the mouse study results, as well as the activity and appetite of rat 1, the authors anticipated recovery of this animal, and therefore rat 2 did not receive a lower, but rather a higher dose than rat 1. Rat 2 showed immediate burrowing into the bedding post exposure, most likely due to irritation at the exposure site. However, the behaviour stopped within 5 minutes. The animal then showed severe swelling, depression and inappetence and died acutely overnight.

Rat 3 received a dose of 123 mg/kg BW. This animal also showed severe subcutaneous swelling and depression for 24 h post dosing, but recovered well, remaining active and appetent and gained weight until 14 days after dosing. Rat 3 also developed a self-induced lesion on the right lateral elbow, which responded well to topical treatment with petroleum jelly and healed effectively.

Given the chronic deterioration of rat 1, it was decided to extend the inter-dosing interval to 5 days. Thus rat 4 was dosed 5 days after rat 3 at a dose of 164 mg/kg BW. Rat 4 showed a similar clinical picture to rat 3; initial swelling and depression, followed by recovery. This animal self-traumatised over both the left lateral elbow and at the exposure site, but both lesions healed well.

Rat 5 was scheduled for dosing at 219 mg/kg BW, 5 days after rat 4 was dosed. This animal was extremely fractious during dosing, causing the needle to dislodge from the subcutaneous

tissue and resulting in a loss of the dose onto the procedure table. As it could not be determined how much the animal had received, it was excluded from the data set and the same dose of 219 mg/kg BW was administered to rat 6. Rat 6 showed severe subcutaneous swelling and depression and died acutely overnight. Mortality in this animal triggered stopping criteria 3 (the likelihood-ratio) and the study was concluded.

In control animals, there was virtually no swelling at the injection site and no dermal irritation. None of these animals exhibited signs of toxicity. All displayed stable weight trends (table 10) and were euthanased, as scheduled, 14 days after vehicle dosing.

Table 8: Weight trends during acclimatisation and study period in Sprague-Dawley rats exposed subcutaneously to ivalin.

Date	8 Aug	16 Aug	21 Aug	23 Aug	25 Aug	28 Aug	30 Aug	5 Sep	6 Sep	13 Sep
Day of study	Day 2 of acclimatisation	Day 10 of acclimatisation	Day 1 of study, weigh rat 1	Day 3 of study; weigh all	Day 5 of study; weigh rat 1 and 3	Day 8 of study; weigh rat 3	Day 10 of study; weigh all	Day 15; weigh rat 3, 4, 5 and 6	Day 16; weigh all rats	Day 23; weigh all rats
Dosing			Dose rat 1	Dose rat 2	Dose rat 3		Dose rat 4	Dose rat 5, 6		
Weight (g)										
Rat 1	213	226	235	235	200	X	X	X	X	X
Rat 2	200	218	-	229	X	X	X	X	X	X
Rat 3	190	212	-	219	213	222	225	245	248	239
Rat 4	190	202	-	218	-	-	225	221	220	227
Rat 5	209	241	-	234	-	-	237	239	250	257
Rat 6	201	219	-	232	-	-	238	235	X	X
Rat 7	196	212	-	225	-	-	219	-	227	229
Rat 8	166	181	-	192	-	-	188	-	192	193

Rat 9	192	200	-	213	-	-	209	-	212	212
Rat 10	194	210	-	219	-	-	222	-	218	223
Rat 11	171	189	-	195	-	-	205	-	209	210
Rat 12	203	220	-	230	-	-	230	-	237	231
Rat 13	189	215	-	224	-	-	228	-	228	234
Rat 14	201	222	-	224	-	-	231	-	228	225
Rat 15	194	214	-	223	-	-	229	-	229	235

Dosing is noted in yellow cells, X denotes mortality.

Table 9: Individual dose and clinical outcomes in Sprague-Dawley rats exposed subcutaneously to ivalin.

Rat ID	Test/Control	Pre-dosing weight (g)	Ivalin dose (mg/kg BW)	Ivalin dose (mg)	Outcome (X/O*)	Time to mortality
1	Exposed	235.0	123	28.91	X	4 day (euthanased)
2	Exposed	229.0	164	37.56	X	< 24 h (found dead)
3	Exposed	213.0	123	26.20	O	-
4	Exposed	225.0	164	36.90	O	-
5	Exposed	239.0	219	52.34	Rodent very fractious; dosing error (only part of dose injected); animal removed from data set	
6	Exposed	235.0	219	51.47	X	< 24 h (found dead)
Study terminated according to OT 425 Likelihood Ratio stopping criteria (stopping criteria 3)						
7	Not used	-	-	-	-	-
8	Not used	-	-	-	-	-
9	Not used	-	-	-	-	-
10	Not used	-	-	-	-	-
11	Control	Drug vehicle only; 0.5 ml PEG 400.			O	-

12	Control	Drug vehicle only; 0.5 ml PEG 400.	O	-
13	Control	Drug vehicle only; 0.5 ml PEG 400.	O	-
14	Control	Drug vehicle only; 0.5 ml PEG 400.	O	-
15	Control	Drug vehicle only; 0.5 ml PEG 400.	O	-

** Exposed animals are highlighted in red. Control group animals are highlighted in green. X = died, O = survived.*

Table 10: Clinical observations over time in Sprague-Dawley rats exposed subcutaneously to ivalin.

	Day 1	Day 2	Day 3-5	Day 6-8	Day 9-14
Exposed animals to ivalin in PEG 400 vehicle (test animals)					
Rat 1	Initially depressed and severe swelling at site of exposure but remained appetent and appeared to improve overnight.	Depressed but remained appetent and alert.	Deterioration and signs of toxicity*, anorexia, weight loss of greater than 10% and self-trauma over ventral sternum. Euthanased in accordance with escape clause of the protocol on D5.	X	X
Rat 2	Burrowing into sawdust after injection. Severe swelling at exposure site, signs of toxicity* and depression.	Died overnight.	X	X	X
Rat 3	Depression and severe swelling at site of exposure.	Bright and alert, eating well.	Bright and alert, weight gain.	Bright and alert. Alopecia and crusting over right lateral elbow.	Bright and alert, lesions over elbow healed.
Rat 4	Depression and severe swelling at site of exposure.	Bright and alert, eating well.	Bright and alert. Alopecia and crusting over right lateral elbow.	Bright and alert. Alopecia and crusting over left lateral elbow.	Bright and alert, lesions over elbow healed. Second lesion developed at injection site on day 13, but also healed.
Rat 5	Animal not used in data set due to dosing error; see table 9.				

6	Severe swelling at exposure site, signs of toxicity* and depression.	Died overnight.	X	X	X
1 - 10	Animal not used.				
Animals exposed to PEG 400 alone (control animals)					
11	No abnormalities detected.				
12	No abnormalities detected.				
13	No abnormalities detected.				
14	No abnormalities detected.				
15	No abnormalities detected.				

** Narrowing of eye orbits, hunched posture, whisker/nose/cheek flattening, as assessed by Rat Grimace Scale (Sotocinal et al., 2011).*

4.2 Median Lethal Dose (LD_{50})

4.2.1 CD-1 Mice

Though the study in mice was not designed to calculate a median lethal dose and there was a complete absence of data points below a dosage of 175 mg/kg BW. The available data followed a quadratic model. A series of 3 scenarios were run using a Monte Carlo simulation, according to the Hill's Equation for pharmacodynamic modelling in Kinetica PK/PD modelling software (Thermo Fisher Scientific®, Philadelphia, USA), to determine an estimated LD_{50}. One of the input scenarios was that obtained in the study itself (scenario 1) and the remaining 2 scenarios were hypothesised outcomes for mortality responses between a dose of 0 mg/kg BW and 175 mg/kg BW. These are shown in table 11 and figure 23 below.

Table 11: Three scenarios hypothesising the effect of subcutaneous ivalin exposure between a dose of 0 and 325 mg/kg BW on mortality in CD-1 mice.

Dose mg/kg BW	**Scenario 1 (actual)**	**Scenario 2 (hypothesis)**	**Scenario 3 (hypothesis)**
	Percentage mortality		
0	0	0	0
25	-	0	0
50	-	-	0
175	83.3	83.3	83.3
250	100	100	100
325	100	100	100

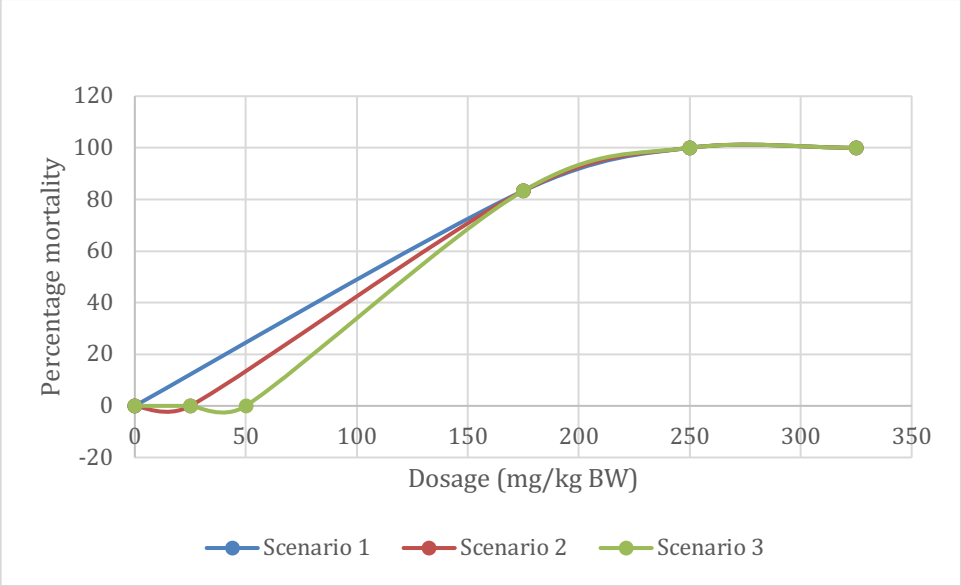

Figure 23: Dose-response curves for subcutaneous ivalin exposure in CD-1 Mice for 3 scenarios for dosages below 175 mg/kg BW.

The Hill's equation is shown below, and describes the dose-response relationship for a given compound;

$$\boldsymbol{E = E_0 \pm \frac{Emax.C^n}{C^n + EC_{50}^n}}$$

Equation 1: The Hill's equation for the relationship between effect and dose.

$$\boldsymbol{EC_{50}^n = \frac{C^n - EC^n}{E}}$$

Equation 2: The Hill's equation for the relationship between effect and dose, rearranged to solve for EC_{50}.

where E = effect, in response to the dose of a given compound, C. E_0 is therefore the baseline effect or effect where C = 0 (in this case 0% mortality or 0) and Emax the maximum effect (in this case 100% mortality or 1). The EC_{50} is the dose at which there is a 50% response or Emax/2 (in this case the LD_{50}). The value for n is the slope of the curve produced by the data points.

1.1. The Hill's equation parameter outputs for the Monte Carlo simulations are shown in table 12 below. The EC_{50}, corresponding to the median lethality, of 164 mg/kg BW was used as the most conservative estimate for determining a more accurate LD_{50} in rats in the second phase of the research. The estimated LD_{50} fell outside the inference range of the model, which was not unexpected given the mortality trend in the 3 dose groups. It is acknowledged that that the estimated LD_{50} is uncertain due to the limitations of the data and modelling.

Table 12: Monte Carlo simulation Hill's equation parameters for 3 scenarios following subcutaneous ivalin exposure in CD-1 mice.

Hill's equation parameter	**Scenario 1 (actual)**	**Scenario 2 (hypothesis)**	**Scenario 3 (hypothesis)**
Emax	100	100	100
EC_{50}	166	164	167
n	33.31	27.49	33.26
E0	-4.44291e-010	-1.18711e-008	-1.61751e-010

4.2.2 Sprague-Dawley Rats

The major objective of the rat study was determination of the LD_{50} for ivalin exposure subcutaneously. The output of the AOT425 statpgm software is shown below in figure 24. In this study, stopping criteria 3, the likelihood ratio, determined the stopping point of the study and the LD_{50} was estimated to be 135.4 mg/kg BW, based on the maximum likelihood method. The 95% confidence intervals provided by the programme were 0 - >20,000.

File Edit Format View Help

Test/Substance: Ivalin LD50 Rat
Test type: Main Test
Limit dose (mg/kg): 2000
Assumed LD50 (mg/kg): 164
Assumed sigma (mg/kg): 0.125

Recommended dose progression: 2000, 1640, 1230, 920, 690, 520, 390, 290, 219, 164, 123, 92, 69, 52, 39, 29, 21.9, 16.4, 12.3, 9.2, 6.9, 5.2, 3.9, 2.9, 2.19, 1.64

DATA:

Test Seq.	Animal ID	Dose (mg/kg)	Short-term Result	Long-term Result
1	1	123	O	X
2	2	164	X	X
3	3	123	O	O
4	4	164	O	O
5	6	219	X	X

(X = Died, O = Survived)

Dose Recommendation: The main test is complete.

Stopping criteria met: LR criterion.

SUMMARY OF LONG-TERM RESULTS:

Dose	O	X	Total
123	1	1	2
164	1	1	2
219	0	1	1
All Doses	2	3	5

Statistical Estimate based on long term outcomes:

Estimated LD50 = 135.4 (Based on maximum likelihood).
95% PL Confidence interval is 0 to Greater than 20,000.

Figure 24: AOT 425 OECD/EPA software output for determining median lethality of subcutaneous ivalin exposure in Sprague-Dawley rats, using the maximum likelihood method.

4.3 Clinical pathology

4.3.1 CD-1 Mice

The clinical pathology results obtained for mouse 3 (exposed group 1 surviving animal) and the group 4 control animals are shown in table 13. The mean, standard deviation and coefficient of variation could only be calculated for the control animals. Although blood was also submitted for exposed group animals 6, 7, 13, 14 and 16, these animals were moribund and the quantity collected at euthanasia was insufficient for biochemistry analysis. In view of the unexpected acuteness of toxicity, electrolytes, urea, creatinine and serum proteins were run on mouse 3 and the control animals.

Without a reference range for CD-1 mice from the test laboratory, the blood from mouse 3 was visually compared to the mean results from the control animals. The AST, ALT and GLDH levels in mouse 3 were 1.6 times, 2.8 times and 6.3 times raised, respectively, compared to the control animals for these parameters. The CK level in the same animal was 3.6 times lower than the mean of the control animals. There was good precision within the control group, except for CK, driven by a low reading in mouse 19.

Table 13: Clinical pathology parameters for ivalin-exposed and control CD-1 mice.

	Parameter	Na^+	K^+	Cl^-	Urea	Creatinine	GGT	AST	CK	ALT	GLDH	TSP	Alb	Glob
	Unit	mmol/l	mmol/l	mmol/l	mmol/l	umol/l	U/l	U/l	U/l	U/l	U/l	g/l	g/l	g/L
Exposed	Group													
Mouse 3	1	148.3	4.20	113.7	7.83	<18	0	**136.4**	59.4	**72.4**	**46.9**	54.7	40.19	14.5
Control	Group													
Mouse 19	4	146.6	4.10	110.7	5.17	18	0	71.3	67.1	26.2	6.0	50.3	37.39	12.9
Mouse 20	4	147.1	4.49	115.6	4.64	<18	0	85.5	211.4	34.0	7.3	49.7	35.43	14.3
Mouse 21	4	148.4	4.82	116.5	6.04	<18	0	99.3	339.3	27.9	8.4	46.0	32.81	13.2
Mouse 22	4	146.7	4.74	113.8	8.18	<18	0	91.1	208.6	30.8	10.5	48.0	36.25	11.8
Mouse 23	4	145.6	5.05	113.8	5.66	<18	0	83.0	262.6	16.1	5.0	46.5	35.48	11.0
Mouse 24	4	148.0	4.29	113.2	5.99	<18	0	77.8	199.9	23.0	7.2	45.5	33.19	12.3
Mean		147.1	4.60	113.9	5.90	18.0	0.0	84.7	214.8	26.3	7.4	47.7	35.1	12.6
Std Dev		0.93	0.32	1.84	1.11	8.78	0.00	8.99	81.52	5.73	1.75	1.83	1.62	1.05
CoV		1%	7%	2%	19%	-	-	11%	**38%**	22%	24%	4%	5%	8%

GGT = Gamma-Glutamyl Transferase, AST = Aspartate Transferase, CK = Creatinine Kinase, ALT = Alanine Transaminase, GLDH = Glutamate Dehydrogenase, TSP = Total Serum Protein, Alb = Albumin, Glob = Globulin.

Exposed animals are highlighted in red. Control group animals are highlighted in green.

Table 14: Haematology parameters for ivalin-exposed and control Sprague-Dawley rats.

Para-meter	Hb	RCC	Ht	MCV	MCH	MCHC	RDW	WCC	Seg. Neuts	Band. Neuts	Lympho -cytes	Mono-cytes	Eosino-phils	Baso-phils	Platelet Count
Unit	**g/L**	**X10^{12}L**	**%**	**fL**	**pg**	**g/dl**	**%**	**X10^{9}L**	**X10^{9}L**	**X10^{9}L**	**X10^{9}L**	**X10^{9}L**	**X10^{9}L**	**X10^{9}L**	**X10^{9}L**
Rat 1	**134**	**7.75**	43	55.9	17.2	30.8	11.3	**1.75**	**0.58**	0	**1.05**	0.12	0.00	0	870
Rat 3	Blood clotted														
Rat 4	Blood clotted														
Rat 11	171	9.77	54	55.2	17.5	31.7	11.9	8.93	1.70	0	6.97	0.27	0.00	0	919
Rat 12	136	8.46	44	51.9	16.1	31.0	12.6	6.69	1.14	0	5.49	0.07	0.00	0	388
Rat 13	146	9.23	44	47.8	15.8	33.1	12.3	6.14	1.11	0	4.91	0.06	0.06	0	43
Rat 14	150	8.85	45	50.4	16.9	33.6	12.2	7.32	1.17	0	5.86	0.15	0.15	0	537
Rat 15	133	8.34	43	51.4	15.9	30.9	12.4	4.80	0.77	0	3.98	0.05	0.00	0	473
Mean	147.20	8.93	46	51.34	16.44	32.06	12.28	6.78	1.18	0.00	5.44	0.12	0.04	0.00	472.00
Std Dev	15.02	0.59	4.53	2.68	0.73	1.23	0.26	1.52	0.33	0.00	1.11	0.09	0.07	0.00	314.30
CoV	10%	7%	10%	5%	4%	4%	2%	22%	28%	-	20%	**77%**	**156%**	-	**67%**

Hb = Haemoglobin, RCC = Red Cell Count, Ht = Haematocrit, MCV = Mean Corpuscular Haemoglobin, MCHC = Mean Corpuscular Haemoglobin Concentration, RDW = Red Diameter Width, WCC = White Cell Count, Seg. Neuts – Segmented neutrophils, Band. Neuts = Banded Neutrophils. Exposed animals are highlighted in red, control animals in green.

Exposed animals are highlighted in red. Control group animals are highlighted in green.

Table 15: Bloodsmear findings for ivalin-exposed and control Sprague-Dawley rats.

Rat ID	Bloodsmear comments
1	2+ Anisocytosis, **2+ polychromasia**, **1+ hypochromasia,** mild monocyte activity, few reactive lymphocytes, high platelet count
3	-
4	-
11	1+ Anisocytosis, 2+ acanthocytes, mild platelet aggregation
12	2+ Anisocytosis, mild macrocytosis, few reactive lymphocytes, 1+ acanthocytes, normal platelets
13	1+ Anisocytosis, 2+ acanthocytes, few reactive lymphocytes, rouleaux, low platelet count
14	1+ Anisocytosis, few reactive lymphocytes, normal platelets, mild platelet aggregation
15	1+ Anisocytosis, few reactive lymphocytes, mild monocyte activity, normal platelet count, mild platelet aggregation, few giant cells

Exposed animals are highlighted in red. Control group animals are highlighted in green.

Table 16: Blood gas parameters for ivalin-exposed and control Sprague-Dawley rats.

Para-meter	Na^+	K^+	Cl^-	iCa^{2+}	pH	CO_2 PP	O_2 PP	HCO_3 Actual	HCO_3 Standard	Base Excess	O_2 Saturation	CO_2 Content	Lactate
Unit	**mmol/L**	**mmol/L**	**mmol/L**	**mmol/L**		**mm Hg**	**mm Hg**	**mEq/L**	**mEq/L**	**mEq/L**	**%**	**mmol/L**	**mmol/L**
Rat 1	137	**5.93**	104	**1.29**	**7.27**	44.1	75.5	19.6	**18.6**	**-7.5**	93.2	21.0	**6.70**
Rat 3	135	3.71	107	1.06	-	-	-	-	-	-	-	-	5.70
Rat 4	135	4.65	107	1.17	-	-	-	-	-	-	-	-	4.70
Rat 11	139	3.35	103	1.16	7.38	38.2	60.0	22.2	22.3	-2.9	90.7	23.4	4.20
Rat 12	140	3.73	106	1.25	7.35	49.1	50.1	26.4	24.2	0.7	83.2	27.9	4.30
Rat 13	-	-	-	-	-	-	-	-	-	-	-	-	-
Rat 14	139	3.30	106	1.23	7.44	31.5	98.2	20.8	22.6	-3.4	97.7	21.8	3.34
Rat 15	138	3.42	105	1.23	7.38	34.0	87.7	19.8	20.9	-5.3	96.6	20.8	5.80
Mean	139.00	3.45	105.00	1.22	7.39	38.20	74.00	22.30	22.50	-2.73	92.05	23.48	4.41
Std Dev	0.82	0.19	1.41	0.04	0.04	7.77	22.66	2.91	1.35	-	6.65	3.14	1.02
CoV	1%	6%	1%	3%	1%	20%	31%	13%	6%	-	7%	13%	23%

iCa^{2+} = inorganic calcium, CO_2 PP = CO_2 Partial Pressure, O_2 PP = O_2 Partial Pressure, HCO_3 = Bicarbonate.
Exposed animals are highlighted in red. Control group animals are highlighted in green.

Table 17: Selected biochemistry parameters and blood smear results for ivalin-exposed and control Sprague-Dawley rats.

Para-meter	AST	CK	GLDH	ALT
Unit	**U/L**	**U/L**	**U/L**	**U/L**
Rat 1	126	185	12	44.3
Rat 3	135	**790**	10	42.4
Rat 4	**356**	**2280**	5	60.0
Mean	**205.67**	**1085.00**	9.00	48.90
Std Dev	106.37	880.35	2.94	7.89
CoV	52%	81%	33%	16%
Rat 11	84	404	9	45.5
Rat 12	115	532	11	43.9
Rat 13	118	664	7	54.5
Rat 14	83	358	7	34.6
Rat 15	103	410	9	49.2
Mean	100.60	473.60	8.60	45.54
Std Dev	16.59	124.41	1.67	7.35
CoV	16%	26%	19%	16%

AST = Aspartate Transferase, CK = Creatinine Kinase, ALT = Alanine Transaminase, GLDH = Glutamate Dehydrogenase. Exposed animals are highlighted in red. Control group animals are highlighted in green.

4.3.2 Sprague-Dawley Rats

A more extensive clinical pathology panel was attempted on the rats. The haematology, blood gas, electrolyte and selected biochemistry parameters are displayed in table 14, 15, 16 and 17.

Unfortunately, bleeding from rats 3 and 4 was difficult, resulting in clotted EDTA samples for haematology and serum tubes for blood gas analysis. As a result, only the biochemistry and electrolyte levels are available for these animals.

4.3.2.1 Haematology

Rat 1 (which received the first dose of ivalin of 123 mg/kg BW, 1 dose-step below the estimated LD_{50}) showed significant neutropaenia (3.8 times lower) and lymphopaenia (5.2 times lower) compared to the mean of the control groups (table 14). Rat 1 also had a mildly reduced red cell count (1.15 times below the mean for the control group animals), and a mild polychromasia and hypochromasia on blood smear evaluation, compared to control animals (table 15).

Within the control group of animals, most parameters showed high precision, with the variability being below 30%. The exceptions to this were higher variability parameters, including eosinophils and monocytes, which had a 77% and 156% coefficient of variation respectively (Aigner and Heuman, 2023). The platelet count variability was also high at 56%, likely due to an outlier low value in rat 13. This value is probably linked to clotting of blood that was not visually detected at the time of sampling (table 14).

4.3.2.2 Electrolyte and blood gas analyses

There were no major differences in electrolyte levels between exposed and non-exposed rats, except for in rat 1 which demonstrated hyperkalaemia and hypercalcaemia compared to the mean of the control animals. Furthermore, rat 1 demonstrated a mild metabolic acidosis, as evidenced by the mild acidaemia (pH 7.27), lower standard HCO_3^- and base excess values, and raised lactate levels, compared to the means of the control animals (table 16).

The reduced PO_2 levels across most rats in the study can probably be attributed to cardiac blood collection under isoflurane-induced general anaesthesia. Within the control group of animals, most parameters showed high precision (table 16).

4.3.2.3 *Biochemistry*

The AST levels in all exposed rats from which samples were obtained (1, 3 and 4) were elevated compared to the mean of the control rats. This was particularly the case for rat 4, where the AST level was 3.5 times higher than the mean of the controls. The CK levels from rats 3 and 4 were also raised; 1.67 and 4.8 times the mean of the control rats (table 17).

Within the control group of animals, most parameters showed high precision (table 17).

4.4 Pathology

4.4.1 CD-1 Mice

There were no significant macroscopic changes in any of the mice, except for the subcutaneous swelling noted in 7.1.1 above.

Selected striated muscle samples from mice in table 18 were evaluated by light microscopy for evidence of histopathology.

Table 18: Ivalin-exposed and control CD-1 mice evaluated for histopathology.

Mouse ID	Group	Dose and clinical outcome
3	1	175 mg/kg BW, surviving animal, euthanased at study end
5	1	175 mg/kg BW, animal died
7	2	250 mg/kg BW, animal died
8	2	250 mg/kg BW, animal died
13	3	325 mg/kg BW, animal euthanased
17	3	325 mg/kg BW, animal died
20	4	Control animal; euthanased at study end
23	4	Control animal; euthanased at study end

4.4.1.1 *Heart*

In both exposed and control mice, there were multifocal singly scattered to small aggregates of slightly swollen hypereosinophilic myocardial fibres with variable loss of cross-striations and hyperchromatic nuclei. These were considered to be contraction artefacts, given their presence in unexposed mice as well. In some mice (5, 13 and 20), aggregates of slightly swollen hypereosinophilic myofibres were associated with haemorrhage, which may be linked to perimortal blood collection by cardiac puncture (figure 25).

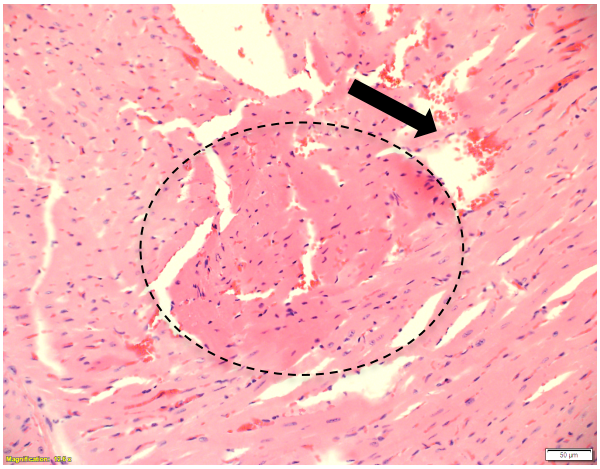

Figure 25: Slightly swollen hypereosinophilic cardiac myofibres (dashed circle), associated with mild haemorrhage (arrow) in control mouse 13 (H&E stain, x 20).

4.4.1.2 Oesophagus and diaphragm

In both the exposed mice (especially mice 3 and 5) and control mice (especially mouse 20), there were multifocal single to occasional small aggregates of slightly swollen hypereosinophilic myofibres. The preservation of cross-striations suggested that these findings were likely artefactual, probably related to contraction artefacts (figure 26).

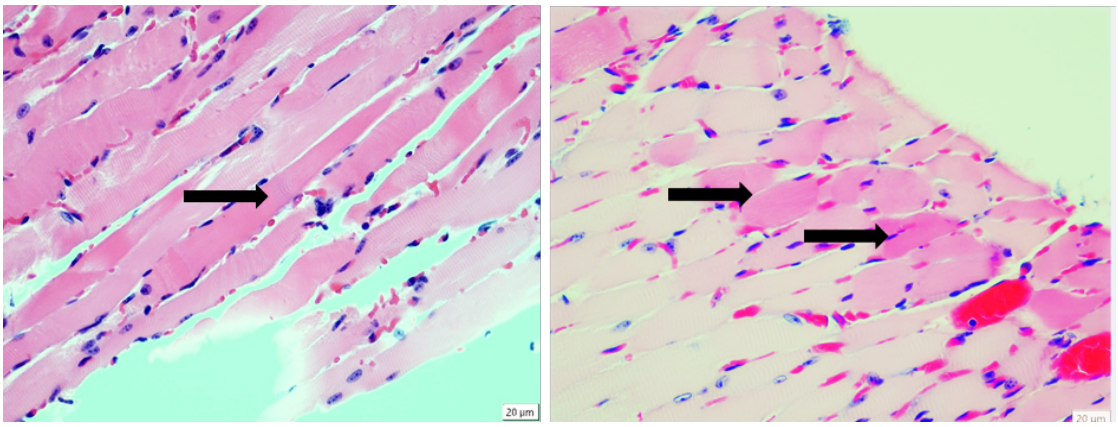

Figure 26: Hypereosinophilic muscle fibres (arrows) in the diaphragm of exposed and control mice. Left: Mouse 13 from exposed group 3 (H&E stain, x 40). Right: Control mouse 20 (H&E stain, x 40).

4.4.1.3 Skeletal muscle; Gluteus maximus *and* Triceps brachii *muscle*

In both exposed and control mice, multifocal hypereosinophilic myofibres were observed (especially in mouse 20 of the control group). The myofibres were not swollen and cross-striations remained visible, indicating that these were likely artefactual contraction bands (figure 27).

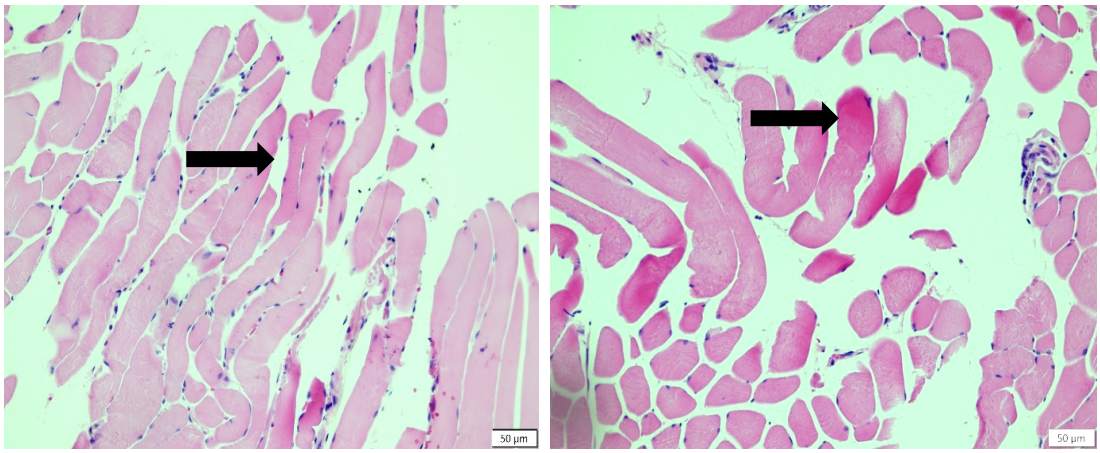

Figure 27: Hypereosinophilic muscle fibres (arrows) in the maximal gluteal muscles of exposed and control mice. Left: Surviving mouse 3 from exposed group 1 (H&E stain, x 20). Right: Control mouse 20 (H&E stain, x 20).

4.4.1.4 Liver

In mouse 5 (exposed, group 1), there were random single to small aggregates of swollen hepatocytes with hypereosinophilic cytoplasm and hyperchromatic (not yet pyknotic) nuclei, in just two liver lobes (figure 28). In the same animal, randomly scattered pyknotic nuclei and karyorrhectic nuclear debris were observed, indicative of cell death, and accompanied by mild lymphocytic inflammation.

In the surviving exposed mouse 3 (group 1) and mouse 20 (control group), small inflammatory foci with neutrophils, lymphocytes, and occasional macrophages, were found around small aggregates of 1 – 2 necrotic hepatocytes. These incidental foci of focal hepatitis, as noted in rats by Percy *et al.* (2016), may account for this finding in mice (Percy *et al*., 2016).

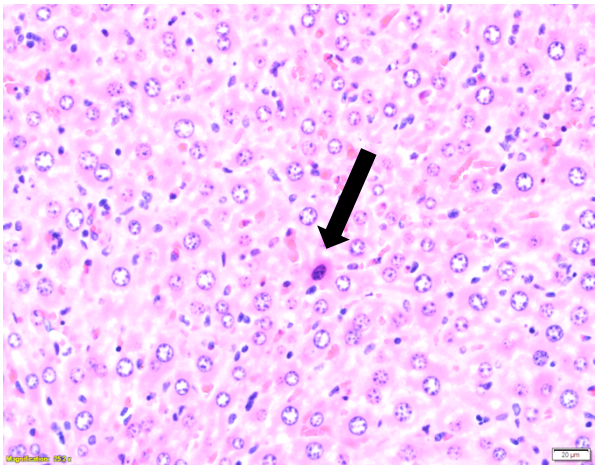

Figure 28: Single hypereosinophilic hepatocyte with a hyperchromatic nucleus (arrow) in ivalin-exposed mouse 5 (H&E stain, x 40).

4.4.1.5 *Lungs*

In some exposed mice, moderate diffuse congestive atelectasis, variable neutrophilic leukostasis, and extramedullary haematopoiesis (EMH) were present. Mice 5, 13 and 17 (from exposed groups 1, 2 and 2 respectively) exhibited scattered pyknotic and karyorrhectic nuclei (indicative of cell death). There were alveolar haemorrhages visible in mice 3 (surviving exposed mouse from group 1) and 5. These haemorrhages are noted by Percy *et al* (2016) to be an inconsistent agonal finding in mice (Percy *et al*., 2016). In addition to the alveolar haemorrhages, mouse 3 exhibited severe bronchiolar dilation and moderate alveolar emphysema, also indicative of agonal changes.

4.4.1.6 *Spleen*

No significant changes were observed.

4.4.1.7 *Kidneys*

No significant changes were observed.

4.4.2 Sprague-Dawley Rats

There were no significant macroscopic changes in any of the rats, aside from the subcutaneous swelling and self-traumatic lesions noted in 7.1.2 above.

Selected striated muscle samples from rats in table 19 were evaluated by light microscopy for evidence of histopathology. Overall, the striated muscle sections exhibited mild to moderate congestion, often accompanied by focal to multifocal small, acute haemorrhages. Singly scattered, well-granulated mast cells were frequently observed in the interstitium of the diaphragm muscle in both control and exposed rats, and very occasionally in the oesophagus and myocardium of some exposed rats.

Table 19: Ivalin-exposed and control Sprague-Dawley rats evaluated for histopathology.

Rat ID	Dose (mg/kg)	Clinical outcome
1	123	Euthanased 4 days after dosing
2	164	Died within 24 h of dosing
3	123	Survived; euthanased at study end
4	164	Survived; euthanased at study end
6	219	Died within 24 h of dosing
11	-	Control animal; euthanased at study end
13	-	Control animal; euthanased at study end
15	-	Control animal; euthanased at study end

4.4.2.1 Heart

In rats 1, 3, 4, 6, and 13, as in the mice, there were singly scattered and/or small groups of slightly shrunken to slightly swollen hypereosinophilic myofibres, often with hyperchromatic myonuclei. These were likely contraction artefacts since in oblique and longitudinal sections, cross-striations were typically visible, and similar findings were observed in both exposed and control animals (figure 29).

In rat 2, the endocardium and subendocardium showed mild to moderate thickening due to macrophage infiltration and mesenchymal cell proliferation. In the myocardium near the endocardial surface, rare, small foci of myofibre lysis were observed, accompanied by infiltrating macrophages and minimal early fibrous repair (figure 30).

In rats 3, 4, and 15, the cardiopuncture sites used for blood sampling were visible. These sites exhibited a linear tract lined by mildly swollen and rounded hypereosinophilic myofibres with hyperchromatic nuclei and acute haemorrhage.

4.4.2.2 Diaphragm and oesophagus

In both exposed (1, 2, 4 and 6) and control rats (11, 13 and 15), similar to the mice, striated muscle fibres in the diaphragm and/or oesophagus displayed isolated or multifocal small aggregates of shrunken to slightly swollen hypereosinophilic myofibres, typically associated with irregular, hyperchromatic myonuclei. These changes were considered contractual artefacts and not significant (figure 29).

In rat 1, the diaphragm exhibited mild multifocal vacuolisation within the myofibre sarcoplasm, typically associated with segmental myofibre enlargement and loss of cross-striations. Additionally, some myonuclei appeared irregularly enlarged and darkly stained, with unstructured chromatin; the nuclear membranes were disrupted, and the nuclear content appeared lysed. Multifocal myofibre segments also showed lytic changes, accompanied by sarcoplasmic fragmentation, and sparse infiltration of macrophages. Increased numbers of internal myonuclei were observed (figure 31). In the connective tissue surrounding the diaphragm, there were increased numbers of perivascular well-granulated mast cells and occasional lymphocytes and neutrophils (figure 30). A bacteraemia was also present in this animal.

In exposed rats 2, 3, 4 and control rat 11, perivascular aggregates of well-granulated mast cells, along with occasional lymphocytes and macrophages, were observed in the fibro-adipose tissue adjacent to the diaphragm.

In exposed rat 6, similar to rat 1, though milder, some myonuclei were swollen and irregular, with darkly staining, unstructured chromatin and loss of nuclear membrane integrity, suggestive of nuclear dissolution.

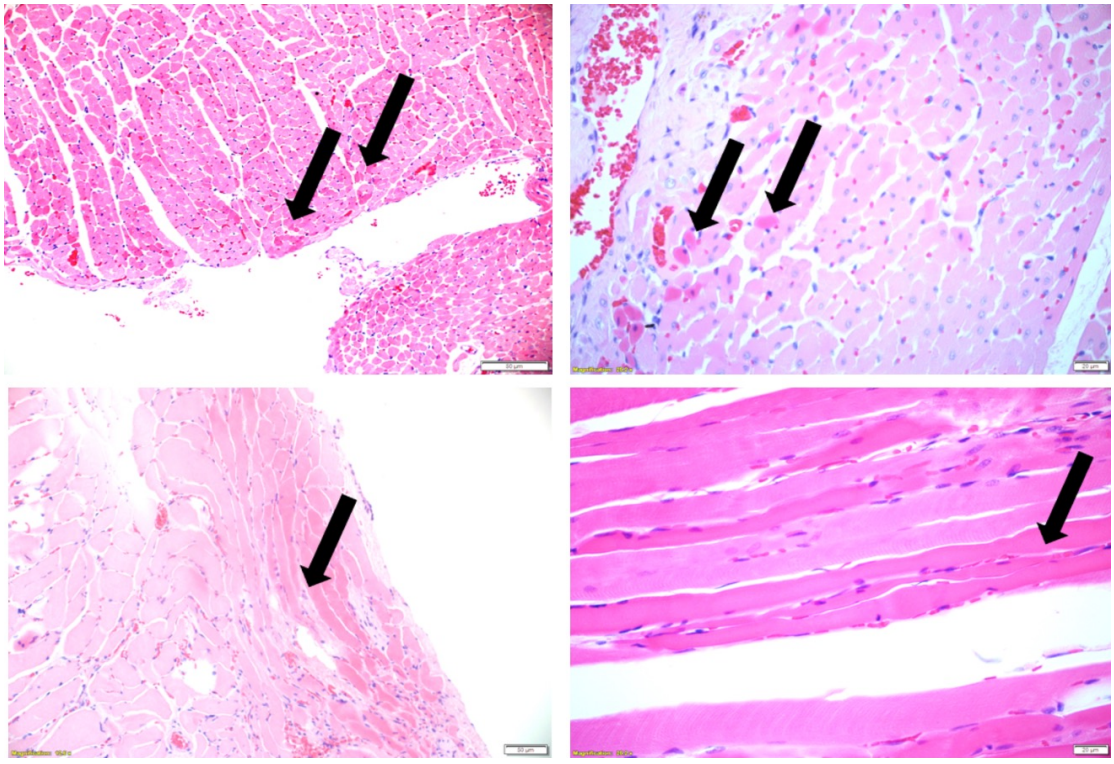

Figure 29: Slightly shrunken hypereosinophilic myofibres with hyperchromatic nuclei (black arrows) in cardiac and diaphragmatic tissue of exposed and control rats.
Top left: Exposed rat 4, myocardium (H&E, x 20). Top right: Control rat 13, myocardium (H&E x 40).
Bottom left: Exposed rat 6, diaphragm (H&E x 20). Bottom right: Control rat 15, diaphragm (H&E, x 40).

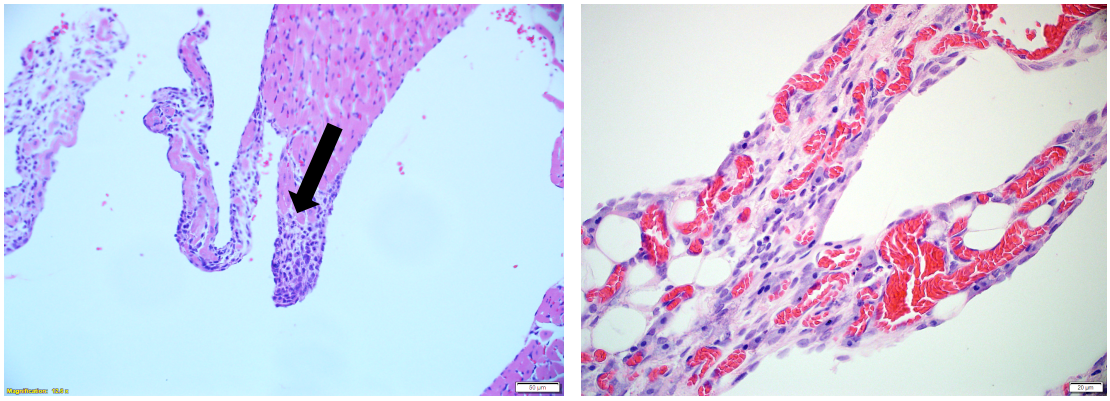

Figure 30: Mononuclear infiltrates in ivalin- exposed Sprague-Dawley rats.
Left: Macrophagic infiltrate in the endocardium of the heart (black arrow) of exposed rat 2 (H&E, x 20). Right: Perivascular mast cells in the connective tissue surrounding the diaphragm of exposed rat 1 (H&E, x 40).

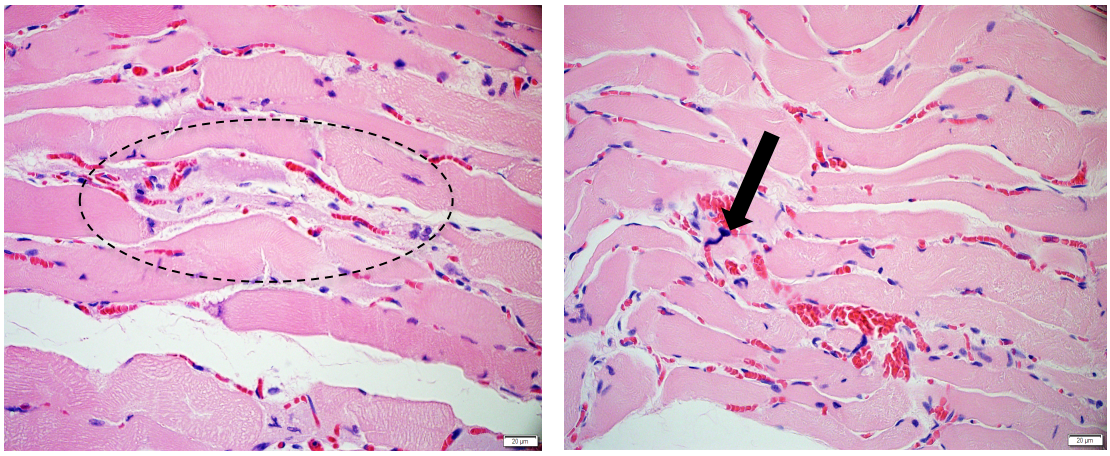

Figure 31: Myofibre and nuclear findings in diaphragm of exposed rat 1.
Segmental myofibre lysis associated with mild macrophagic infiltration (left, dashed oval) and enlarged, irregular, hyperchromatic nuclei (right, arrow) (H&E, x40).

4.4.2.3 Skeletal muscle; Gluteus maximus *and* Triceps brachii *muscle*

In rat 2, a single small section of skeletal muscle exhibited moderate, multifocal widespread segmental necrosis with fragmentation of myofibres. This was accompanied by moderate infiltration of macrophages, and activation of satellite cells/satellitosis (figure 32).

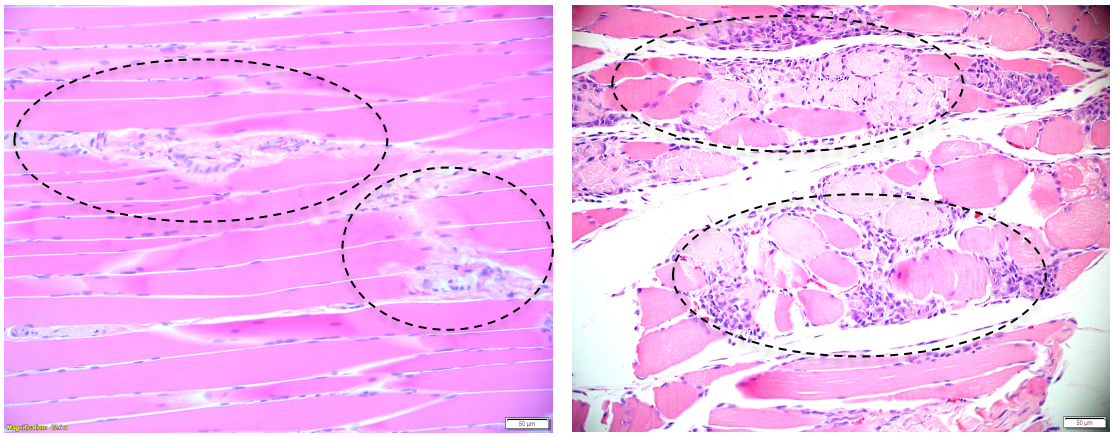

Figure 32: Mild multifocal segmental myofibre lysis and fragmentation, accompanied by macrophagic infiltration (dashed ovals), in the skeletal muscle of exposed rat 2.
Left: Longitudinal section (H&E x 40). Right: cross-section (H&E x 20).

4.4.2.4 Liver

Mild leukocytic infiltrates were present in the periportal interstitium and within portal venule walls of most exposed rats (2, 3, 4 and 6) as well as control rats (13 and 15) (figure 33). Similar small aggregates were scattered in the midzonal area of the hepatic lobules. These infiltrates, occasionally associated with megakaryocytes and also present in control animals, likely EMH.

Mild hepatocyte vacuolation was observed in one exposed animal (rat 2) and three control animals (rats 11, 13 and 15).

In rats 2 and 6, scattered periportal hepatocytes, particularly in the limiting plate, appeared hypereosinophilic with misshapen, pyknotic nuclei, indicating early cellular injury (figure 33). Additionally, the liver of rat 2 displayed moderate congestion, and rat 6 had karyorrhectic nuclear debris scattered in the sinusoids and periportal interstitium. These changes were similar to those reported in mouse 5 and are of unknown significance.

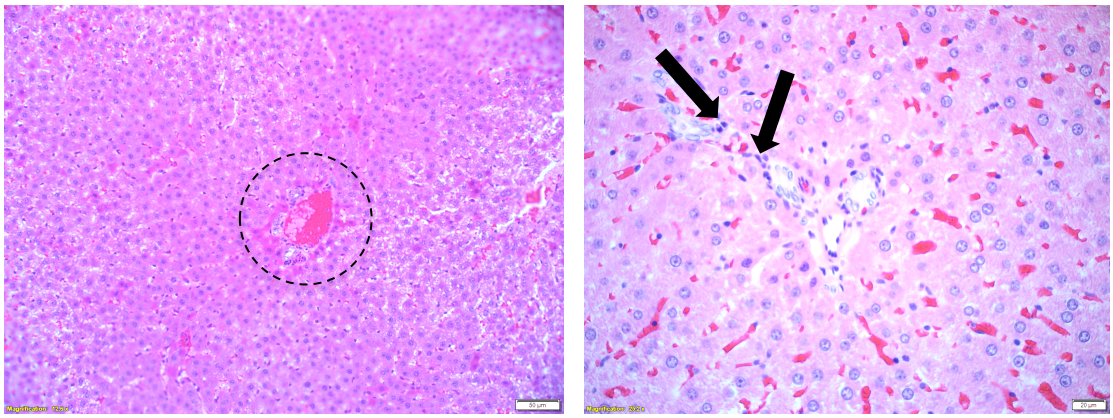

Figure 33: Periportal leukocytic infiltrate and hypereosinophilic hepatocytes in the periportal area of exposed and control rats.
Left: Periportal hypereosinophilia and pyknotic nuclei in exposed rat 2 (within dashed circle). Periportal leukocytic infiltration in control rat 13 (right) (black arrows). H&E stain, x 40.

4.4.2.5 Lungs

In all exposed and control rats, severe congestive atelectasis was observed. Similar to the findings in mice, this change was considered to be a result of terminal cardiorespiratory failure and post mortem changes.

4.5 Desmin immunohistochemistry (IHC)

4.5.1 CD-1 Mice and ruminants

Desmin IHC was performed on diaphragm, oesophagus, heart and triceps muscle sections from exposed mouse 3 (surviving mouse from exposed group 1) and control mouse 20. Additionally, IHC was applied to the oesophageal sections from two diagnostic cases (a sheep and a cow) suspected of succumbing to vermeersiekte.

In general, desmin immunoreactivity varied across muscle specimens from mice and ruminant diagnostic cases, showing inconsistency between and even within individual striated myofibres of both skeletal and cardiac tissues. In the ruminant diagnostic cases, obviously degenerate and necrotic myofibres exhibited a notable lack of desmin immunoreactivity. However, desmin positivity was also reduced to absent in some morphologically normal myofibres in the ruminant oesophageal specimens (figure 34). Similarly, non-swollen

hypereosinophilic myofibres in both mice lacked desmin reactivity, despite retaining visible cross striations in longitudinal sections.

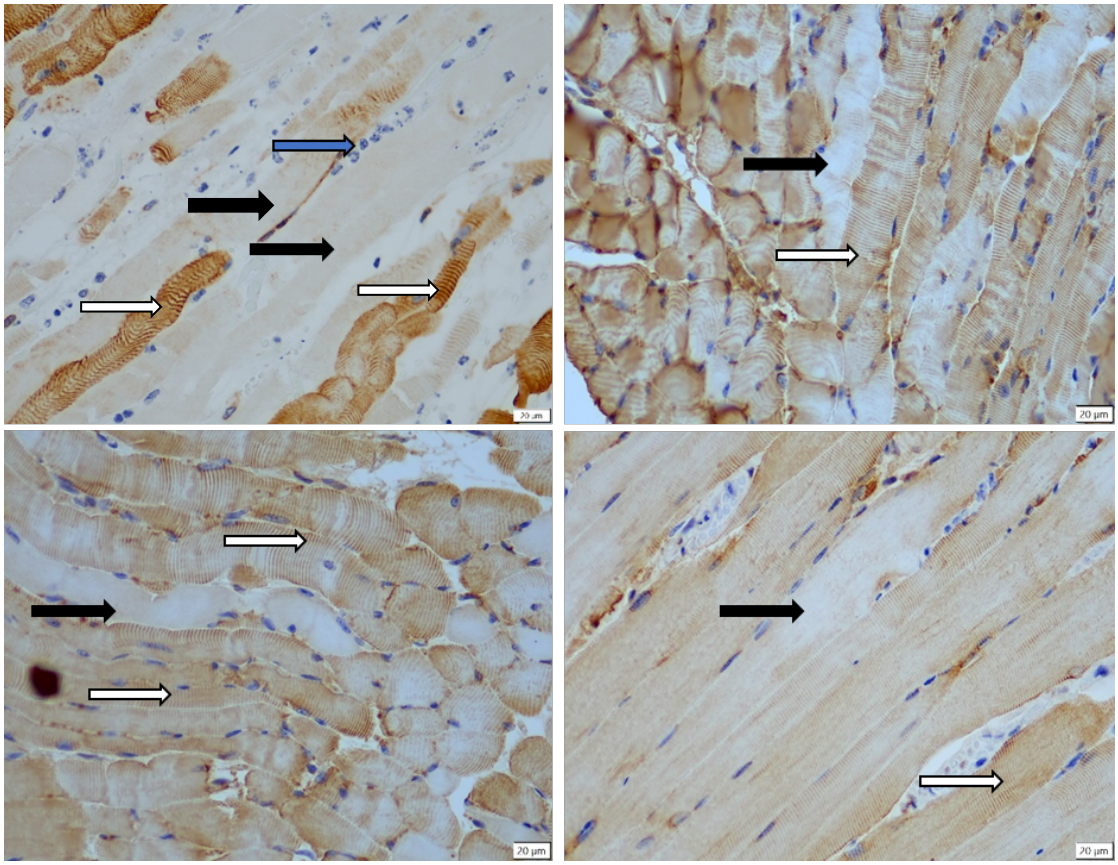

Figure 34: Variable desmin reactivity in ovine and mouse oesophageal tissue.
Top left: Sheep diagnosed with vermeersiekte (x 40). Top right: Diaphragmatic tissue from exposed mouse 3 (x 40). Bottom left: Diaphragm from control mouse 20 (x 40). Bottom right: Skeletal muscle from control mouse 20 (x 40). Black arrows denote myofibres or segments of myofibres showing a lack of desmin reactivity. White arrows show myofibres with desmin reactivity. Note in the ovine tissue (top left), the presence of neutrophils in an area of muscle pathology (blue arrow).

4.5.2 Sprague-Dawley Rats

Desmin IHC was performed on all tissues previously examined under light microscopy (section 7.4.2).

Rat 1 (exposed) exhibited generally reduced immunoreactivity in the heart, oesophagus, diaphragm and skeletal muscle. The reduced immunoreactivity corresponded to areas of suspected contraction artefacts and mildly swollen myofibres, but myofibres not obviously affected by contraction also exhibited reduced immunoreactivity.

Rat 2 (exposed) exhibited generally reduced immunoreactivity in the heart and skeletal muscle, with stronger immunoreactivity in the oesophagus and diaphragm. The reduced immunoreactivity correlated with contraction artefacts in the heart and skeletal muscle,

although non-contracted myofibres also exhibited reduced immunoreactivity. Satellite cells among the macrophagic cell infiltrate in the skeletal muscle displayed immunoreactivity.

Rat 3 (exposed) exhibited generally moderate to strong immunoreactivity in the oesophagus, diaphragm, heart and skeletal muscle. Areas of reduced immunoreactivity were associated with suspected contraction artefacts, but non-contracted myofibres also demonstrated reduced immunoreactivity.

Rat 4 (exposed) exhibited generally moderate to strong immunoreactivity in the oesophagus, diaphragm, heart and skeletal muscle. Areas of reduced immunoreactivity correlated with foci of hypereosinophilic, slightly swollen fibres in the oesophagus and diaphragm (figure 35). In the heart, hypereosinophilic and swollen myofibres surrounding the suspected cardiopuncture site also showed loss of immunoreactivity.

Rat 6 showed reduced immunoreactivity in the diaphragm, but stronger immunoreactivity in the oesophagus, heart and skeletal muscle. Reduced immunoreactivity aligned with suspected contraction artefacts, although reduced immunoreactivity was also observed in non-contracted myofibres.

In the control rats (11, 13 and 15), immunoreactivity varied, corresponding to contracted myofibres, and also appearing in non-contracted myofibres. Rats 13 and 15 exhibited reduced skeletal muscle reactivity, and the hypereosinophilic and swollen myofibres surrounding rat 15's cardiac puncture site also showed reduced reactivity (figure 35).

Additionally, as a general observation, only rare myofibre nuclei exhibited desmin reactivity. Variable desmin staining was also noted in the vascular smooth muscle of the liver and bronchiolar smooth muscle of the lung.

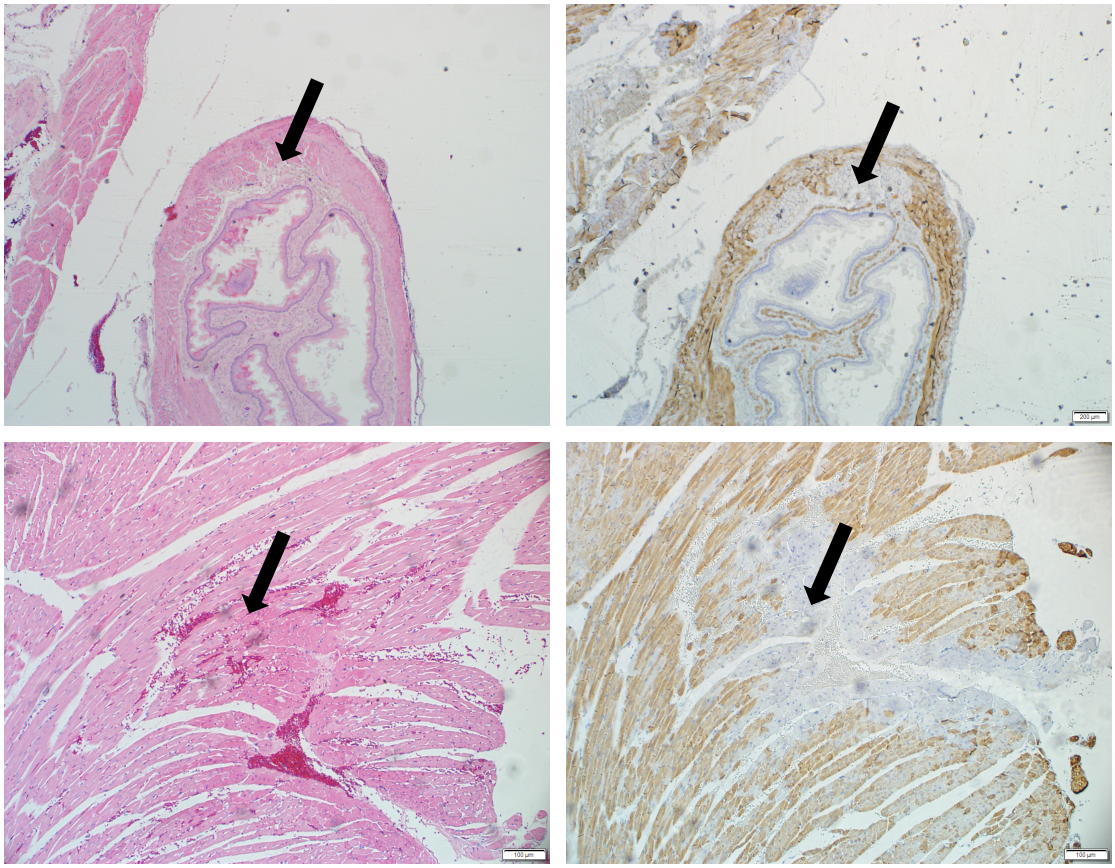

Figure 35: H&E staining and desmin immunohistochemistry applied to the same oesophageal and cardiac tissue specimens in exposed and control rats.
Top left and right: Rat 4 (x 4). Note the lack of desmin reactivity in areas with aggregates of hypereosinophilic myofibres (black arrows).
Bottom left and right: Rat 15 (x 10) Note the lack of desmin reactivity in hypereosinophilic myofibres at the suspected cardiocentesis site (black arrows).

4.6 TEM

4.6.1 Sprague-Dawley Rats

The ultrastructure of the diaphragm, oesophagus, cardiac muscle and skeletal muscle from all exposed rats (1, 2, 3, 4 and 6) and two control rats (11 and 13) were qualitatively evaluated using transmission electron microscopy (TEM).

4.6.1.1 Heart

Examination of heart muscle from the exposed group revealed several pathological ultrastructural changes that were also observed in control samples, though less frequently.

All exposed rats and both control rats presented with varying degrees of abnormally folded myonuclear profiles. Occasionally myonuclei were elongated (particularly in rats 1 and 6), became fragmented (rat 1, 2 and 6), had chromatin condensation with marginalisation and

early pyknotic changes (all rats) and/or exhibited multiple prominent nucleoli (rat 1, 2, 3 and 6).

The extent and severity of mitochondrial abnormalities observed were less than those seen in other tissues such as the diaphragm and skeletal muscle. However, the abnormal changes found included hydropic change (rat 3), shape changes (rat 2 and 3), the presence of inclusions (rat 1), and alterations in the cristae (pattern abnormalities, cristae loss and type I para crystalline inclusions in rat 1, 2, 3, 6 and 13).

Small degrees of myofibrillar degeneration and dilation of the sarcoplasmic reticulum were observed. However, similar changes were present in the control samples and were not considered pathological.

Abnormalities were found in the majority of endomysial capillaries and blood vessels in the exposed group. These included hypertrophy and microvillus transformation of the endothelial cells, as well as electron dense inclusions within the endothelial cells and the underlying connective tissue.

4.6.1.2 Diaphragm

Nuclear abnormalities, most notably an irregularly folded nuclear envelope, were observed in rats 1, 2, 3, 4 and 11. A few myonuclei were located more centrally within the myocytes, occasionally showing mild chromatin condensation, marginalisation, and early pyknotic changes (rat 1, 2, 4 and 11) (figure 36).

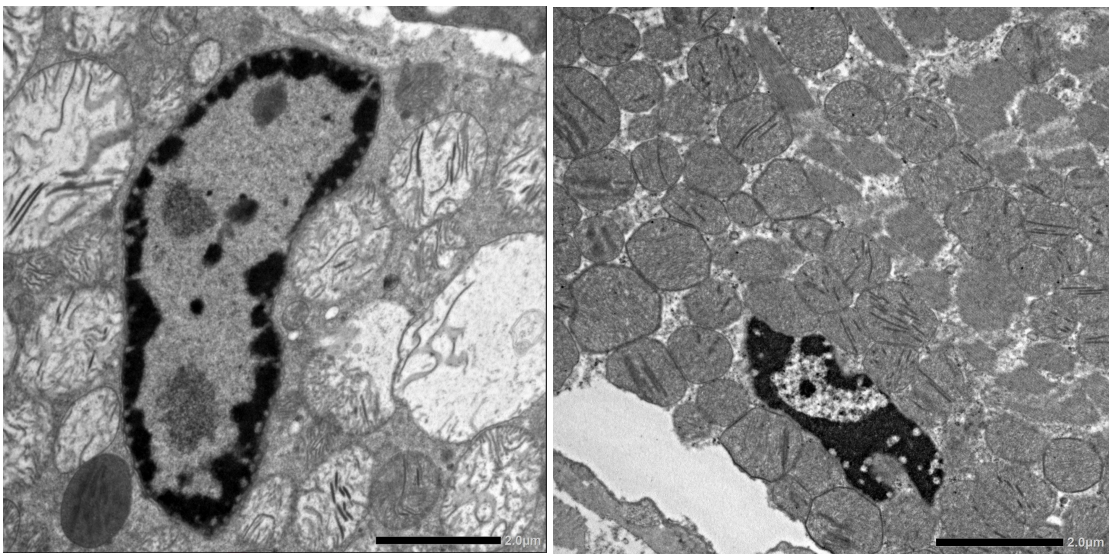

Figure 36: TEM nuclear findings in exposed rats.
Left: Chromatin condensation and marginalisation in the diaphragm of exposed rat 1.
Right: Early pyknotic changes and mitochondrial proliferation in the diaphragm of exposed rat 4.
.

Mitochondrial abnormalities were noted in all evaluated rats, including hydropic change, shape alterations, proliferation, inclusions, compartmentalisation and alterations in the cristae (pattern abnormalities, cristae loss, and type I paracrystalline inclusions) (figures 36, 37 and 39).

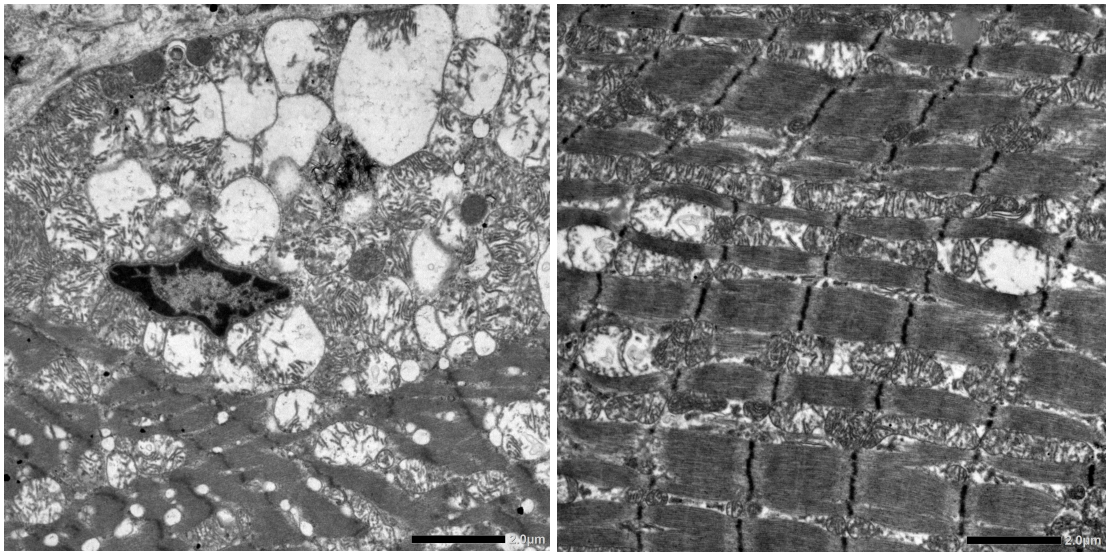

Figure 37: TEM mitochondrial swelling, proliferation and loss of cristae in the diaphragm of exposed and control rats.
Left: Exposed rat 2. Right: Control rat 11.

Myofibrillar loss, varying degrees of disorganisation of the fibrils, and dilation of the sarcoplasmic reticulum were noted in rats 1, 3, 4, 6 and 11. Some z-line streaming was seen in rats 3 and 4 (figure 39). In fibres with myofibrillar loss, subsarcolemmal accumulations of amorphous and granular material were prominent (figure 38). A few myocytes presented with a circular myofibrillar arrangement (rat 3 and 4). Necrotic fibres with a complete loss of myofibrils and containing granular, granulofilamentous, electron dense amorphous, as well as crystalline material were observed in rats 1, 2, 3 and 11 (figure 38).

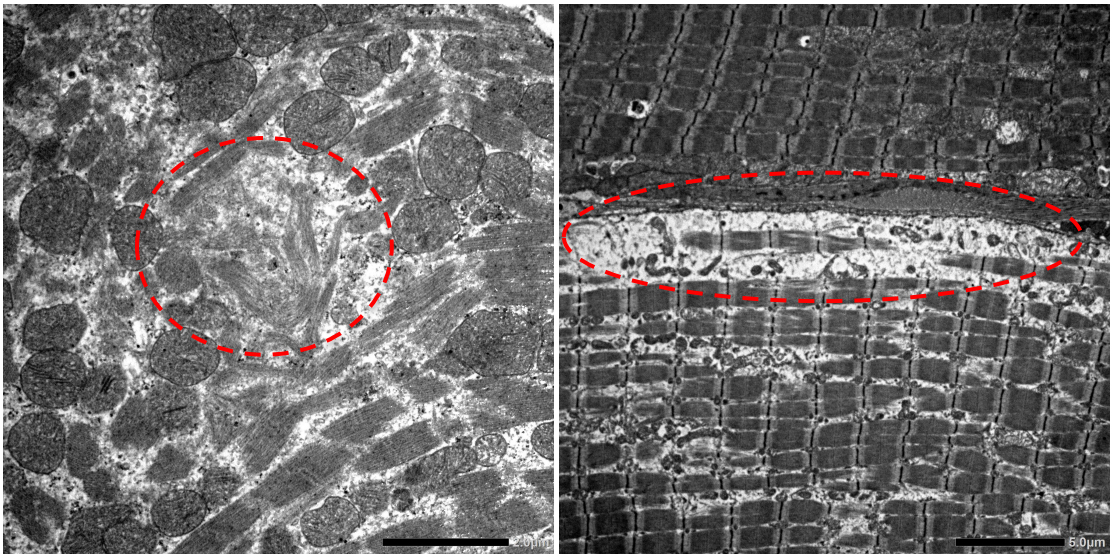

Figure 38: TEM myofibrillar changes in exposed and control rats.
Left: Myofibrillar loss and disorganisation in the diaphragm of exposed rat 4 (dashed oval). Right: Myofibrillar loss and subsarcolemmal amorphous and granular appearance in the diaphragm of control rat 11 (dashed oval).

The majority of abnormal ultrastructural features observed were noted in the diaphragm samples of all animals (control and exposed). However, z-line streaming, and mitochondrial inclusions and compartmentalisation were only seen in the exposed animals. The extent and severity of pathological changes were greater in exposed animals, especially rats 1, 3 and 4 (figure 39).

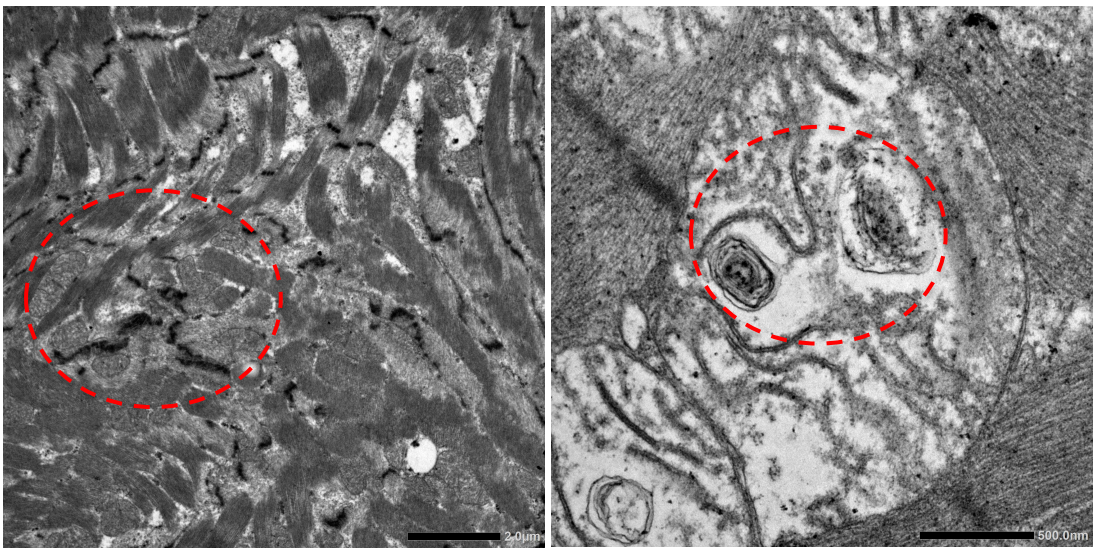

Figure 39: TEM-diagnosed pathological features in the diaphragms of exposed rats only.
Left: Z-line streaming in the diaphragm of exposed rat 3 (dashed oval).
Right: Mitochondrial inclusions in the diaphragm of rat 1 (dashed oval).

4.6.1.3 Oesophagus

Although several ultrastructural abnormalities were observed in the oesophageal tissue, the differences between control and exposed samples were minor. The most prominent

pathological features included changes in the myocyte nucleus, myofibrils, and to a lesser extent, the mitochondria.

Myonuclei often exhibited irregular nuclear profiles, sometimes appearing elongated and abnormally positioned in the centre of the myocyte (all rats, but more consistently in 1 and 4). A few mitochondrial changes were also observed, including swelling with matrical lucency, shape changes, and occasionally type I paracrystalline inclusions (particularly in rats 1, 3, 6 and 11).

Several fibres presented with varying degrees of myofibrillar loss (all rats) and subsarcolemmal accumulations of granular material (rats 3, 4 and 6). Occasionally, and only in some samples, myofibrillar disorganisation, abnormal circular myofibrillar arrangement, and minor sarcoplasmic reticulum dilation were observed (rats 1, 3, 6 and 11).

The most pronounced difference between the exposed and control groups was the length of the nucleus; several myonuclei were elongated in the exposed group, while few to none were elongated in the control group (figure 40). In addition, the control group exhibited less myofibrillar loss and fewer subsarcolemmal granular accumulations.

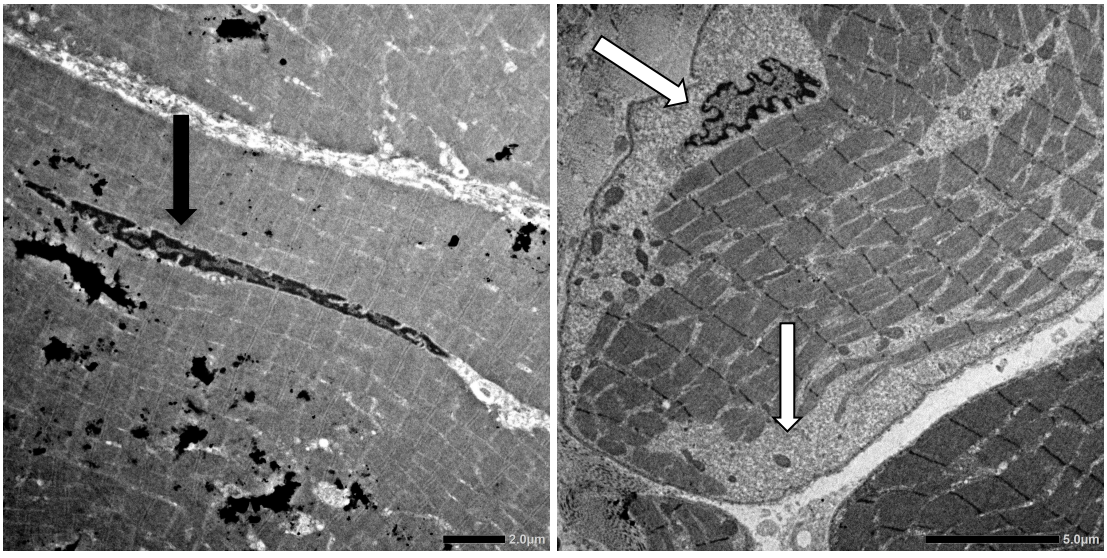

Figure 40: TEM oesophageal nuclear and myofibrillar changes noted in exposed rats.
Left: Myonuclear elongation in oesophageal tissue of exposed rat 1 (black arrow). The dark irregular patches in this image are artefactual stains.
Right: Irregular myonuclear profile and myofibrillar loss (white arrows) in oesophageal tissue of exposed rat 3.

4.6.1.4 Skeletal muscle

Myonuclei in all samples from both the exposed and control rats exhibited ultrastructural abnormalities, most notably irregularly folded nuclear profiles. Other nuclear changes, such as abnormal central positioning (rats 3 and 4), elongation, and condensation and margination

of the chromatin (rats 1, 4 and 6) were observed only in some of the exposed rat samples. A marked increase in the number of mitochondria was observed in skeletal muscle from some of the exposed rats (rats 1, 3, 4 and 6). Other mitochondrial changes (swelling, shape changes, type I para-crystalline inclusions) varied between the exposed muscle samples in extent and severity, and also occurred in the control rat samples. Dilation of the sarcoplasmic reticulum, as well as myofibrillar degeneration, disorganisation, and circular arrangement, were observed in some samples from both the exposed and control groups. However, the muscle in the exposed rat group was more severely affected.

5 DISCUSSION

The high level of mortality seen in CD-1 mice was not anticipated in view of literature suggestions that a subcutaneous dose of 250 mg/kg in guinea pigs and mice was toxic, but not lethal (Vermeulen, 1978; Coleman *et al.*, 1984). The most conservative estimate of median lethality calculated using the Hill's model, 164 mg/kg BW, was selected as the starting point for more accurate LD_{50} determination in rats, using the OECD UDP. Similarly, the slope of the most conservative dose-response curve in mice was used to inform the dose increments for the OECD UDP in rats, though it was felt that a gradient of 33 was too steep and practically unworkable. Therefore, a slope value of 8 was used.

The LD_{50} in rats of 135.4 mg/kg, as estimated by the maximum likelihood method in the OECD UDP, is thus in line with the simulations and predictions made for the mice. However, it should be noted that the OECD UDP is designed to estimate median lethality for risk assessment purposes and the stopping criteria are therefore to minimise animal usage, thus giving a very wide confidence interval. Whilst this was a pilot study, ascertaining median lethality more accurately, and within a narrower confidence interval, would require a more traditional lethality study using larger number of rodents. OECD TG 401 provides for such research, nevertheless, it is no longer endorsed by the OECD (OECD, 1987) and is not ethically warranted in view of the aims of this study.

There is a paucity of data published on rodent sesquiterpene lactone median lethality, though two studies are relevant. Firstly, Kim *et al.* (1980) reported median lethal doses of 3.08 to >200 mg/kg BW for different *Helenium* and *Hymenoxys* spp. sesquiterpene compounds, dissolved in a dimethyl sulphoxide vehicle, and injected intraperitoneally in female albino mice. Mexicanin-E (LD_{50} 3.08 mg/kg BW) and helenalin (LD_{50} 9.86 mg/kg BW), both containing a

cyclopentenone and a α-methylene-y-lactone alkylating functional group, had toxicity levels of *c.* 10 – 60 times that of other sesquiterpene lactones each containing only one alkylating centre, such as psiltropin (LD_{50} of 112.25 mg/kg BW), hymenoxon dimethyl ether (LD_{50} of 141.42 mg/kg BW) and tenulin (LD_{50} of 184.65 mg/kg BW). Mexicanin-E was also dosed subcutaneously in mice and the LD_{50} from this route of exposure was 1.59 mg/kg (Kim, 1980). Secondly, a study by Shivappa *et al.* (2016) demonstrated the oral LD_{50} of synthetic parthenolide in Swiss albino mice to be *c.* 200 mg/kg BW (Shivappa, 2016).

Ivalin, with one conjugated α-methylene-y-lactone (Fouche *et al*. 2021) therefore has an LD_{50} more consistent with psilotropin, hymenoxon dimethyl ether and tenulin. The lower subcutaneous median lethality for mexicanin-E in mice, suggests slightly greater bioavailability of highly lipophilic sesquiterpene compounds in an amphoteric vehicle, from subcutaneous exposure compared to oral exposure. This toxicokinetic difference may be due to gastrointestinal presystemic elimination or the presence of efflux transporters (Yu *et al*., 2021), and is further discussed with reference to vermeersiekte in sheep below. Though a subcutaneous LD_{50} for parthenolide in mice or rats is not readily available in the literature, the oral median lethality of this sesquiterpene lactone of *c.* 200 mg/kg, which has both a conjugated α-methylene-y-lactone and an epoxide functional group (Freund *et al*. 2020), is much higher than that of mexicanin, following oral exposure. It is possible that gastrointestinal metabolism or transporter protein efflux mechanisms may also reduce oral bioavailability of parthenolide, however more work is needed to investigate this further.

Systemic clinical signs from animals in the study by Kim *et al.* (1980) were consistent with those observed in mice and rats dosed with ivalin in this study; anorexia, significant weight loss, depression and convulsions (mainly noted in mice). In the study by Kim *et al.* (1980), mice dosed orally developed peritonitis and abdominal fluid accumulation and mice dosed subcutaneously developed dermal erosions (Kim *et al*, 1980). In subcutaneous ivalin-exposed mice and rats from this study, severe subcutaneous oedema and dermal erosions were also noted.

The irritant effects of sesquiterpene lactones in some edible, herbaceous and ornamental Asteraceae are noted in the literature, including plants such as Chicory (*Cichorium intybus* var. *sativum* L.) containing grosheimin and guaianolide ixerisoside D, Dandelion (*Taraxacum officinale* L) containing Taraxinic acid-1ƒ-O-b—glucopyranoside and Feverfew (*Tanacetum parthenium*) containing parthenolide (Denisow-Pietrzyk *et al,* 2019). Hypersensitisation and

local contact pruritis, oedema and inflammation are reported to be a major reason why some sesquiterpene lactone therapies, such as parthenolide as a chemotherapeutic agent, are still not in clinical use (da Silva *et al* 2021). A recent review of sesquiterpene lactone dermal toxicity suggests that up regulatory effects on gene expression of inflammatory cytokines such as TNF-α, IL-1, IL-4, IL-6, IL-8, IL-12, MCP-1, 5-LOX, and COX-2 may be involved (da Silva *et al* 2021). The chronic deterioration and weight loss observed in rat 1, which also showed mild anaemia, electrolyte disturbances and bacteraemia on histopathology, could also be attributed to the severe irritation and self-trauma experienced by the animal following ivalin exposure.

The mildly swollen, hypereosinophilic myofibres noted in light microscopy studies of the striated muscle in exposed mice, which often retained cross-striations, did not show a concurrent inflammatory response or internalised nuclei. These findings were also observed in control mice, suggesting that they were likely artefacts. Notably, the typical hypereosinophilic contraction bands described in the literature were not convincingly present (McInnes, 2017). In mouse 3, which was also evaluated for biochemistry, this interpretation was supported by a normal CK level compared to control animals. Similarly, mildly swollen hypereosinophilic myofibres, also thought to be artefacts, were noted in rat cardiac, oesophageal and diaphragmatic tissues from the majority of both exposed and control rats, sometimes accompanied by hyperchromatic myonuclei. Although muscles were pinned to reduce contraction artefacts, this method was not entirely effective. The authors suggest more complete clamping of the entire muscle belly, perhaps by cutting thin sections of 2 – 3 mm and using a staple or muscle crimping system.

In addition to myofibres thought to be affected by contraction (though lacking the characteristic light microscopy banded appearance), there were areas of myofibrillar damage in rats. This damage was particularly notable in the diaphragm of rat 1, myocardium of rat 2, and, to a lesser extent, the skeletal muscle of rat 2. However, the affected areas were isolated and difficult to find, with only a single focus observed in the skeletal muscle of rat 2. Generally, changes in these myofibres included vacuolisation, enlargement and loss of cross-striations, sometimes accompanied by mild lysis, macrophagic infiltration and regeneration. Nuclear changes included centralisation, enlargement, membrane disruption and loss of chromatin structure. Due to the sporadic and inconsistent nature of the lesions, rat tissue samples were submitted for TEM.

Whilst myofibrillar loss, disorganisation and necrosis were noted on TEM analysis of the diaphragm in rat 1, some or all these findings were also noted in all the other exposed rats and in control rat 11. Similarly, nuclear changes correlating to histopathology such as irregular nuclear profiles, nuclear centralisation and early pyknotic changes were noted in rat 1, but this was also the case in some other exposed rats (rats 2, 3 and 4) and control rat 11. In rat 2, which had a single focal lesion of myonecrosis in the skeletal muscle on light microscopy, TEM did not reveal any myofibrillar disorganisation, necrosis, or z-line streaming (note that light microscopy and TEM were not performed on exactly the same muscle specimens).

Ultrastructural study therefore supports the histopathology findings of myofibrillar damage and associated nuclear changes in rats 1 and 2 as being either fairly isolated and mild, or incidental. Furthermore, whilst muscle damage from sesquiterpene lactone exposure may have been expected to occur in rat 1, which was euthanased 4 days after dosing, it would not have been expected in rat 2, which died acutely overnight. In rats 3 and 4, both of which survived following ivalin exposure, there was minimal noticeable pathology compared to the controls, even at an ultrastructural level. Despite this, both rats had moderately raised AST and CK levels. Therefore, there was a poor correlation between the dose, clinical observations, and pathological findings, as well as inconsistency between the methods (light microscopy, ultramicroscopy and clinical pathology) used to assess muscle damage.

Desmin staining was ineffective at distinguishing injured from non-injured myofibres. In both mice and rats, desmin immunoreactivity varied in intensity and distribution across all striated muscle tissues. Even within the same myofibre, immunoreactivity displayed a gradient from strong to no reactivity, with varying degrees of partial reactivity in between. Typically, desmin immunoreactivity was reduced in myofibres with suspected contraction artefacts and in areas of suspected isolated myofibre injury. However, it was also greatly reduced or even segmentally absent in some normal myofibres. Consequently, in our experience, loss of desmin expression in striated myofibres was not specific to injury, as it also occurred in uninjured fibres. This phenomenon is not described in the literature, indicating a need for further investigation. Future studies should ensure more careful muscle sampling to prevent artefacts, implement automated staining, and explore the use of alternative antibodies and immunodetection kits.

In view of the effect sesquiterpene lactones have *in vitro* on mitochondrial function (Hanson *et al.*, 1970; van Aswegen *et al*, 1979; Hall *et al.*, 1980; Klimek *et al.*, 1981; Woynarowski *et al.*,

1981; van Aswegen *et al*, 1982; Coleman *et al.*, 1984; Caspar *et al.*, 1986; Narasimhan *et al.*, 1989), and the findings noted by van der Lugt and van Heerden (1993), these organelles were also evaluated under TEM. Whilst pathological mitochondrial changes were observed in exposed rats in the current study, they were also present in control rats. The diaphragm was noted as displaying mitochondrial hydropic changes, shape changes, proliferation, the presence of inclusions, compartmentalisation and alterations in the cristae. This occurred with higher frequency in exposed rats 1, 3 and 4 compared to other exposed or control rats. However, in the heart, it was exposed rats 1, 2 and 3 which appeared to display more frequent mitochondrial changes and all exposed rats and control rats displayed similar mitochondrial changes in skeletal muscle. Therefore, although proper quantification is needed for definitive conclusions, there does not appear to be a correlation between findings in tissues from the same animal.

In the liver of rodents in this study, hypereosinophilic hepatocytes with hyperchromatic nuclei and surrounding foci of karyorrhectic nuclear debris and inflammation were noted in exposed mouse 5 and both exposed rats 2 and 6 suggesting mild, isolated hepatonecrosis. Although no blood could be collected from any of these animals due to acute death overnight, hepatic biochemistry markers in exposed mouse 3 and exposed rats 1, 3 and 4 were not significantly raised compared to control animals. In the absence of clinical signs associated with hepatobiliary disease and clinical pathology assessment, the significance of this finding in relation to ivalin exposure is unknown.

In domestic sheep and cattle affected by vermeersiekte, the disease is one of chronic striated muscle damage, with mortality often resulting from aspiration pneumonia and progressive debilitation. Histopathology and ultrastructural changes of myofibrillar necrosis and inflammatory cell infiltration are notable and consistent, and fit with this clinical picture (Pienaar *et al*., 1973; van der Lugt and van Heerden, 1993). In this study using mice and rats, mortality was acute, with either no or mild pathological findings that were infrequent and inconsistent in both rodent species evaluated. Furthermore, desmin staining of striated muscle could not distinguish pathology from contraction artefacts or even normal muscle tissue.

Acute single-dose parenteral exposure of rodents to purified sesquiterpene lactones, therefore, does not provide a viable laboratory animal model for further study of *Geigeria* spp. ingestion in ruminants. However, the calculated LD_{50} from rats could provide an estimated starting dose for further study of *Geigeria* extracts in sheep, potentially reducing

the need for large dosing volumes or oral administration of plant material. A possible reason for the different clinical and pathological outcomes observed in sheep ingesting *Geigeria* plants may be related to differences in exposure duration and route. Although kinetic data on sesquiterpene lactones are limited, a recent review indicates that while these compounds are highly lipophilic and therefore well absorbed, they are extensively metabolised by both phase 1 and 2 enzyme systems in the gastrointestinal tract (Yu *et al.*, 2021). Furthermore, gastrointestinal pGp transporter efflux proteins further contribute to variable or reduced oral absorption. Interspecies anatomical and physiological variation may also play a role (Yu *et al.*, 2021). Therefore, pre-systemic elimination (including possible ruminal microbial degradation), combined with chronic plant ingestion over several weeks, may lead to prolonged, but lower levels of exposure to sesquiterpene lactones in sheep, resulting in muscle pathology. This contrasts with the acute mortality and minimal pathology observed following a single large dose administered subcutaneously in rodents.

There is also a possible difference in the mechanism of acute versus chronic sesquiterpene lactone toxicity. While pathology from affected ruminants and *in vitro* cell culture studies suggest that desmin disruption may play a role in loss of muscle integrity, this could not be verified *in vivo* in this study. Desmin aggregation has been noted in Arabian horses with exertional rhabdomyolysis and warmblood horses with myofibrillar myopathy (McKenzie *et al.,* 2016; Valberg *et al*., 2017. In both studies, desmin aggregation occurred to a higher degree in horses affected by the respective condition compared to control horses (McKenzie *et al.,* 2016; Valberg *et al*., 2017). While desmin aggregation occurred in murine myoblastic cell lines following sesquiterpene lactone exposure (Botha *et al.* 2019; Botha *et* al., 2020), this was not observed in this study following *in vivo* ivalin exposure.

Furthermore, whilst no major differences existed in mitochondrial pathology between exposed and control rats, the studies by van Aswegen *et al.* (1979) and van Aswegen *et al.* (1982) suggest that interference with mitochondrial oxidative phosphorylation could account for the acute death seen in rodents, and even on occasion, in sheep. This is supported by several other reports of sesquiterpene interference with glycolytic and mitochondrial energy processes (Hanson *et al.*, 1970; Hall *et al.*, 1980; Klimek *et al.*, 1981; Woynarowski *et al.*, 1981; Coleman *et al.*, 1984; Caspar *et al.*, 1986; Narasimhan *et al.*, 1989). This suggests that the mechanism of toxicity following acute sesquiterpene lactone exposure is related to mitochondrial dysfunction and not muscle pathology, as occurs following chronic exposure. It is also possible that in chronic exposure, both desmin disruption and related effects on

mitochondria, and direct effects on mitochondrial functioning may be involved in muscle pathology. This may explain the mitochondrial pathology noted by van der Lugt and van Heerden (1993) and is also commented on in a recent paper by Agnetti *et al.*, 2022 (Agnetti *et al.*, 2022), though there were no major mitochondrial ultrastructural differences noted between exposed and control rats in this study.

6 CONCLUSION

The approximate subcutaneous LD_{50} of ivalin, purified from *Geigeria aspera*, in Sprague-Dawley rats is 134.5 mg/kg. Whilst this route of exposure to purified plant extract is not the usual route of exposure to sesquiterpene lactones from plants in ruminants, the calculated median lethality could provide a starting point for further studies in sheep. It is concluded that acute toxicity, with high mortality and little pathology, is a result of different toxicodynamics, compared to chronic toxicity where significant muscle pathology occurs. It is possible that longer exposure to lower doses of sesquiterpene lactones, as occurs orally in vermeersiekte, compared to acute subcutaneous exposure to a larger dose, may account for this difference in toxic mechanism of action.

Toxicokinetic studies of ivalin via oral and parenteral routes of exposure in both ruminant and rodent species would potentially enhance our understanding of the pathogenesis of the muscle pathology in vermeersiekte. As the subcutaneous administration of these compounds appears extremely irritant, intravenous exposure at lower starting doses, could potentially reduce inflammatory effects at the site of exposure and bypass pre-systemic elimination. This would negate the need for using large volumes of plant extract.

7 REFERENCES

Agbulut, O., Li, Z., Périé, S., et al. (2001). Lack of desmin results in abortive muscle regeneration and modifications in synaptic structure, *Cell Motility and the Cytoskeleton*, 49 (2); pp 51-66. DOI: 10.1002/cm.1020.

Agnetti, G., Herrmann, H. & Cohen, S. (2022). New roles for desmin in the maintenance of muscle homeostasis, *The FEBS journal,* 289, pp. 2755-2770. DOI: 10.1111/febs.15864.

Anderson, L. A., De Kock, W. T., Pachler, K. G., et al. (1967). The structure of vermeerin: A sesquiterpenoid dilactone from *Geigeria africana* Gries, *Tetrahedron,* 23, pp. 4153-4160. DOI: 10.1016/S0040-4020(01)97928-1.

Anderson, L. A., De Kock, W. T., Nel, W., et al. (1968). Gafrinin, a sesquiterpenoid lactone from *Geigeria Africana* gries—I: Revised structure, *Tetrahedron,* 24, pp. 1687-1699. https://doi.org/10.1016/S0040-4020(01)82475-3.

ASTM. 1987. *E 1163-87, Standard Test Method for Estimating Acute Oral Toxicity in Rats*, American Society for Testing and Materials, Philadelphia, US.

Aigner, B. C., Heumann, C. I. & Ahmad I. E. (2023). Variability of clinical chemical and hematological parameters, immunological parameters, and behavioral tests in data sets of the Mouse Phenome Database, *Plos One*, 18 (7). DOI: 10.1371/journal.pone.0288209.

Barton, D. H. & Levisalles, J. E. (1958). Sesquiterpenoids. Part XI. The constitution of geigerin, *Journal of the Chemical Society (Resumed)*, 912, 4518. DOI: 10.1039/jr9580004518.

Bohlmann, F. & Gupta, R. K. (1982). Guaianolides and furanosesquiterpenes from *Ursinia nana*, *Phytochemistry,* 21, pp. 1309-1312. DOI: 10.1016/0031-9422(82)80131-3.

Botha, C. J., Gous, T. A., Penrith, M. L., et al. (1997). Vermeersiekte caused by *Geigeria burkei* Harv. subsp. *burkei* var. hirtella merxm. in the northern province of South Africa, *Journal of the South African Veterinary Association,* 68, pp. 97-101.

Botha, C. J., Clift, S. J., Ferreira, G. C. H., et al. (2017). Geigerin-induced cytotoxicity in a murine myoblast cell line (C2C12), *The Onderstepoort Journal of Veterinary Research,* 84, pp. e1-e7. DOI: 10.4102/ojvr.v84i1.1465.

Botha, C. J., Venter, E. A., Ferreira, G. C. H., et al. (2019). Geigerin-induced disorganization of desmin, an intermediate filament of the cytoskeleton, in a murine myoblast cell line (C2C12), *Toxicon,* 167, pp. 162-167. DOI: 10.1016/j.toxicon.2019.06.014.

Botha, C. J., Mathe, Y. Z., Ferreira, G. C. H., et al. (2020). Cytotoxicity of the Sesquiterpene Lactones, Ivalin and Parthenolide in Murine Muscle Cell Lines and Their Effect on Desmin, a Cytoskeletal Intermediate Filament, *Toxins,* 12. DOI: 10.3390/toxins12070459.

Bruce, R. D. (1985). An up-and-down procedure for acute toxicity testing, *Fundamental and Applied Toxicology,* 5, pp. 151-7. Accession Number: 3987991 DOI: 10.1016/0272-0590(85)90059-4.

Caspar, A. R., Potgieter, D. J. & Vermeulen N., M. (1986). The effect of the sesquiterpene lactones from Geigeria on glycolytic enzymes, *Biochemical Pharmacology*, 35 (3), pp. 493-497. DOI: 10.1016/0006-2952(86)90225-X.

Capetanaki, Y. (2002). Desmin cytoskeleton: a potential regulator of muscle mitochondrial behavior and function, *Trends in cardiovascular medicine,* 12, pp. 339-48.

Chen, Z. (2015). *Sesquiterpene Drugs as Potential Treatment for Hepatocellular Carcinoma (HCC): Preclinical Evaluation of Parthenolide Administered Via Transarterial Chemoembolization in a Rat HCC Tumour Model*. Doctoral dissertation, University of Arkansas for Medical Sciences.

Coleman, P. C., Potgieter, D. J., Aswegen, C. H., et al. (1984). Flavonoids of geigeria, *Phytochemistry,* 23, pp. 1202-1203. DOI: 10.1016/S0031-9422(00)82648-5.

Costa, M. L. S. (2014). Cytoskeleton and Adhesion in Myogenesis, *ISRN Developmental Biology,* 2014, pp. 1-15. DOI: 10.1155/2014/713631.

da Silva, L. P., Borges, B. A., Veloso, M. P., et al. (2021). Impact of sesquiterpene lactones on the skin and skin-related cells? A systematic review of in vitro and in vivo evidence, *Life Sciences*, 265. DOI: 10.1016/j.lfs.2020.118815.

De Kock, W. T., Pachler, K. G. R., Ross, W. F., et al. (1968). Griesenin and dihydrogriesenin, two new sesquiterpenoid lactones from *Geigeria africana* Gries—I: Structures, *Tetrahedron,* 24, pp. 6037-6043. DOI: 10.1016/S0040-4020(01)90987-1.

De Villiers, J. P. (1959). 483. The isolation and structure of geigerinin, a guaianolide, *Journal of the Chemical Society (Resumed)*, 2412. DOI: 10.1039/jr9590002412.

De Villiers, J. P. (1961). 389. The isolation and structure of gafrinin, a sesquiterpenoid lactone from *Geigeria africana*, *Journal of the Chemical Society (Resumed)*, 2049. DOI: 10.1039/jr9610002049.

Denisow-Pietrzyk, M., Pietrzyk Ł. & Denisow, B. E. (2019). Asteraceae species as potential environmental factors of allergy, *Environmental Science and Pollution Research*, 26 (7), pp. 6290-6300. DOI: 10.1007/s11356-019-04146-w.

Dixon, W. J. (1991). Staircase bioassay: the up-and-down method, *Neuroscience and biobehavioral reviews,* 15, pp. 47-50. Accession Number: 2052197 DOI: 10.1016/s0149-7634(05)80090-9.

Domínguez-Oliva, A., Hernández-Ávalos, I., Martínez-Burnes, J., et al. (2023). The Importance of Animal Models in Biomedical Research: Current Insights and Applications, *Animals*, 13, p. 1223. Accession Number: doi:10.3390/ani13071223. https://www.mdpi.com/2076-2615/13/7/1223.

Du Toit, P. J. (1928). Investigations into the cause of Vomeersiekte in sheep, *13th and 14th Reports of the Director of Veterinary Education and Research Part 1.*

Dubińska-Magiera, M., Jabłońska, J., Saczko, J., et al. (2014). Contribution of small heat shock proteins to muscle development and function, *FEBS Letters,* 588, pp. 517-530. DOI: 10.1016/j.febslet.2014.01.005.

EPA. (2023). *Acute Oral Toxicity Up-And-Down-Procedure* [Online], Environmental Protection Agency, Available: https://www.epa.gov/pesticide-science-and-assessing-pesticide-risks/acute-oral-toxicity-and-down-procedure, [Accessed November 2022 2023].

Fletcher, D. A. & Mullins, R. D. (2010). Cell mechanics and the cytoskeleton, *Nature: International Weekly Journal of Science,* 463, pp. 485-492. DOI: 10.1038/nature08908.

Ford, E. J. (1974). Activity of gamma-glutamyl transpeptidase and other enzymes in the serum of sheep with liver or kidney damage, *Journal of Comparative Pathology*, 84 (2), pp 231-243. DOI: https://doi.org/10.1016/0021-9975(74)90064-4.

Fouche, G., Ackerman, L. G. J., Venter, E. A., et al. (2021). Sesquiterpene lactones from *Geigeria aspera* Harv. and their cytotoxicity, *Natural Product Research,* 35, pp. 2353-2359. DOI: 10.1080/14786419.2019.1675068.

Fourie, N. (1991). *Vermeersiekte*. Internal report. Onderstepoort Veterinary Institute. Unpublished.

Fourie, N. (1992). Vermeersiekte. Internal report. Onderstepoort Veterinary Institute. Unpublished.

Freund, R. R., Gobrecht, P., Fischer D., et al. (2020). Advances in chemistry and bioactivity of parthenolide, *Natural Product Reports*, 37 (4), pp. 541-565. DOI: 10.1039/c9np00049f.

Gach, K., Długosz, A. & Janecka, A. (2015). The role of oxidative stress in anticancer activity of sesquiterpene lactones, *Naunyn-Schmiedeberg's Archives of Pharmacology,* 388, pp. 477-486. DOI: 10.1007/s00210-015-1096-3.

Grosskopf, J. F. W. (1964). *Our present knowledge of "vermeersiekte" (geigeria poisoning)*, Printed by the Govt. Printer, Pretoria.

Hall, I. H., Lee, K. H., Williams, W. L Jr., et al. (1980). Antitumor agents XLI: Effects of eupaformosanin on nucleic acid, protein, and anaerobic and aerobic glycolytic metabolism of Ehrlich ascites cells, *Journal of Pharmaceutical Sciences*, 69 (3), pp. 294-7. Accession Number: 7381705 DOI: 10.1002/jps.2600690313.

Hamilton, J. A., Mcphail, A. T. & Sim, G. A. (1962). The structure of geigerin: X-ray analysis of bromogeigerin acetate, *Journal of the Chemical Society (Resumed)*, pp. 708-716. DOI: 10.1039/JR9620000708.

Hanson, R. L., Lardy, H. A. & Kupchan S. M. (1970). Inhibition of Phosphofructokinase by Quinone Methide and α-Methylene Lactone Tumor Inhibitors, *Science*, 168 (3929), pp. 378-380.

Hardy, W. T. (1931). *Bitterweed poisoning in sheep*, Texas Agricultural Experiment Station, College Station, Texas.

Herz, W., Aota, K., Holub, M., et al. (1970). Sesquiterpene lactones and lactone glycosides from *Hymenoxys* species, *The Journal of Organic Chemistry,* 35, pp. 2611-2624. DOI: 10.1021/jo00833a029.

Hutcheon, D. (1893). Vomeerziekte or vomit sickness, *Agricultural Journal of the Cape of Good Hope,* 6, p 24.

Joubert, J. P. (1983). Attempted prevention and treatment of *Geigeria filifolia* Mattf. poisoning (vermeersiekte) in sheep, *Journal of the South African Veterinary Association,* 54, pp. 255-8.

Kellerman, T. S., Naudé, T. W. & Fourie, N. (1996). The distribution, diagnoses and estimated economic impact of plant poisonings and mycotoxicoses in South Africa, *The Onderstepoort Journal of Veterinary Research,* 63, pp. 65-90.

Kellerman, T. S., Coetzer, J. A., Naudé, T. W., et al. (2005). *Plant poisonings and mycotoxicoses of livestock in Southern Africa*, Oxford University Press, Cape Town, South Africa.

H. L. Kim. (1980). Toxicity of sesquiterpene lactones, *Research communications in chemical pathology and pharmacology*, 28 (1) pp,189-92.

Klimek, D., Chemiel, J. & Baer, W. (1981). The effect of sesquiterpene lactones on the synthesis of nucleic acid in cultures of human lymphocytes stimulated by phytohemagglutinin, *Archivum Immunologiae et Therapiae Experimentalis,* 29 (2), pp. 195-203. Accession Number: 6171235.

Kolm, H. P. (1984). Protective effects of antioxidants on bitterweed (*Hymenoxys odorata* DC) toxicity in sheep, *Toxicon,* 22, p 992. DOI: 10.1016/0041-0101(84)90204-6.

Konieczny, P., Fuchs, P., Reipert, S., et al. (2008). Myofiber integrity depends on desmin network targeting to Z-disks and costameres via distinct plectin isoforms, *The Journal of Cell Biology,* 181 (4) pp. 667-81. DOI: 10.1083/jcb.200711058.

Kupchan, S. M. (1974). Selective alkylation: a mechanism of tumor inhibition. *Intra-Science Chemistry Reports*, 8, pp. 57-66.

Langford, D. J., Bailey, A. L., Chanda, M. L., et al. (2010). Coding of facial expressions of pain in the laboratory mouse, *Nature methods,* 7, pp. 447-9. *DOI: 10.1038/nmeth.1455*.

Makowska, I. J. & Weary, D. M. (2021). A Good Life for Laboratory Rodents?, *Institute for Laboratory Animal Research Journal,* 60, pp. 373-388. Accession Number: 32311030 DOI: 10.1093/ilar/ilaa001.

McInnes, E. F. (2017). Pathology for toxicologists: principles and practices of laboratory animal pathology for study personnel, Wiley Blackwell. DOI: 10.1002/9781118755174.

McKenzie, E.C., Eyrich, L.V., Payton, M.E., et al. (2016). Clinical, histopathological and metabolic responses following exercise in Arabian horses with a history of exertional rhabdomyolysis, *The Veterinary Journal*, 216, pp 196-201. DOI: 10.1016/j.tvjl.2016.08.011

Mermelstein, C. S., Amaral, L. M., Rebello, M. I., et al. (2005). Changes in cell shape and desmin intermediate filament distribution are associated with down-regulation of desmin expression in C2C12 myoblasts grown in the absence of extracellular Ca2+, *Brazilian Journal of Medical and Biological Research = Revista Brasileira de Pesquisas Medicas e Biologicas,* 38, pp. 1025-32.

Milner, D. J., Weitzer, G., Tran, D., et al. (1996). Disruption of muscle architecture and myocardial degeneration in mice lacking desmin, *The Journal of Cell Biology*, 134 (5), pp. 1255-1270.

Milner, D. J., Mavroidis, M., Weisleder, N., et al. (2000). Desmin Cytoskeleton Linked to Muscle Mitochondrial Distribution and Respiratory Function, *The Journal of Cell Biology*, 150 (6), pp. 1283-1298.

Mizuno, Y., Thompson, T. G., Guyon, J. R., et al. (2001). Desmuslin, an intermediate filament protein that interacts with α-dystrobrevin and desmin, *Proceedings of the National Academy of Sciences,* 98, pp. 6156-6161. DOI: 10.1073/pnas.111153298.

Morris, J. J. (1945). 'Die vermeerbosvraagstuk in Griekwaland-Wes', *Boerdery in Suid-Afrika.*

Myburgh, J. (2020). *Ursinia nana subsp nana (Asteraceae) – the cause of "vermeersiekte" in sheep in South Africa.* University of Pretoria. Unpublished.

Narasimham, T. R., Kim, H. L. & Safe, S. H. (1989). *Effects of sesquiterpene lactones on mitochondrial oxidative phosphorylation*, *General Pharmacology*, 20 (5), pp. 681-7.

O'Neill, A., Williams, M. W., Resneck, W. G., et al. (2002). Sarcolemmal organization in skeletal muscle lacking desmin: evidence for cytokeratins associated with the membrane skeleton at costameres, *Molecular biology of the cell*, 13, pp. 2347-59.

OECD. (1987). *Test No. 401: Acute Oral Toxicity*.
DOI: https://doi.org/10.1787/9789264040113-en.
https://www.oecd-ilibrary.org/content/publication/9789264040113-en

OECD (2022). *Test No. 425: Acute Oral Toxicity: Up-and-Down Procedure*.
DOI: https://doi.org/10.1787/9789264071049-en.
https://www.oecd-ilibrary.org/content/publication/9789264071049-en.

Paul, M. & Skalli, O. (2016). Synemin: Molecular Features and the Use of Proximity Ligation Assay to Study Its Interactions, *Intermediate Filament Proteins,* 568, pp. 537-555. DOI: 10.1016/bs.mie.2015.08.005.

Paulin, D. & Li, Z. (2004). Desmin: a major intermediate filament protein essential for the structural integrity and function of muscle, *Experimental Cell Research,* 301, pp. 1-7. DOI: 10.1016/j.yexcr.2004.08.004.

Percy, D. H., Barthold S. W. & Griffey S. M. (2016). *Pathology of laboratory rodents and rabbits.* Fourth edn. John Wiley & Sons, Inc. New Jersey, USA.

Pei, S. *Characterization of the Anti-leukemia Mechanism of Parthenolide*, Doctoral dissertation, University of Rochester. http://hdl.handle.net/1802/27310.

Picman, A. K. (1986). Biological activities of sesquiterpene lactones, *Biochemical Systematics and Ecology,* 14, pp. 255-281. DOI: 10.1016/0305-1978(86)90101-8.

Pienaar, J. G., Kriek, N. P., Naudé, T. W., et al. (1973). Lesions in sheep skeletal and oesophageal muscle in vermeersiekte (*Geigeria ornativa* O. Hoffm. poisoning), *The Onderstepoort Journal of Veterinary Research,* 40, pp. 127-37.

Rimington, C. (1936a). *Chemical studies upon the vermeerbos, Geigeria Aspera Harv. I.: isolation of a bitter principle "Geigerin"*, Govt. Printer, Pretoria.

Rimington, C., Roets, G.C., Steyn, D.G., et al. (1936b). Chemical studies upon the vermeerbos, *Geigeria aspera* Harv. II. Isolation of the active principle "vermeeric acid", *Onderstepoort Journal of Veterinary Science and Animal Industry,* 7.

Rodriguez, E., Towers, G. H. & Mitchell, J. C. (1976). Biological activities of sesquiterpene lactones, *Phytochemistry,* 15**,** pp. 1573-1580. DOI: 10.1016/S0031-9422(00)97430-2.

Rowe, L. D., Kim, H. L. & Camp, B. J. (1980). The antagonistic effect of L-cysteine in experimental hymenoxon intoxication in sheep, *American Journal of Veterinary Research,* 41**,** pp. 484-6. Accession Number: 7406268.

Shivappa, P., Shetty, P., Kumari, S., et al. V. (2016). Evaluation of acute and sub-acute toxicity of the leaf extract of *Tanacetum parthenium* (Asteraceae) and synthetic parthenolide, *World Journal of Pharmacy and Pharmaceutical Sciences5*, pp. 703-713. DOI: 10.20959/wjpps20168-7269.

Schmutz, E. M., Reed, R. E. & Freeman, B. M. (1974). *Livestock-poisoning plants of Arizona*, University of Arizona Press, Tucson, USA.

Snyman, L. D., Schultz, R. A., Kellerman, T. S., et al. (2002). Continuous exposure to an aversive mixture as a means of maintaining aversion to vermeerbos (*Geigeria ornativa* O. Hoffm.) in the presence of non-averted sheep, *The Onderstepoort Journal of Veterinary Research,* 69, pp. 321-5.

Sotocinal, S. G., Sorge, R. E., Zaloum, A., et al. (2011). The Rat Grimace Scale: A partially automated method for quantifying pain in the laboratory rat via facial expressions, *Molecular Pain,* 7, pp. 1-10. DOI: 10.1186/1744-8069-7-55.

Steyn, D. G. (1935). Recent Investigations into the Toxicity of Known and Unknown Poisonous Plants in the Union of South Africa, *Onderstepoort Journal of Veterinary Research and Animal Science,* 4, pp. 399–415.

Steyn, D. G. (1943). 'Vermeersiekte by veediere', *Boerdery in Suid- Afrika.*

Sun, Y. (2010). *The radiosensitization effect of parthenolide in prostate cancer: implications for selective cancer killing by modulation of intracellular redox state.* Doctoral dissertation, University of Kentucky. http://uknowledge.uky.edu/gradschool_diss/768.

Thornell, L. E., Carlsson, L., Li, Z., et al. (1997). Null Mutation in the Desmin Gene Gives Rise to a Cardiomyopathy, *Journal of Molecular and Cellular Cardiology*, 29 (8), pp. 2107-2124. DOI: 10.1006/jmcc.1997.0446.

Vahrmeijer, J. (1981). *Poisonous plants of Southern Africa that cause stock losses*, Tafelberg, Cape Town, South Africa.

Valberg, S. J., Nicholson, A.M., Lewis, S.S., et al. (2017). Clinical and histopathological features of myofibrillar myopathy in Warmblood horses, *Equine Veterinary Journal*, 49 (6), pp 739-745. DOI: 10.1111/evj.12702.

van Aswegen, C.H., Vermeulen, N.M., Potgieter D. 1979. Inhibition of oxidative phosphorylation by sesquiterpene lactones from *Geigeria aspera*, *South African Journal of Science*, 75, pp. 84-85.

van Aswegen C.H., Vermeulen N.M., Potgieter, D. (1982). Site of respiratory inhibition by sesquiterpene lactones from *Geigeria*, *South African Journal of Science*, pp. 125–127.

van Der Lugt, J. J. & van Heerden, J. (1993). Experimental vermeersiekte (*Geigeria ornativa* O. Hoffm. poisoning) in sheep. II: Histological and ultrastructural lesions, *Journal of the South African Veterinary Association,* 64, pp. 82-8.

van Heerden, J., van Der Lugt, J. J. & Durante, E. (1993). Experimental vermeersiekte (Geigeria ornativa O. Hoffm. poisoning) in sheep. I: An evaluation of diagnostic aids and an assessment of the preventive effect of ethoxyquin, *Journal of the South African Veterinary Association,* 64, pp. 76-81.

Vermeulen, N. M., Vogelzang M. E., Potgieter, D. J. (1978). Dihydrogriesenin in *Geigera aspera* Harv, *Agrochemophysica,* 10, pp. 01-03.

Vogelzang, M. E., Vermeulen, N. M., Potgieter, D. L., et al. (1978). Ivalin in Geigeria aspera, *Phytochemistry,* 17, pp. 2030-2031. DOI: 10.1016/S0031-9422(00)88760-9.

Woynarowski, J. W., Beerman, T. A. & Konopa, J. (1981). Induction of deoxyribonucleic acid damage in HeLa S3 cells by cytotoxic and antitumor sesquiterpene lactones, *Biochemical Pharmacology*, 30 (21), pp. 3005-3007. DOI: https://doi.org/10.1016/0006-2952(81)90268-9.

Yu, Z., Chen, Z. Li, Q., et al. (2021). What dominates the changeable pharmacokinetics of natural sesquiterpene lactones and diterpene lactones: a review focusing on absorption and metabolism, *Drug Metabolism Reviews*, 53 (1), pp.122-140. DOI: 10.1080/03602532.2020.1853151. DOI: 10.1080/03602532.2020.1853151.

Appendix 1: The Mouse Grimace Scale

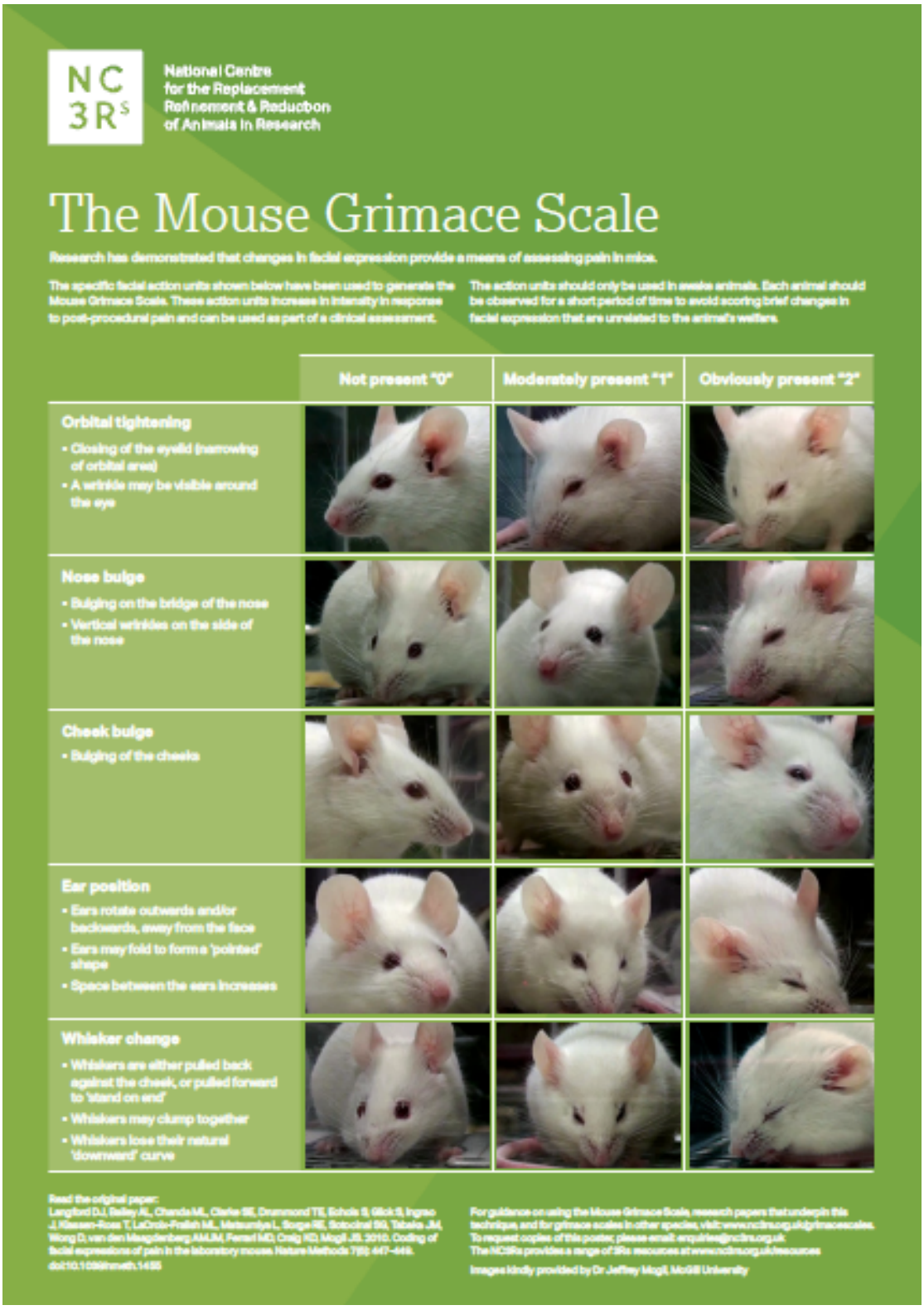

NC 3Rs
National Centre for the Replacement Refinement & Reduction of Animals in Research

The Mouse Grimace Scale

Research has demonstrated that changes in facial expression provide a means of assessing pain in mice.

The specific facial action units shown below have been used to generate the Mouse Grimace Scale. These action units increase in intensity in response to post-procedural pain and can be used as part of a clinical assessment.

The action units should only be used in awake animals. Each animal should be observed for a short period of time to avoid scoring brief changes in facial expression that are unrelated to the animal's welfare.

	Not present "0"	Moderately present "1"	Obviously present "2"
Orbital tightening • Closing of the eyelid (narrowing of orbital area) • A wrinkle may be visible around the eye			
Nose bulge • Bulging on the bridge of the nose • Vertical wrinkles on the side of the nose			
Cheek bulge • Bulging of the cheeks			
Ear position • Ears rotate outwards and/or backwards, away from the face • Ears may fold to form a 'pointed' shape • Space between the ears increases			
Whisker change • Whiskers are either pulled back against the cheek, or pulled forward to 'stand on end' • Whiskers may clump together • Whiskers lose their natural 'downward' curve			

Read the original paper:
Langford D.J, Bailey AL, Chanda ML, Clarke SE, Drummond TE, Echols S, Glick S, Ingrao J, Klassen-Ross T, LaCroix-Fralish ML, Matsumiya L, Sorge RE, Sotocinal SG, Tabaka JM, Wong D, van den Maagdenberg AMJM, Ferrari MD, Craig KD, Mogil JS. 2010. Coding of facial expressions of pain in the laboratory mouse. Nature Methods 7(6):447–449.
doi:10.1038/nmeth.1455

For guidance on using the Mouse Grimace Scale, research papers that underpin this technique, and for grimace scales in other species, visit: www.nc3rs.org.uk/grimacescales.
To request copies of this poster, please email: enquiries@nc3rs.org.uk
The NC3Rs provides a range of 3Rs resources at www.nc3rs.org.uk/resources

Images kindly provided by Dr Jeffrey Mogil, McGill University

Appendix 2: The Rat Grimace Scale